Fall 1985

Depositional Model for the Auriferous Gravels in the Payan Mining District Department of Narino, Columbia, South America

Jim R. Garrett
Old Dominion University

DEPOSITIONAL MODEL FOR THE AURIFEROUS GRAVELS IN THE PAYAN MINING DISTRICT DEPARTMENT OF NARINO, COLOMBIA, SOUTH AMERICA

by

Jim R. Garrett
B.S. December 1981, Old Dominion University

A Thesis Submitted to the Faculty of
Old Dominion University in Partial Fulfillment of the
Requirements for the Degree of

MASTER OF SCIENCE
GEOLOGICAL SCIENCES

OLD DOMINION UNIVERSITY
DECEMBER, 1985

Approved by:

Dr. Dennis A. Darby

G. Richard Whittecar

Ramesh Venkatakrishnan

ABSTRACT

DEPOSITIONAL MODEL FOR THE AURIFEROUS GRAVELS THE PAYAN MINING DISTRICT DEPARTMENT OF NARINO, COLOMBIA, SOUTH AMERICA

Unlike placer deposits in arid and semi-arid environments where gold concentration is closely tied to the position of the bedrock, Payan placer deposits have no association with bedrock. Gold concentration values show highest gold concentrations occur at the contact of a coarse sand unit and its underlying gravel unit. Comparisons of the size and shape distributions of gold grain populations with their associated black sand populations indicate the gold and black sand were not deposited in hydraulic equilibrium. The mean size of each gold population is consistently coarser than the mean size of its associated black sand population despite the large density difference. Flood events and subsequent entrainment sorting occurring during waning flow conditions can account for the observed areas of highest gold concentration as well as the anomalous size relationship between gold grain populations and their associated black sand populations. Morphological characteristics of gold grains observed under SEM establish that two types of gold exist in the Payan Mining District. One type probably travelled a distance of 80 to 100 km from its source, while the other type probably travelled less than 25 km from its source.

DEDICATION

Mom and Dad

In recognition of many years

of guidance and support

TABLE OF CONTENTS

APPENDIXES Page

LIST OF FIGURES

FIGURE PAGE

LIST OF TABLES

LIST OF PLATES

CHAPTER I

INTRODUCTION

The Payan Mining District is located sixty kilometers inland from the Pacific Ocean on the coastal plain of southwest Colombia. The village of Payan, situated on the floodplain of the Rio Magui, a tributary of the Rio Patia, is the center of population for the Payan Mining District (Figure 1). Approximately sixty kilometers to the east lies the Cordillera Occidental, one of the three Andean ranges in Colombia. Historically the coastal plain of Colombia has been an important producer of placer gold. Recent increases in gold prices have renewed interests in the placer gold in the Pleistocene river terraces of this district and exploration for new deposits has raised the question of the origin and distribution of this gold. Mining operations adjacent to the Payan area (Figure 1) have been successful in exploiting gold in economic proportions, mostly by dredging. At present, mining in the Payan District has been limited to very small unmechanized operations. In 1982, Cal-Colombian Mining Company, and its subsidary, Compania Minera de Colombia y Texas acquired

Figure 1. Map showing location of Rio Magui, Payan Mining District, and Barbacoas Mining District.

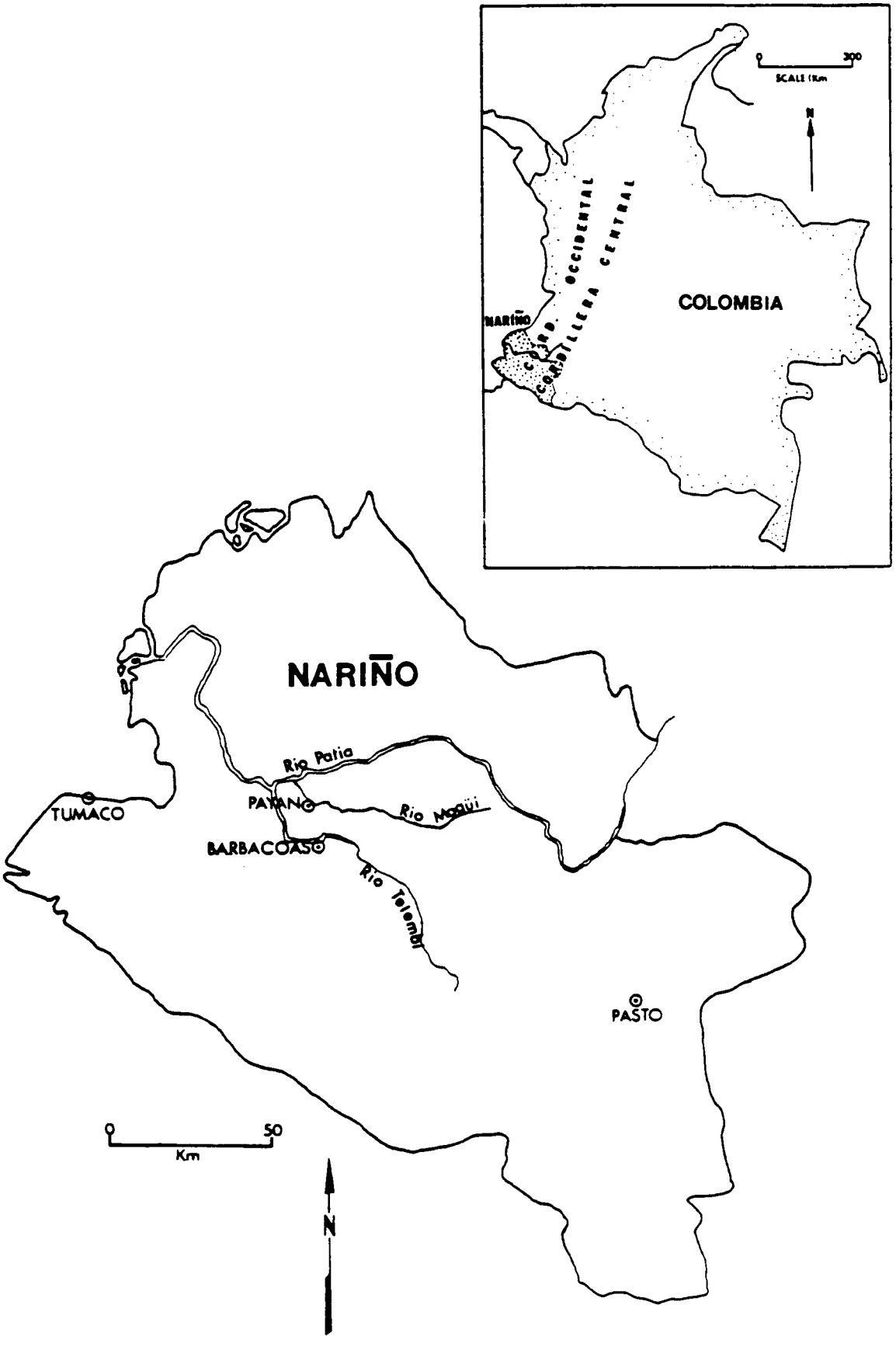
0 300
SCALE 1 Km
N
COLOMBIA
NARIÑO
C. OCCIDENTAL
C. CENTRAL
NARIÑO
Rio Patia
PATIANO
Rio Mayi
TUMACO
BARBACOAS
Rio Telembi
PASTO
0 50
Km
N

mineral rights to the Payan area and subsequently made funding available for this research.

Understanding the dynamics and genesis of placer deposits has always been a complex problem in both mining and sedimentology. Each placer deposit, whether modern or ancient, exposed or buried, affords its individual and peculiar problems (Crampton, 1937). Although the location, size and shape of a placer will reflect the regional forces of erosion, transportation, and deposition which created it, its final form will be controlled or modified by purely local conditions. Past studies have shown that due to the complex history of most valleys, regularity of concentration of heavy minerals at favorable points is rare (Kartashov, 1971). Placer deposits generally show many stages of deposition and erosion causing a great deal of variability of heavy mineral concentration in all three dimensions of the river system (Schumm, 1977, pp 221-241).

The purpose of this research has been to determine the nature and approximate distribution of the placer gold contained in the various lithologies of the Rio Magui terrace deposits and, to develop a depositional model for these auriferous units. In order to determine the sedimentary processes responsible for the implacement of fluvial placers, sedimentologists have generally focused attention to the physical characteristics of the rock record and studies of the heavy minerals associated with

the precious metal grains. Rarely have these studies included a detailed analysis of the precious metal grains themselves. The approach here will be to examine the size, shape, and surface texture of gold particles found in the Payan placer deposits. Size distributions of gold and their associated black sands will be interpreted in the context of hydraulic equivalence.

Hydraulic equivalence is the concept that describes the relationship between grains of a mineral of a given size and specific gravity and smaller grains of heavier minerals that are deposited simultaneously under given hydraulic conditions. Hydraulic-equivalent grains have the same settling velocity under the same hydraulic conditions. Tyrell (1912) used the concept in refering to equivalent volumes and weights of gold that a given stream velocity can move. Rubey (1933) studied the effect of specific gravity on the size distribution of other heavy minerals. Rittenhouse (1943) formalized the term, particularly in the form "hydraulic-equivalent sizes."

Scope of Research

Due to the remoteness and dense jungle vegetation of the study area, initially available geologic and topographic maps were limited to rough sketch maps based on pace and compass surveys (Ortiz, 1982). Consequently, the first objective of this investigation was to further refine and develop additional detail regarding the stratigraphic framework of the Rio Magui terrace deposits. This was accomplished by using a combination of aerial photographs and alidade-planetable surveys conducted during the three month field study (May 10 - August 10, 1983).

After developing a working topographic and stratigraphic framework the next objective of this study was to determine the amount and variability of gold concentration in the Rio Magui terrace deposits near Payan. These data are important to the interpretation of sedimentary processes responsible for these placer concentrations, as well as to the evaluation of the economic potential for future mining. It may also be possible that a relationship exists between high gold concentration and specific geologic characteristics readily observable in the field. These relationships could be useful in guiding future exploration and sampling.

The third objective of this research is to determine the depositional relationship between the gold, its

associated heavy minerals, and their host sands and gravels. Sedimentologic data on detrital precious metal grains and host sediments has proven to be useful for interpreting the nature and genesis of some placer deposits (Tourtelot and Riley, 1973; Utter, 1979; Slingerland, 1984). Size, shape, and textural analysis of gold grains and associated black sands are used in the present study to determine their hydraulic equivalence, which should yield important implications as to the depositional history of the gold-bearing terraces of the Payan Mining District. The following questions invariably arise in any placer examination and will be addressed in this research:

1. Is gold from a single source or multiple sources?
2. What is the lateral and vertical variability of gold concentration throughout the terraces?
3. Was all of the gold deposited contemporaneously with associated gravels or was part or all of it concentrated as a sieve deposit?
4. Was the final emplacement of auriferous gravels exclusively due to fluvial processes or some other process such as debris flows or a combination of the two?
5. Can areas of high gold concentration be related to specific characteristics in the host material which are observeable in the field?
6. What is the relationship between gold concentration and local stratigraphy?
7. Where is the source(s) of the Payan gold?
8. What caused the placer deposits?

Regional and Local Geologic Setting

The Payan Mining District lies on the coastal plain of southwest Colombia in the Pacific Coastal Basin, locally referèd to as the Tumaco Basin. The Pacific Coastal Basin of Colombia covers an area of 56,000 square kilometers and is considered part of the Bolivar Geosyncline (Nygren, 1950), which is thought to extend along the west coast of South America (Figure 2). It is bordered on the east by the mafic and ultra-mafic complex of the Western Cordillera of the Andes Mountains, where the "Diabase Porphry Group" crops out extensively (Buena and Govea, 1976). The lower portion of this group is a series of hard dark shales and slates, interbedded with altered limestones and cherts, with flows of diabase and diabase porphry. This group is generally assigned a Cretaceous age. To the east of the Western Cordillera lies the Central Cordillera, the oldest existing range in the Colombian Andes. The Central and Western Cordilleras were uplifted and intruded during the late Mesozoic and Cenozoic, followed by Tertiary volcanism which built numerous large peaks and formed many of the mineralized zones found in southern Colombia (Ramirez, 1977). This uplift and resulting erosion induced the deposition of a thick sequence of sediments (in the Pacific Coastal Basin) ranging in age from middle Miocene through the Quaternary. Duque Caro (1972) recognized a regional

Figure 2. Generalized tectonic map of western Colombia and Ecuador showing Bolivar Geosyncline and trends of of the three Cordilleras of the Andes Mountain Range. The small diamond represents the Payan Mining District. (modified from West, 1957).

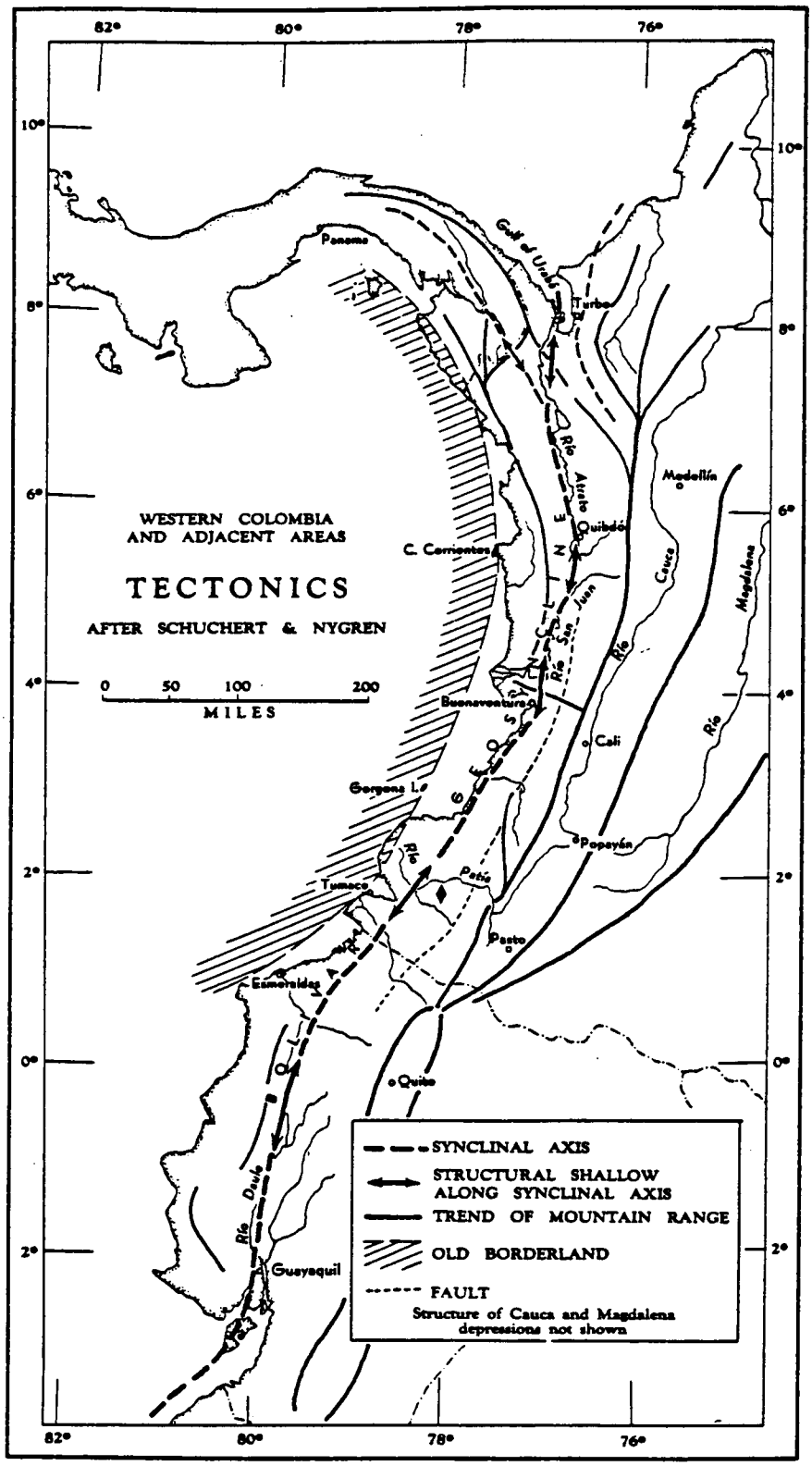
WESTERN COLOMBIA
AND ADJACENT AREAS
TECTONICS
AFTER SCHUCHERT & NYGREN
0 50 100 200
MILES
SYNCLINAL AXIS
STRUCTURAL SHALLOW ALONG SYNCLINAL AXIS
TREND OF MOUNTAIN RANGE
OLD BORDERLAND
FAULT
Structure of Cauca and Magdalena depressions not shown
Panama
Gulf of Urabá
Turbo
Río Atrato
Quibdó
Medellín
C. Corrientes
Río San Juan
Río Cauca
Río Magdalena
Buenaventura
Cali
Gorgona I.
Popayán
Tumaco
Río Patía
Pasto
Esmeraldas
Quito
Río Daule
Guayaquil
82°
80°
78°
76°
10°
8°
6°
4°
2°
0°

hiatus of deposition between the upper Cretaceous and the middle Eocene based on faunal successions.

Middle Eocene shales and siltstones are common throughout the coastal basin of Colombia. However, an exploratory well drilled by Mobil Oil near Tumaco (about 30 Km from study area) failed to reach Eocene stata at a depth of 13,107 feet (3,995m). The same well encountered over 3,000 meters of Oligocene strata consisting of tightly cemented coarse conglomerates, interbedded with claystones and siltstones, with tuffaceous sandstones near the upper portions (Buena, 1977). The Miocene is represented by up to 2,000 meters of olive-green and grey siltstones with interbeded tuffaceous sandstones and fine conglomerates. In the Tumaco area three facies make up the Pliocene section: marine, continental, and sedimentary-volcanic. The volcanic facies is thought to be contemporaneous with at least the upper sections of the continental and marine facies; it is composed of tuff, ash, and volcanic breccia and is only present in the Department of Narino.

Quaternary deposits consist of beach sands, lagoonal clays and silts, and fluvial deposits of boulder-to-gravel conglomerates along the mountain front, to sandstones and finer grained units in the lower valleys of most rivers.

In Plio-Pleistocene time the rivers draining the western slope of the Cordillera Occidental formed a continuous belt of auriferous and platiniferous gravels

extending from Esmeraldas, Equador to the Atrato Basin in northern Colombia (West, 1957). The auriferous gravels found in the Payan Mining District were deposited by the ancestral Rio Patia and/or Rio Telembi (Darby and Whittecar, 1985) in the southern portion of this linear band (Figure 3).

The Rio Patia is the only river in Colombia whose drainage area (24,000 sq km) includes the igneous and metamorphic rocks of both the Cordillera Occidental and Cordillera Central. The smaller Rio Telembi only drains from the western slope of the Cordillera Occidental and covers an area of 4,350 square kilometers. The Rio Magui, a tributary of the Rio Patia, is the major river in the Payan area. Its drainage basin covers approximately 500 square kilometers of the inner coastal plain and Andean foothills. Placer gold in the southwestern Colombia was eroded from gold ore occuring in veins and batholiths in the Central and Western Cordilleras and later deposited by one or all of these rivers (West, 1957).

Local Stratigraphy

The stratigraphy of the Pacific Coastal Basin of Colombia is poorly covered in the published literature. Climate, dense vegetation, and the remoteness of this tropical region makes field work very difficult. The

Figure 3. Map of Western Colombia showing the band of auriferous and platiniferous gravels deposited by rivers draining the western versant of the Cordillera Occidental (after West, 1957).

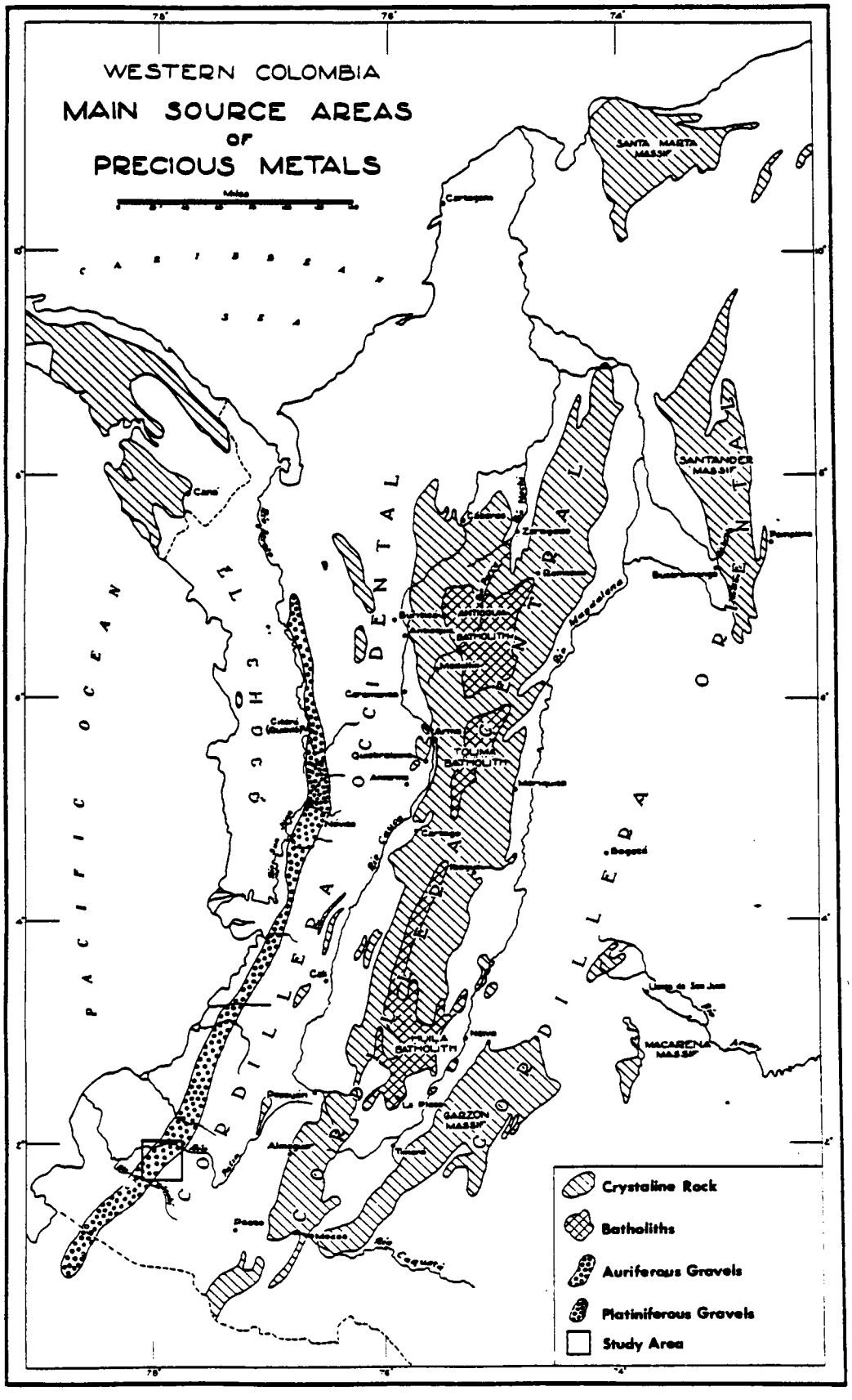
WESTERN COLOMBIA
MAIN SOURCE AREAS
or
PRECIOUS METALS
Miles
PACIFIC OCEAN
CARIBBEAN SEA
SANTA MARTA MASSIF
SANTANDER MASSIF
CORDILLERA OCCIDENTAL
CORDILLERA CENTRAL
CORDILLERA ORIENTAL
SIERRA NEVADA DEL COCUY
ANTIOQUIA BATHOLITH
TOLIMA BATHOLITH
GARZON MASSIF
MACARENA MASSIF
Crystaline Rock
Batholiths
Auriferous Gravels
Platiniferous Gravels
Study Area

problem is further complicated by the complex sedimentary history of the area, where abrupt vertical and horizontal facies changes are the rule rather than exception (Buena and Govea, 1976).

The sediments contained in the Payan terraces (Figure 4) were refered to as "terraces and fans of fluvio-volcanic origin" and described as alternating cobble-to boulder gravels with volcanic stones, capped by pumice and ash, and lenses of sand silt and clay with high carbonaceous content (Arango and Ponce, 1982). Ortiz (1982) further refined the stratigraphy of the Payan terraces. He identified and mapped several gravel-rich units, one volcanic ash bed, and two bedrock or false bedrock strata. Ortiz assigned the first formation names to these deposits (Table 1).

The most recent stratigraphic revisions, based on extensive field observations and radiometric dating, are described in Darby and Whittecar (1984). Although their proposed stratigraphy closely follows that of Ortiz (Table 1), they recognized six stratigraphically and geomorphically distinct formations: three units of volcanic ash, and three consisting of fluvial gravels, sands, and muds.

Description of Stratigraphic Units

The oldest formation observed (Ananias Formation)

Figure 4. Sketch map of Payan area showing the major auriferous terraces: Piccinini (1), Santa Ana (2), La Travesia (3), Hipolito (4), Marta (5), Magdalena (6), Alcose (7), Mirabel (8), Payan (9), Ananias (10), and Panambi (11). Terraces are outlined by the 50 meter contour line. Also shown are the path to Barbacoas, ponds, the Rio Magui, and minor drainage ways.

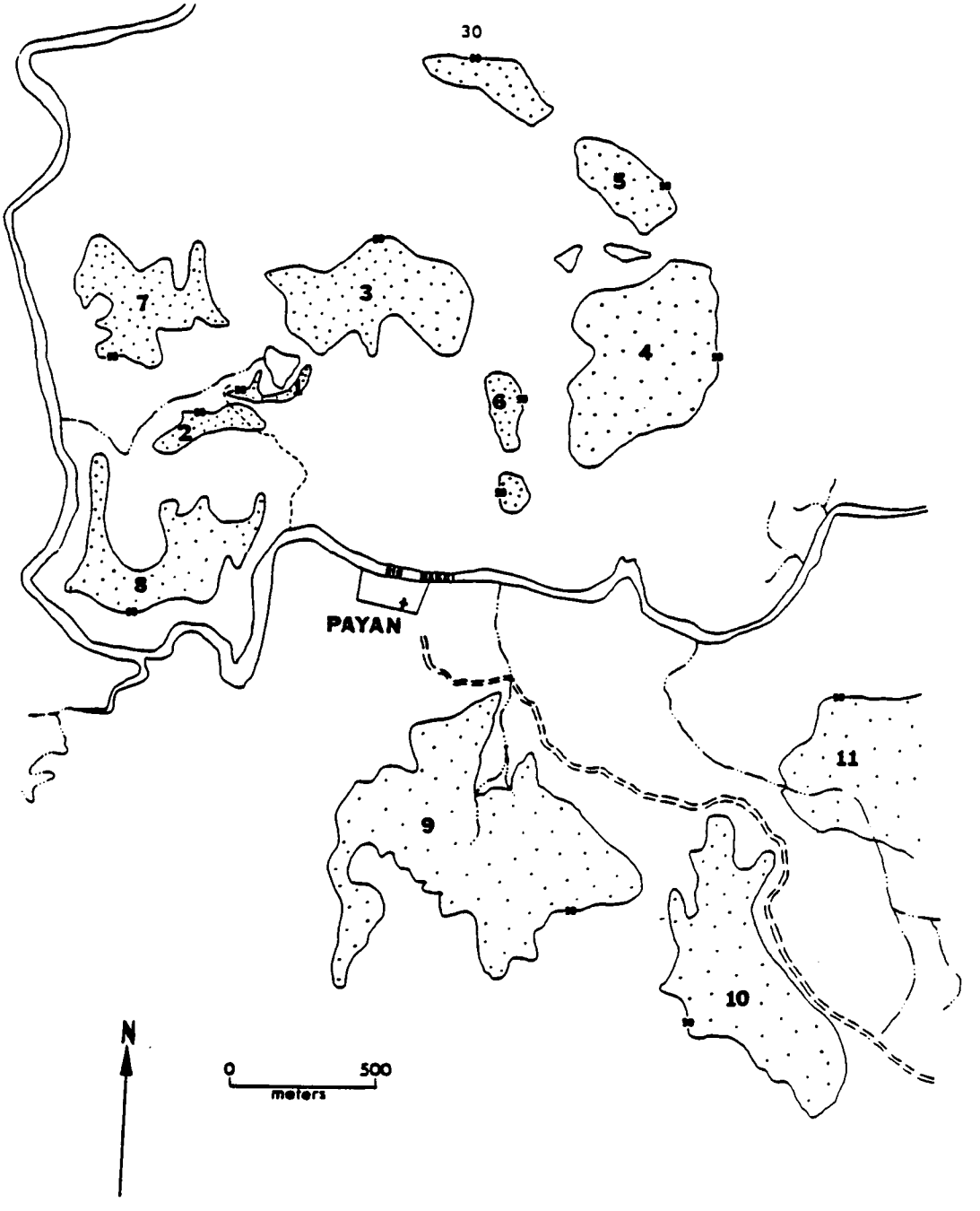
30
5
7
3
4
6
2
8
PAYAN
11
9
10
N
0
500
meters

TABLE 1. Correlation chart for surficial deposits, Payan Minining District, Narino, Colombia.

	ARANGO and PONCE 1982	ORTIZ 1982	DARBY and WHITTECAR 1984
QUATERNARY	UNNAMED FORMATION "terraces and fans of fluvio-volcanic origin...."	PAYAN FORMATION	PAYAN FORMATION
			MAGUI ASH included in San Juan Fm. of Ortiz
			PAÑAMBISITO FORMATION included in Piccinini Fm. of Ortiz
		SAN JUAN FORMATION	SAN JUAN ASH
		PICCININI FORMATION -upper conglomerate member -middle sandstone member -lower conglomerate member	ANTIGUA FORMATION
		SAN JOAQUIN FORMATION	
TERTIARY (?)		MAGDALENA FORMATION	ANANIAS FORMATION
		ANANIAS FORMATION	

consists of a volcanic ash and agglomerate, lithified sufficiently to form "bedrock" or "false bedrock". The younger five unconsolidated formations (Antigua, San Juan, Panambi, Magui, and Payan) resulted either from the episodic erosion and deposition of streams or eruptions of large Andean volcanoes to the east. Each alluvial unit is associated with a set of active or abandoned fluvial terraces lying within a certain range of elevations, and rests upon a stream-cut unconformity. The following stratigraphic descriptions are based on those presented by Darby and Whittecar (1984).

Ananias Formation

The Ananias formation is the oldest exposed unit in the Payan area. It consists of lithified, compacted ash and agglomerate layers with angular volcanic fragments. The total thickness of this unit is unknown, but thickness greater than 10 meters have been observed. This formation is devoid of gold and is unconformably overlain by the Antigua Formation.

Antigua Formation

The Antigua Formation is classified as an entirely fluvial terrace deposit containing relatively high

percentages of well-rounded basalt or porphyritic basalt cobbles. Antigua sediments are exposed throughout the study area, typically at elevations greater than 35 meters. The thickest measured section is located at the Piccinini Mine where more than 30 meters of cobbly sands and gravels have been observed in outcrop and drill sections.

The Antigua Formation is generally composed of cobbly gravels with a coarse sandy matrix. This matrix is often weathered entirely to clay, but the ghost texture of the original sand grains can be clearly seen. Minor amounts of chert, quartz, and various other igneous and metamorphic cobble types also occur in this unit. Cobbles are usually slightly elongated, frequently imbricated, and well rounded. Weathering rinds are common and vary in thickness from one millimeter to 10 centimeters at different exposures. Boulders over one meter in diameter have been observed in some horizons. Wood debris and logs up to several meters in length are also common in this unit. The Antigua gravels contain numerous discontinuous lenses of sand and mud. Wood debris is especially concentrated near the bases of these lenses along with black sands. Rare sedimentary structures consist of small trough cross-bedding, cut-and-fill structures, parallel laminae, and shadow deposits. Stringers of concentrated black sands, mostly magnetite, have been observed near contacts

of gravel and overlying sand and are associated with high gold values.

The Antigua formation is the major gold-bearing unit in the Payan Mining District. It is interpreted as a high gradient, braided channel deposit which was part of a wet alluvial fan (Darby and Whittecar, 1984). These gravels are considered to be Late Pleistocene in age based upon C^{14} dates that range between 30,000 to greater than 40,000 years before present.

San Juan Ash

The volcanic ash and agglomerate overlying the Antigua formation have been named the San Juan Ash Formation (after Ortiz, 1982). This formation is also extensively exposed throughout the Payan terraces. Individual beds range from 0.5 to 8 meters in thickness, however the total thickness of unit is unknown because of the erosional nature of the ash surface. Lithologically this formation consists of a white bedded ash mostly weathered to clay. The unweathered fragments include quartz, magnetite, biotite, and rarely hornblende. The San Juan Ash is considered to be the result of Late Pleistocene eruptions of Andean volcanoes to the east (Darby and Whittecar, 1984).

Panambi Formation

The chert-rich gravels with sand and mud lenses overlying the San Juan Ash make up the Panambi Formation. These deposits are found in terraces of less than 65 meters in elevation. The Panambi gravels are easily distinguished from Antigua gravels on the basis of cobble lithology, size of clasts, and topographic elevation. Panambi gravels are primarily quartz and chert, ranging in size from 4 to 10 centimeters, while the cobbles in the Antigua Formation consist mainly of basalts that range in size from 8 to 40 centimeters. Organic material in the form of logs, leaves, fruits, and nuts are abundant. Gold has been found to occur in relatively high concentrations, for this area, at the type section for this unit (Panambisito Mine). Based on the similarity of pebble and cobble lithologies, the greater content of muddy strata, and organic material similar to present-day Rio Magui system, the Panambi sediments are interpreted to be the result of more stable single channel stream deposition as opposed to braided stream deposition for the older Antigua Formation (Darby and Whittecar, 1985). The near-absense of easily weatherable clasts and smaller average grain size indicates that the Panambi deposits were reworked from the Antigua Formation sediments.

Magui Ash

Lying conformably on top of the Panambi Formation is the Magui Ash. This pyroclastic unit is similar in composition to the San Juan Ash, but probably represents a later volcanic eruption. At only one site (Piccinini Mine) are two ash units observed in the same outcrop with a thin gravel between which might represent the Panambi Formation. The observed thickness of the Magui Ash varies from 5 to 10 meters. The Magui Ash covers nearly all surfaces in the study area except flood plains and recent alluvium. This formation has not been found to contain significant concentrations of gold and is considered locally as overburden.

Payan Formation

Channel and overbank deposits of the present Rio Magui and its tributaries are termed the Payan Formation. The Payan Formation includes sediments ranging in size from cobbly gravels to fine muds which were deposited in channels, on side bars, mid-channel bars, and flood plain deposits. Cobble lithologies are dominated by quartz and chert with minor amounts of basalt. The sand fraction in this formation is less weathered than any other unit and is composed of quartz, feldspar, and basalt fragments. The Payan formation does contain gold, but economic concentrations have yet to be encountered.

CHAPTER 2

METHODOLOGY

Field Methods

Surveying and Mapping

High altitude aerial photographic coverage of the study area was used to construct planimetric base maps by projecting the aerial imagery at a scale of 1:2500 onto acetate field sheets. Rivers, ponds, tree lines, and other landmarks were traced onto these sheets for field survey references. A planetable, alidade, and stadia rod were used to plot the location and calculate the change in elevation for each surveyed point. From a brass benchmark in Payan (47.2 meters elevation, H. Ortiz, personal communication) traverses were made to all known mine sites in order to generate topographic maps and to determine the location and elevation of all exposed stratigraphic contacts in the study area. This work required much clearing of jungle vegetation by machete. In addition to surveying and mapping, detailed stratigraphic descriptions were made at each outcrop. A more thorough explanation of surveying and mapping techniques is presented by Darby and

Whittecar (1984). The geologic and topographic maps and geologic cross-sections that resulted from this work are included in this report (Plates 1,2, and 3). These maps represent the most extensive and detailed mapping completed thus far in this remote region.

Sampling Methods

Representative placer samples are seldom easy to obtain and in most cases sample results require a large measure of interpretation. By themselves small samples obtained from existing exposures can seldom be expected to accurately indicate the quantity of gold available. Small samples, may at best, merely indicate the presence of gold. However analyses of larger samples, if correctly interpreted, can indicate a range of gold values to be expected. One of the main problems associated with placer sampling is the larger particle sizes encountered such as cobbles and boulders. For example, a typical gravel found in the Payan terrace deposits contains a wide range of clast sizes (up to 80cm.). A representative sample should contain all of the constituents of a deposit in exactly the same proportions in which they occur in the outcrop. Therefore it is virtually impossible to take a small representative sample. For these reasons a sample size of 0.5 to 1.0 cubic meters was chosen to evaluate the placers in the Payan Mining District. Twenty samples of this size were

excavated throughout the Payan terraces in both the Antigua and Panambi formations. Sample locations are shown in Figure 5. Sample sites were selected based on the availability of water to wash the samples, and the location of existing exposures. Sampling for placer evaluation was only performed in fluvial sands and gravels because preliminary investigations have shown the volcanic strata to be barren of gold (Ortiz, 1982). Where exposures revealed both sand and gravel units, each unit was sampled. Excavation of samples was accomplished by smoothing the face of the outcrop and marking a one meter square on it, followed by digging straight walls 0.5 to 1.0 meters into the outcrop. Excavated materials were allowed to fall on a canvas placed at the bottom of the excavated wall. The excavated walls stood well facilitating direct measurement of the volume of material removed.

The next step in the field sampling was to thoroughly wash and remove the pebbles and cobbles so that the finer materials could be panned for heavy minerals (black sands and gold). This was achieved by placing a screen with half-inch squares over a large collection pan filled with water. The material less than 0.5 inches in diameter was collected in the pan and the cleaned cobbles and pebbles were discarded. Under our close scrutiny, the collected material was panned by an experienced native panner down to

Figure 5. Sketch map of Payan area. Crossed-hammers represent mine sites sampled for gold content. Appendix A and Plates 1 and 2 give more detailed locations of these sample sites.


PAYAN
N
0
500
meters

the black sand fraction. The black sands from each sample location were then packed and shipped to the laboratory in Norfolk, Virginia for assessment of gold content and, granulometric and morphologic analyses.

Laboratory Methods

Amalgamation Separation

Upon arrival at the laboratory the black sands were dried, weighed, and the amount of black sand per cubic meter was calculated for each sample. The next step was to separate the gold from the black sands (Figure 6). Several methods have been sucessfully employed in the past for gold separation (Peele and Church, 1959). Mercury amalgamation, the process selected here, has proven to be very effective in removing gold (Rossiter, 1973, pp 221-241). Unfortunately, since gold usually goes into solution with the mercury, this process destroys the original characteristics of the gold grains, rendering them useless for analysis of surface texture, size, and shape. Therefore, gold grains were extracted using a water elutriator for a 1/3 split of each of the original black sand samples before amalgamation. In order to increase the efficiency of this gravity separation technique, this split was sieved at quarter-phi intervals before elutriation.

Figure 6. Flow chart of gold separation procedures.

Flow Chart of Gold Separation Procedures

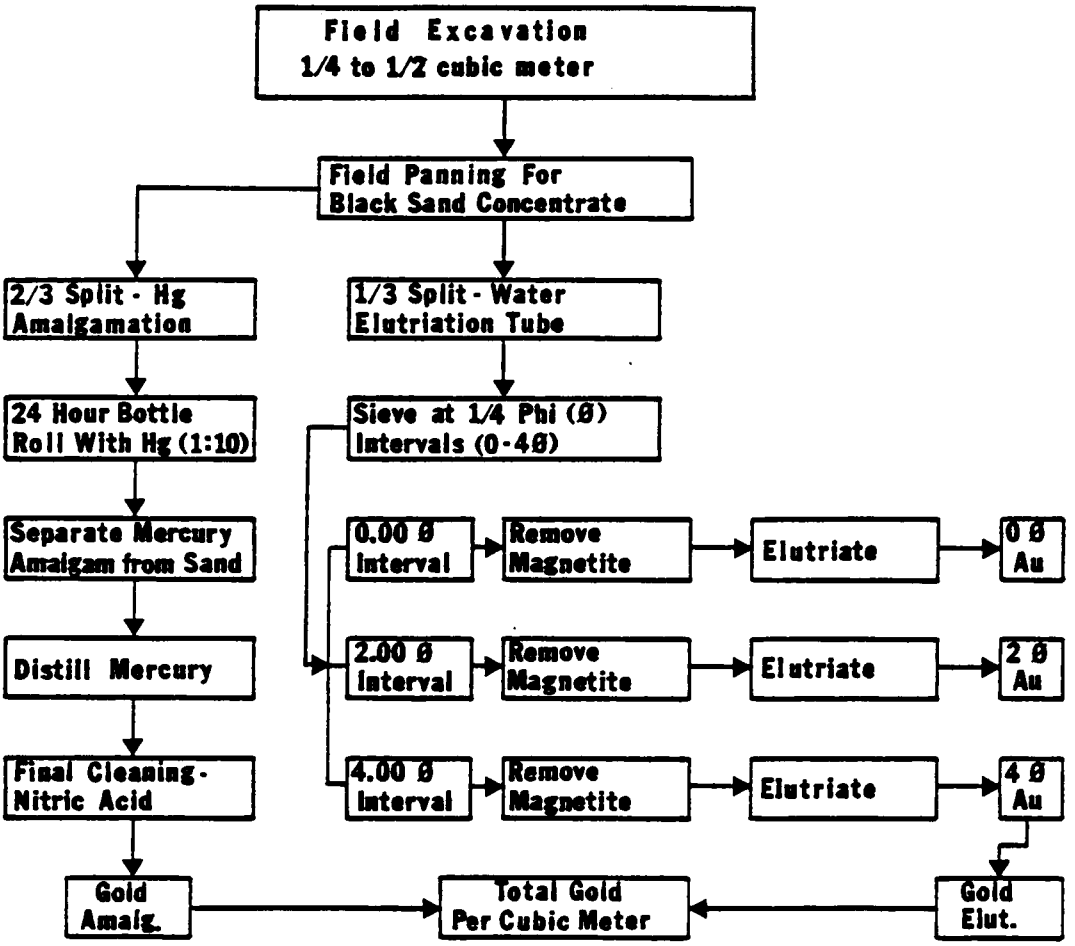

The separation of gold by amalgamation involved weighing the black sand concentrate not used in the elutriate separation. The black sands were then placed in a large wide-mouthed jar along with 50 to 75 grams of mercury and some distilled water. The jar was placed on an electric bottle roller and rolled for 24 hours allowing the gold to completely amalgamate with the mercury. The mercury amalgam was separated from the sand by slowly pouring the mix onto a stainless steel trough inclined at an angle that would allow the mercury beads to roll to the bottom leaving the barren black sands at the top. The mercury amalgam was then placed in a vacuum distillation apparatus and the mercury was boiled off at a temperature of 250-275^{o}C with a vacuum pressure of 500 millimeters of mercury. The recovered mercury was weighed for loss. The recovered gold was cleaned with concentrated HNO_3, dried, and examined under the microscope for contaminating grains. Finally, the gold was weighed to the nearest 0.00001 gram and gold concentration values were calculated in troy oz./cubic meter

Elutriation Separation

As previously mentioned a 1/3 split of the original black sand concentrate was extracted for gold removal by a water elutriation tube (Frost, 1959). This method was especially desirable for this research because it allowed

the gold to be separated from the black sand, and generated size distribution data for both, without altering the original size, shape, or texture of the gold grains.

The increasing cross-sectional areas of the elutriation tube were chosen so as to reduce the velocity of rising water by fifty percent with its entry into each larger section (Figure 7). As each quarter-phi sieve fraction was introduced into the top of the tube, the velocity of rising water was adjusted so that the black sands would remain suspended and the gold settled to the collection flask at the bottom of the tube. The narrow size range of the fractions that were elutriated readily facilitated separation of the gold grains due to their high specific gravity. Because of the bulk of the black sands (1000 to 6000g) a hand magnet was used to remove the magnetic minerals and reduce the amount of material to be elutriated. Recovered gold was examined under the microscope for impurities. The weights of black sands and gold in each size fraction were used to construct cumulative frequency size curves.

Since two methods were used to extract the gold, it was possible to calculate the gold concentration (gram/cubic meter) for each sample, by each method. The percent difference in gold recovery between elutriation and amalgamation ranged from 1.5 to 4.8 percent, which implies that equally efficient gold recovery was accomplished by both methods.

Figure 7. Elutriation Apparatus (after Frost, 1959) (not to scale).

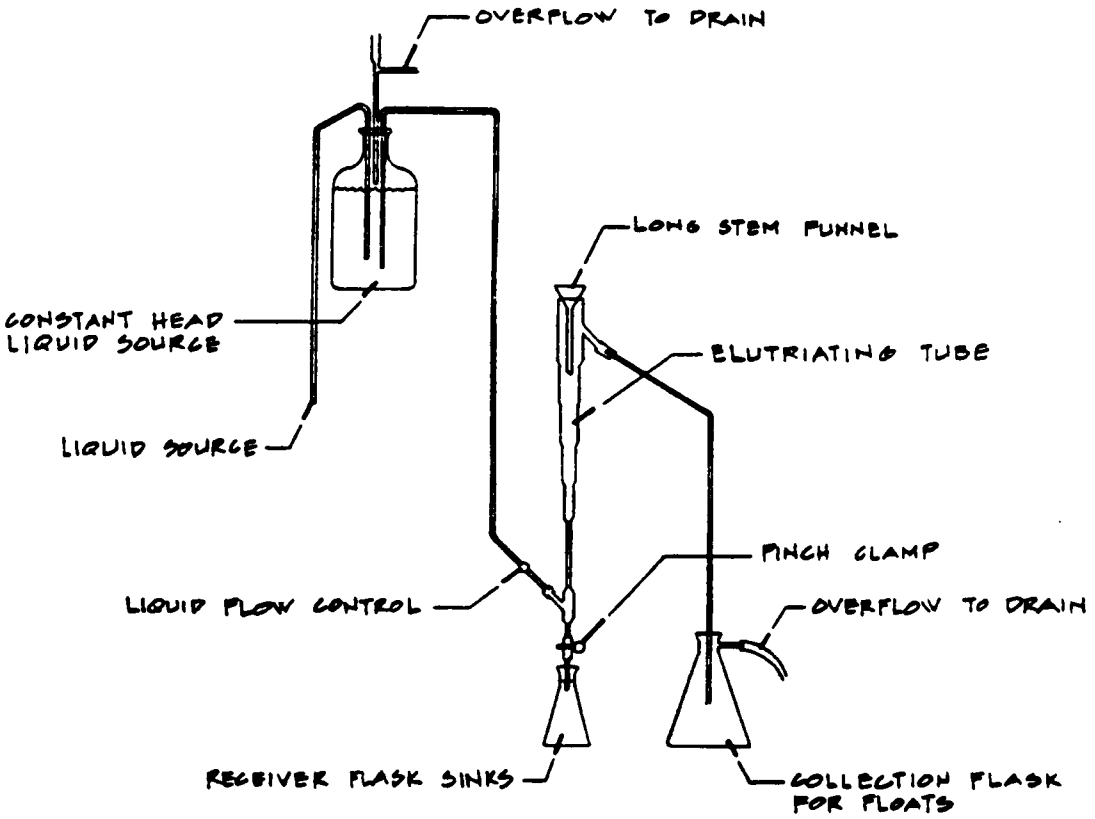
OVERFLOW TO DRAIN
LONG STEM FUNNEL
CONSTANT HEAD
LIQUID SOURCE
ELUTRIATING TUBE
LIQUID SOURCE
PINCH CLAMP
LIQUID FLOW CONTROL
OVERFLOW TO DRAIN
RECEIVER FLASK SINKS
COLLECTION FLASK
FOR FLOATS

Shape Analysis

Shape descriptions for samples were made from microscopic measurements of the gold grains from each sieve fraction. The coarser size fractions contained only a few grains and all were measured. The finer fractions contained hundreds of grains, so a random sample of about 30 grains was taken from each by a micro-cone and quarter procedure under the microscope. The first dimension determined for each grain was the length, which is defined here as the longest measurable dimension of the grain. The length was recorded as the distance intercepted on the ocular micrometer. Next, the grain was rotated 90 degrees and the breadth was recorded in the same way. The thickness of the grain was determined by focusing sharply on the slide and measuring the difference in the fine focus vernier to the top of the grain.

A computer program was written to translate the ocular micrometer intercepts to millimeters, taking into account the magnification of the objective that was used. The program also calculated the difference between vernier readings and converted the difference to millimeters. Duplicate determinations of thickness obtained in this way have a precision of plus-or-minus six microns.

The computer program also calculated the Corey Shape Factor (Corey, 1949), and the maximum projection sphericity

(Sneed and Folk, 1958). Computer plotting techniques were used to plot shape factors against intermediate axis diameters of the grains. The Corey shape factor was chosen rather than the maximum projection spericity because it is widely used in engineering problems of sedimentation (Inter-Agency Commission on Water Resources, 1957):

$$\text{Corey Shape Factor} = T^2/(LB)^{1/2}$$

where T=thickness (smallest dimension), L=length, and B=breadth. Corey shape factors range from 0 to 1.0. Small factors indicate flaky grains and larger factors indicate more spherical grains.

Settling Tube Analysis

In order to better understand the relationship between size, shape, settling velocity, and hydraulic equivalence; size distributions based on fall-equivalent quartz spheres were generated for the black sands and gold . This was done by recombining the sieve fractions of gold and black sands separately to obtain the original size distributions. Each recombined sample was then separately introduced into a Rapid Sediment Analyzer with a water column of 100 centimeters. Cumulative frequency percent size curves were constructed based on the settling velocity of the gold and black sand grains. These distributions

were then compared to the ones based on mechanical sieving. Only five samples contained enough gold to perform this comparison.

Surface Texture Analysis

Because of its pronounced malleability, gold acquires characteristic textural features which reflect each grains transportational history. Scanning Electron Microscopy (SEM) has been shown to be an effective tool in recognizing these features (Hallbauer and Utter, 1977; Utter, 1979). Several gold grains were randomly selected from several sample locations in the Payan Mining District and examined under SEM. Both textural and morphological descriptions were made.

CHAPTER 3

RESULTS

Gold Concentration Values

The mercury amalgamation process was effective in removing all of the gold from the 18 assay samples (0.5-1.0 cubic meter) extracted from the Payan terrace deposits. Gold was present and recovered in all samples analyzed; however, the gold concentration values were found to be quite variable over short distances (often less than a few meters). This variability in gold concentration was observed between samples separated by a short lateral distance as well as samples taken from the same exposure, at different stratigraphic horizons.

Gold concentration values ranged from 0.003 oz/cu m to 0.059 oz/cu m and black sand concentration values ranged from 2,540 gm/cu m to over 7,000 gm/cu m (Table 2). No trends relating geographic areas within the study area to high gold concentration values could be ascertained. For example, the 0.035 oz/cu m value for the Domingo II mine is considerably higher than the 0.004 oz/cu m value for the adjacent Domingo I mine site. Erratic values such as

TABLE 2. Sample elevations, host formation, lithologies, gold concentration values, black sand concentration values, and map locations.

SAMPLE LOCATION	ELEVATION OF SAMPLE (meters)	FORMATION	LITOHLOGY	GOLD VALUE (oz/cu m)	BLACK SAND VALUE (gm/cu m)	LOCATION (PLATES 1,2) DESCRIPTION*
Panambisito	51.9	Panambi	Gravel	0.014	3,354	Plate 2
Mariana	76.5	Antigua	Cobble Gravel	0.003	4,984	Plate 1
Mariana	74.7	Antigua	Coarse Sand	0.012	2,068	Plate 1
Mariana	67.3	Antigua	Cobble Gravel	0.015	6,784	Plate 1
Marta	70.1	Antigua	Coarse Sand	0.012	1,000	Plate 1
Marta	67.5	Antigua	Cobble Gravel	0.040	1,000	Plate 1
Panambisito	54.0	Panambi	Cobble Gravel	0.046	5,640	Plate 2
Domingo I	81.0	Antigua	Cobble Gravel	0.003	5,548	Plate 2
Domingo II	78.0	Antigua	Cobble Gravel	0.027	3,660	Plate 2
Travesia	65.5	Antigua	Cobble Gravel	0.018	7,435	Plate 1
Travesia	67.0	Antigua	Coarse Sand	0.015	1,640	Plate 1
Hipolito	72.1	Antigua	Cobble Gravel	0.002	5,552	Plate 1
Hipolito	71.0	Antigua	Coarse Sand	0.008	4,952	Plate 1
Blandito	64.5	Antigua	Cobble Gravel	0.012	5,692	Plate 2
Hipolito	84.0	Antigua	Cobble Gravel	0.010	2,540	Plate 1
Anguino	50.2	Panambi	Pebble Gravel	0.021	5,436	Plate 2
Anguino	49.1	Panambi	Pebble Gravel	0.011	4,052	Plate 2
Alcose	51.3	Antigua	Cobble Gravel	0.015	4,420	Plate 1

* Detailed stratigraphic descriptions and sample locations are in Appendix A.

these in the Payan terraces are normally encountered in placers (Nicholas, 1897; Kartashov, 1971). High variations in gold values were documented by Ortiz (1982) in his analysis of the Piccinini and Santa Anna terraces.

Six of the ten exposures sampled for gold analyses included samples taken from more than one horizon (Panambisito Mine, Anguino Mine, Mariana Mine, Hipolito Mine, Travesia Mine, and Marta Mine). Ortiz (1982) calculated gold concentration values from several horizons in vertical sequences at the La Junta Mine, Piccinini Mine, and the Santa Anna terrace (Appendix A).

These data show that gold values vary with increasing depth at one location as much as they do laterally between locations. Unlike "bedrock placers" where gold values commonly increase with depth, the Payan placers fluctuate with depth and even decrease near "bedrock" which is herein defined as any semi-consolidated ash which is underlying an auriferous gravel. To illustrate, the Piccinini Mine yields a very low gold value in the upper gravel just below the capping ash. Lower into this unit the values increase, reaching a maximum just above the contact with the underlying sand unit. The values then decrease in the sand unit only to increase again around the contact between the sand and lower gravel. In the thicker, lower gravel, gold values fluctuate with two zones of relatively high concentrations (Appendix A).

Apparently the only stratigraphic trend is that the highest gold values in any particular unit occur at or just below the contact of a sand unit and its underlying gravel. This observation is especially apparent in the Piccinini, Luis, Marta, Panambisito, and Santa Anna Mines. Secondary thin zones of higher gold concentrations are often identified within gravel units, although they are not apparent in the lithologies of the outcrop. Any model proposed for the depositional processes of these placers should account for these zones.

The highest gold values were found to occur in the gravel units, although some of the sand units showed moderate values, especially near their bases. The Panambisito gravel sample and the Marta gravel sample had the highest gold values (0.061 oz/cu m and 0.053 oz/cu m, respectively). The Panambisito sample was taken from the chert-rich gravels of the Panambi Formation, while the Marta sample represents the basalt-rich gravels of the older Antigua Formation (Table 1). A total of 14 samples were taken from the Antigua Formation with concentration vaues ranging from 0.003 to 0.052 oz/cu m. A total of four samples were taken from the Panambi Formation with concentration values ranging from 0.014 to 0.061 oz/cu m. The average gold value for Antigua samples is 0.018 oz/cu m (n=14) compared to 0.029 oz/cu m (n=4) for Panambi samples.

High gold concentration values did not correlate with high black sand concentration values (Table 2). This observation may have important implications as to the hydraulic equivalence between these mineral groups.

Size Distributions

Previous studies have reported that gold owing to its higher specific gravity, will always be smaller in grain size than the lighter grains with which they are associated (Clifton, 1966; Tourtelot, 1968). This means that a cumulative frequency size curve for a particular gold population should plot on the fine side of the cumulative size curve representing its associated black sand population. Contrary to what was expected, the gold curves for the 18 Payan District samples consistently plotted on the coarse side of the black sand curves (Appendix B).

The average mean size for all gold distributions is 1.84 phi while the average mean size for black sands is 2.53 phi, an average difference of 0.69 phi (Table 3). In general the mean size of gold and black sand taken from gravel units was found to be slightly coarser than those from sand units. The average mean size of gold and black sand from sand units is 1.98 phi and 2.79 phi, respectively. The average mean size values for gold and black sand in the gravel units is 1.64 phi and 2.43 phi, respectively.

TABLE 3. Gold concentration values and grain size statistics of sieve analysis. All sizes are in phi units.

SAMPLE NAME	GOLD VALUE OZ/CU M	MEAN SIZE		SORTING		SKEWNESS		KURTOSIS		MEDIAN SIZE	
		GOLD	BLK SAND	GOLD	BLK SAND	GOLD	BLK SAND	GOLD	BLK SAND	GOLD	BLK SAND
Panambisito (sand)	0.014	2.081	2.539	0.770	0.558	0.034	0.527	2.31	2.84	2.23	2.48
Mariana (gravel)	0.003	1.843	2.529	0.590	0.471	0.873	0.240	2.91	3.32	1.69	2.55
Mariana (sand)	0.012	1.826	2.684	0.740	0.625	0.387	0.166	2.16	2.77	1.79	2.71
Mariana (gravel)	0.015	2.118	2.402	0.707	0.539	0.047	0.118	2.25	3.17	2.22	2.42
Marta (sand)	0.012	2.130	2.896	0.752	0.585	0.029	0.017	2.18	2.39	2.15	2.83
Marta (gravel)	0.040	1.532	2.481	0.608	0.560	0.819	0.475	3.27	3.08	1.43	2.43
Panambisito (gravel)	0.046	1.447	2.463	0.612	0.548	0.268	0.272	2.81	2.95	1.41	2.46
Domingo I (gravel)	0.003	1.560	2.398	0.549	0.507	0.962	0.400	2.65	3.30	1.24	2.39
Domingo II (gravel)	0.027	1.377	2.540	0.723	0.501	0.188	0.261	2.77	3.51	1.37	2.55
Travesia (gravel)	0.018	2.036	2.584	0.826	0.478	0.027	0.448	2.14	3.46	2.04	2.56
Travesia (sand)	0.015	2.368	3.136	0.809	0.474	0.290	0.159	2.14	2.61	2.28	3.05
Hipolito (gravel)	0.002	1.924	2.312	0.860	0.524	0.594	0.542	2.15	3.39	1.75	2.25
Hipolito (sand)	0.008	1.836	2.685	0.720	0.626	0.371	0.161	2.24	2.75	1.80	2.71
Blandito (gravel)	0.012	1.831	2.473	0.813	0.570	0.666	0.207	2.52	2.89	1.67	2.47
Hipolito (gravel)	0.010	1.875	2.465	0.808	0.579	0.624	0.204	2.38	2.80	1.70	2.45
Anguino (up gravel)	0.021	1.770	2.346	0.679	0.470	0.910	0.411	3.25	3.24	1.62	2.31
Anguino (low gravel)	0.011	1.843	2.383	0.633	0.542	0.592	0.268	2.98	3.52	1.71	2.37
Alcose (gravel)	0.015	2.036	2.368	0.783	0.639	0.179	0.194	2.40	3.15	2.15	2.33

In all samples analyzed the gold was always better sorted than the associated black sand (Table 3). Sorting values ranged from 0.54 to 0.86 for the gold distributions and 0.47 to 0.63 for the black sands. There appears to be no correlation between degree of sorting and gold concentration values.

A relationship between size distributions of gold and black sand-to-gold concentration values was not clearly defined by this data. However, in samples taken from mines where higher gold values were found, the bulk of the gold grains were coarser regardless of whether they were from a sand or a gravel unit (Figure 8). In the rich sample from the Panambisito Mine, 80 percent of the gold by weight was contained in the 0.0 to 2.0 phi size interval. Only 24 percent of the black sand occurred in this size range. By comparison, the Domingo I sample shows much lower weights of gold in coarser sieves (0.0 to 2.0 phi) corresponding to its lower gold values.

Tourtelot and Riley (1973) used sieve-size distributions of gold grains and their host black sands in order to determine their hydraulic equivalence. If the gold and black sands of the Payan terraces were deposited in hydraulic equilibrium, size distribution curves should reflect this. Gold and black sand size distribution curves should plot parallel to each other, with the gold plotting on the fine side of the black sand due to its higher

Figure 8. Size frequency curves showing differences in gold and black sand sizes between high gold value and low gold value samples. Upper graph represents the high value Panambisito Mine sample, lower graph represents the low value Domingo II Mine sample. Dashed lines = gold distributions, solid lines = black sand distributions.

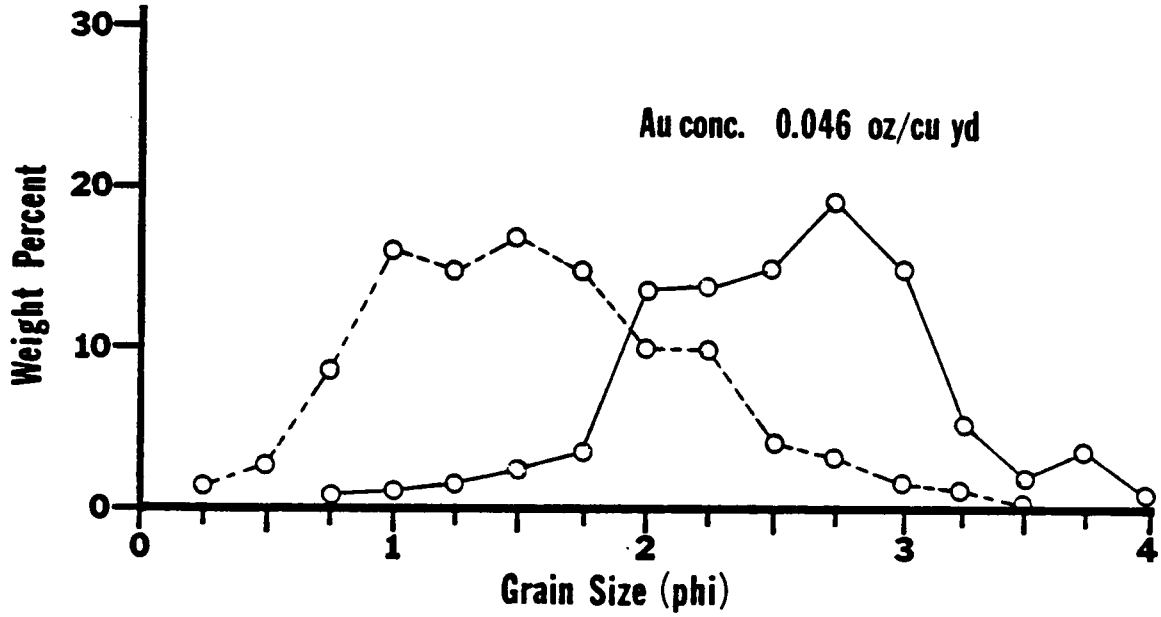
Au conc. 0.046 oz/cu yd
Weight Percent
30
20
10
0
0
1
2
3
4
Grain Size (phi)

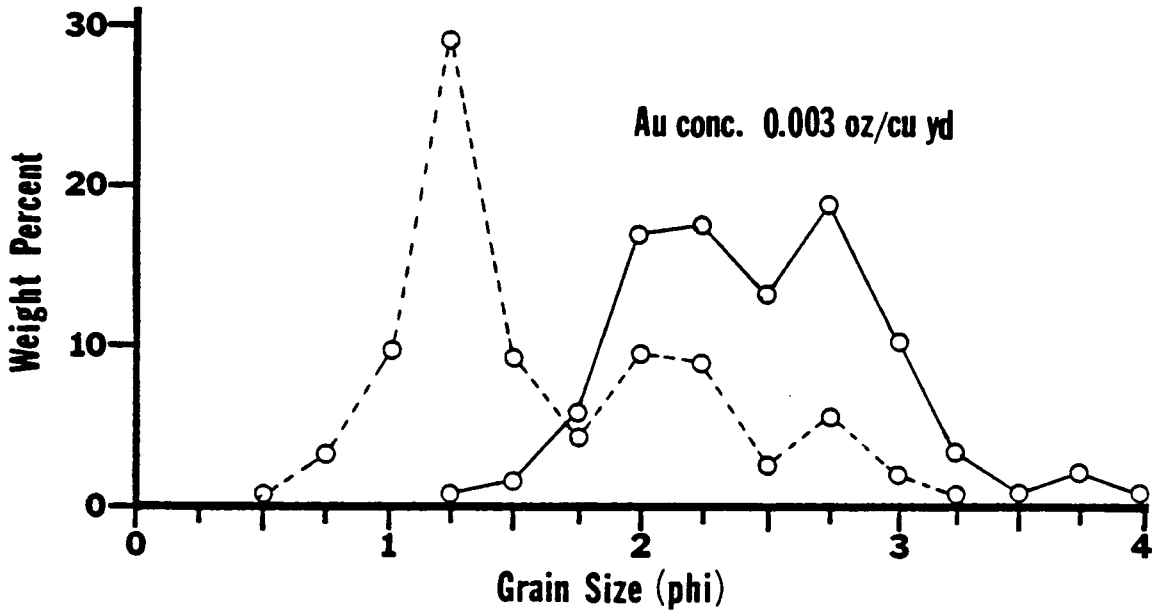
Au conc. 0.003 oz/cu yd
Weight Percent
30
20
10
0
0
1
2
3
4
Grain Size (phi)

density. The general parallelism between the gold and black sand curves generated in this study (Appendix B) indicate a condition of hydraulic equilibrium. On the other hand, the gold grain populations are coarser than the black sand populations, contradicting the findings of Tourtelot (1968) for hydraulically equivalent black sands and gold.

The effect of the shape of detrital grains upon the settling velocity, and thus hydraulic equivalence has been considered by many workers (Heywood, 1933; Wadell, 1936; Krumbien, 1942; Schultz et al., 1954). A primary feature of sediment transport is the settling velocity of grains in water. The velocity necessary to maintain a grain in suspended transport is directly related to the settling velocity of that grain ($W \frac{1}{4} 0.8U*$, where $U*$ is the shear velocity of the flow) (Middleton and Southard, 1977). The same might be true for grains transported along the bed (Rubey, 1933). Therefore the settling velocity alone can be used to examine the behavior of grains of different specific gravities by assuming that the conditions that permitted the deposition of a certain size of quartz grain would also have permitted the deposition of grains having a different specific gravity but with the same settling velocity (Rubey, 1933). For these reasons, shape analyses and settling tube analyses were performed. Shape analysis should help to explain the settling characteristics of gold

grains. Settling tube analyses resulted in direct measurement of settling velocities of gold grains and black sand facilitating more accurate determinations of hydraulic equivalence.

Shape Distributions and Descriptions

Microscopic measurements of several hundred gold grains from several Payan samples were made. A plot of Corey shape factors for the high gold value Panambisito Mine sample shows that the resulting shape distribution is similar to a hyperbolic function (Figure 9). The smaller grains (0.06mm to 0.1mm) approach a Corey shape factor of 1.0 which is a perfect sphere. As the grains increase in size the Corey Factor rapidly decreases to between 0.175 to 0.250 for grains 0.3 millimeters and larger. These larger sizes contain the bulk of the gold by weight. Corey shape factors of this magnitude describe grains that are extremely flakey, having large length to thickness ratios. All of the Payan Mine samples showed the same relationship between Corey shape factor and intermediate axis diameter except the Marta Mine gravel sample. Although the shape to intermediate diameter plot for this sample approximates a hyperbola there is a greater amount of scatter in the larger sizes relative to other samples (Figure 10). The average shape factor for the Marta gravel sample is 2.57

Figure 9. Shape plot of gold grains for Panambisito Mine gravel sample.

Figure 10. Shape plot of gold grains for Marta Mine gravel sample.

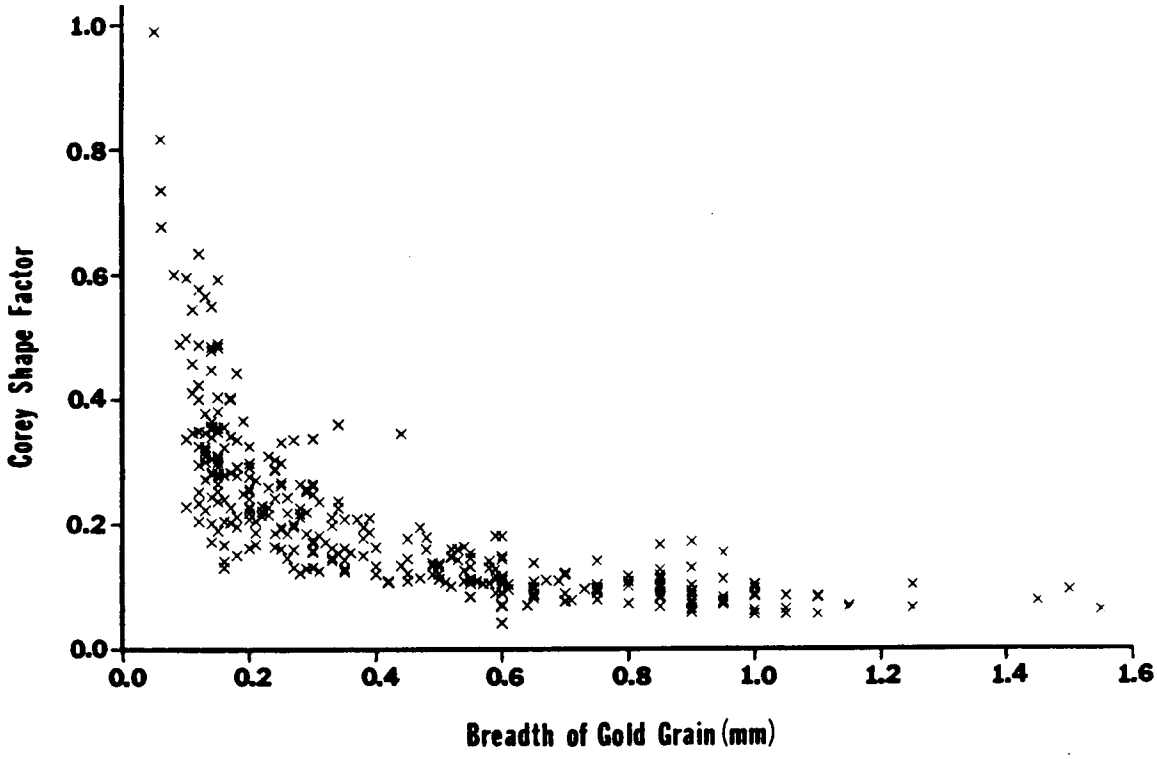
Corey Shape Factor
1.0
0.8
0.6
0.4
0.2
0.0
0.0
0.2
0.4
0.6
0.8
1.0
1.2
1.4
1.6
Breadth of Gold Grain (mm)

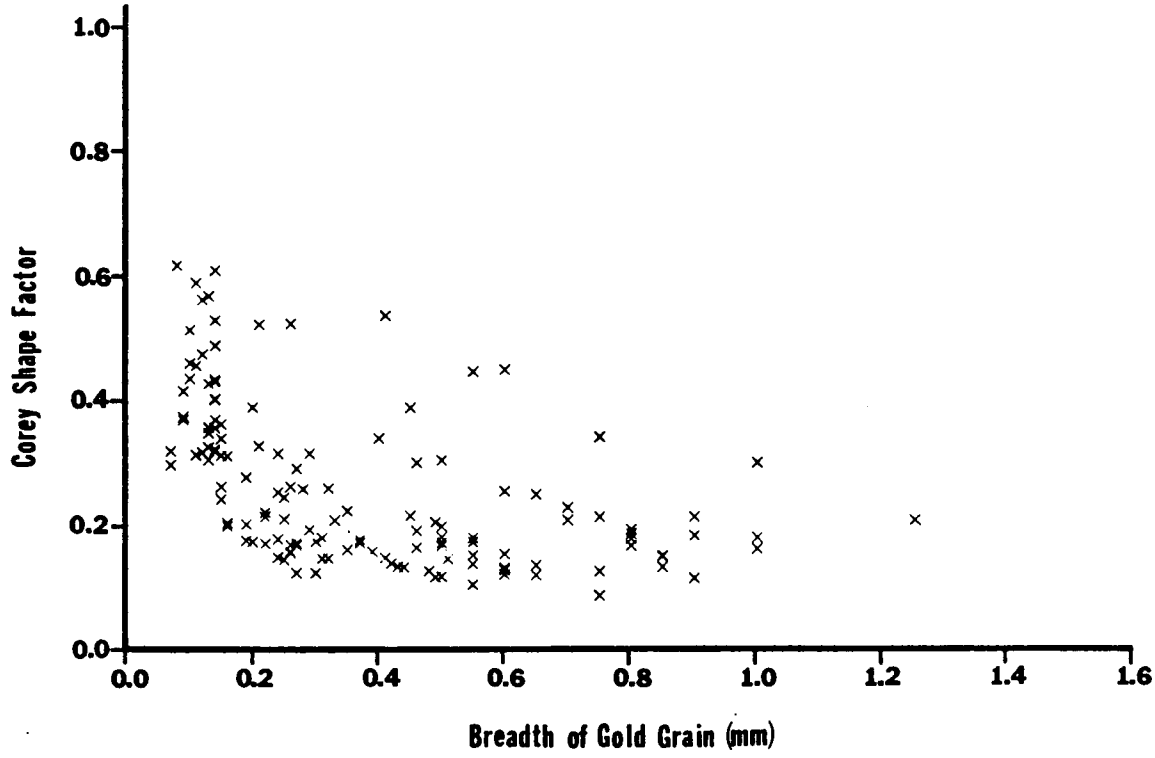
Corey Shape Factor
1.0
0.8
0.6
0.4
0.2
0.0
0.0
0.2
0.4
0.6
0.8
1.0
1.2
1.4
1.6
Breadth of Gold Grain (mm)

compared to a smaller average factor of 1.75 in all other samples analyzed. This difference could be significant as the Marta gravel sample had the second highest measured gold concentration value.

Another important finding resulting from this shape analysis as relates to the transportation and deposition of gold grains is the extreme flakiness of the majority of the gold particles. Tourtelot (1968) studied the fall velocity of gold grains of different shapes. He determined that a flake of gold with a diameter/thickness ratio of 30 settles at a velocity of only 12.5 percent of a gold sphere of the same diameter.

Settling Tube Analysis

Five samples contained enough gold to conduct settling tube studies (RSA). This type of analysis allowed direct measurement of the settling velocity of gold grains and their associated black sands. Cumulative size frequency curves were generated by converting settling velocities of the flakey gold grains and the black sands to diameters of quartz spheres with equivalent fall velocities (Appendix D). This accounted for the effects of shape on the size distribution and facilitated a more efficient comparison of the two mineral populations in terms of hydraulic equivalence.

The results were different than expected. In all five samples tested the gold distributions were coarser than the black sand distributions, even though grain sizes were based on actual settling velocities (Figure 11). After comparing the size distributions generated from mechanical sieve analysis to those based on fall-equivalent quartz spheres, it is apparent that the mean size of Payan gold actually is hydraulically coarser than its associated black sand. In fact, the effective settling size difference between gold and black sand was found to be greater than the difference measured by sieve analysis. For example, the difference in median size between gold and black sand in the Marta gravel sample is 1.43 phi based on settling velocities, while the difference based on sieving was 0.73 phi (Figure 12).

As discussed earlier the gold was found to be better sorted than the black sand. Settling tube analyses have shown the gold to be even better sorted than the sieve results showed (Figure 12), while the black sand fraction was more poorly sorted based on settling relative to sieve data. Gold grains become more spherical with decrease in grain size, however the black sands showed very little change in shape with a decrease in size. Therefore settling velocities increase relative to intermediate axis diameter; thus gold grain sizes based on settling velocites are larger for the smaller more spherical grains, giving

Figure 11. Cumulative size frequency curve for gold and black sands (Panambisito Gravel Sample) based on settling sizes (RSA). Dashed lines = gold grains, solid lines = black sands.

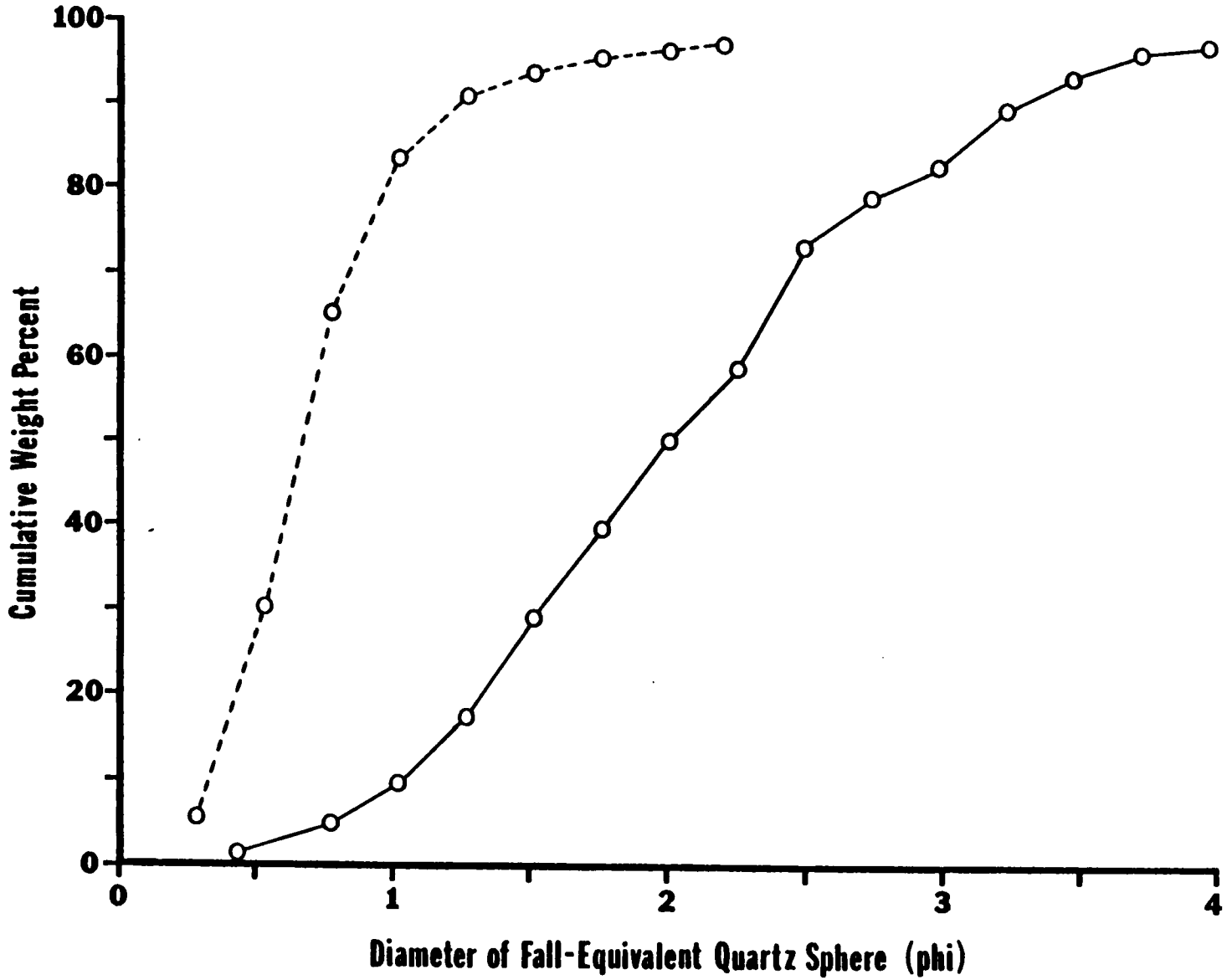
100
80
60
40
20
0
Cumulative Weight Percent
0
1
2
3
4
Diameter of Fall-Equivalent Quartz Sphere (phi)

Figure 12. Comparison of size distributions based on sieve analysis to those generated by RSA analysis for the Panambisito gravel sample. Upper graph shows sieve sizes, lower graph shows settling sizes. Dashed lines = gold, solid lines = black sands.

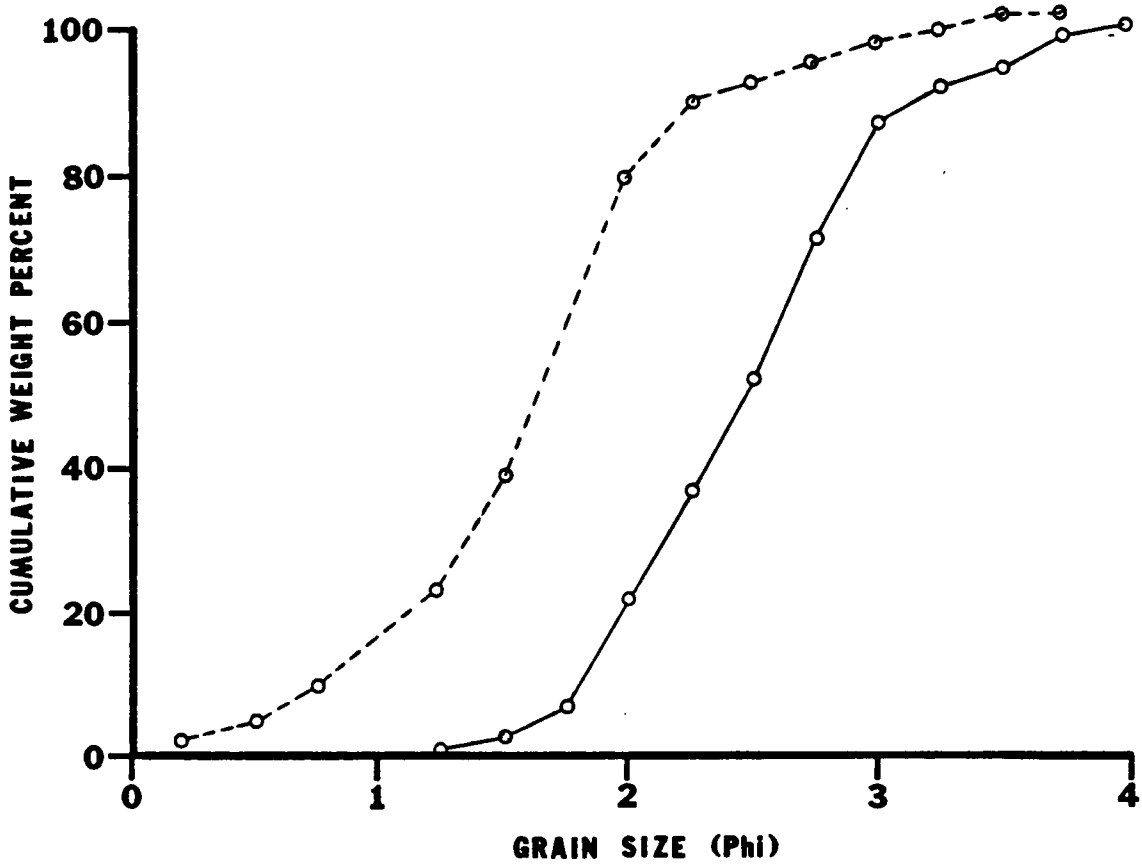
100
80
60
40
20
0
CUMULATIVE WEIGHT PERCENT
0
1
2
3
4
GRAIN SIZE (Phi)

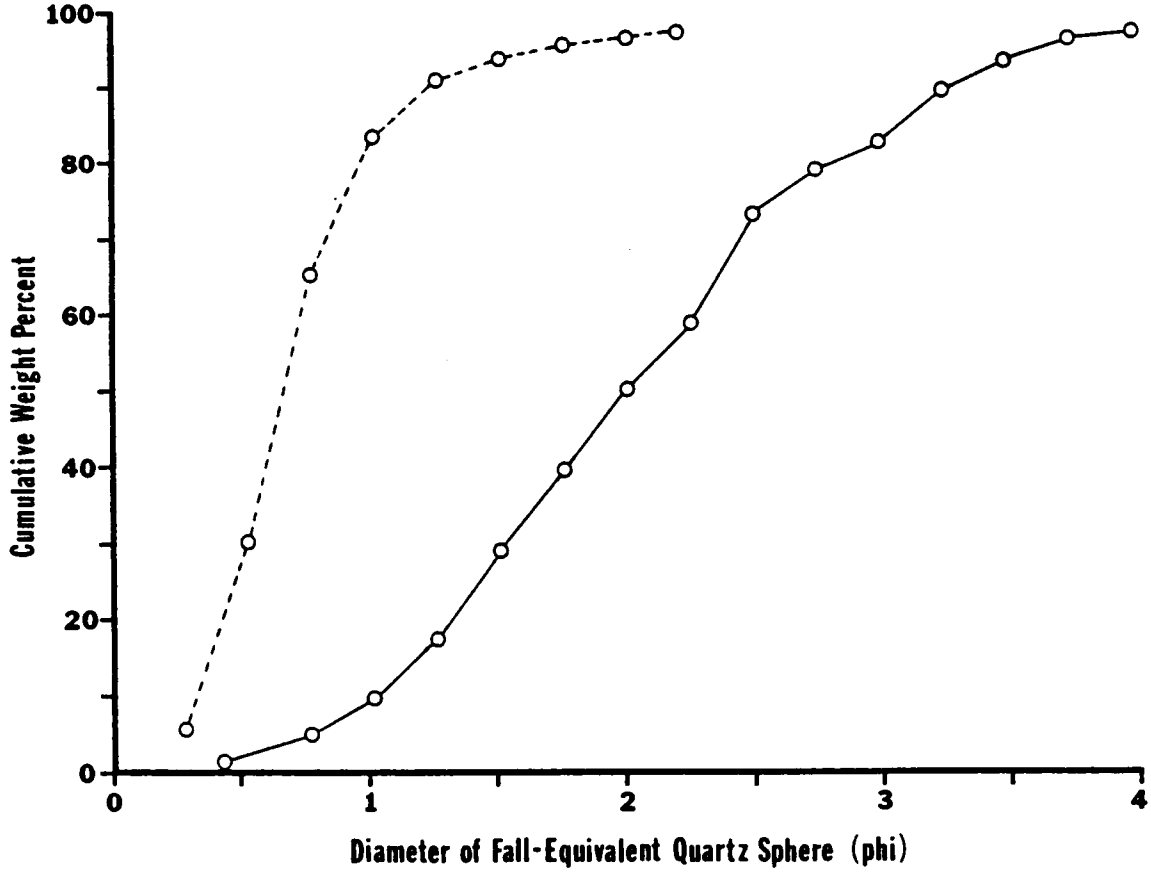
100
80
60
40
20
0
Cumulative Weight Percent
0
1
2
3
4
Diameter of Fall-Equivalent Quartz Sphere (phi)

the appearance of a better sorted population.

Surface Texture of Gold Grains

Scanning Electron Microscopy (SEM) revealed several interesting textural and morphological features, although none of these characteristics were indicative of a particular formation or lithologic unit (sand or gravel). In other words, the gold grains in all samples, regardless of their host formation or lithology, showed the same set of textural and morphological features.

The gold contained in the sands and gravels in the Payan Mining District can be divided into two main groups according to the morphology of gold grains with characteristics that are somewhat genetic but dominantly acquired during transport. The first type which accounts for less than 10 percent of the total gold is here referred to as crystalline gold. This type, although detrital in nature, is most characterized by a preservation of at least part of its original crystalline structure (Figure 13a-c). The parallel lines visible on the flat surfaces of these grains are a reflection of the crystalline nature of the primary gold which crystallized in the source rocks (Halbauer and Utter, 1977). Other characteristics observed for this gold type include irregular shapes, angular proturbances, jagged edges, and occasional bent and

Figure 13. Scanning Electron Photomicrograph of crystalline type gold grains. Scale is indicated at the top of each photograph. (A) Parallel lineations reflecting primary crystalline structure and angular and jagged edges which indicate a short distance of transport. (B) Shingle-like structure is visible. (C) This gold particle shows the initial formation of a bent and hammered edge. The outer surface of this edge (see zoom magnification) is begining to acquire the dough-like micro texture that is common in the highly deformed gold type (Figure 14).


10KV WD 6MM

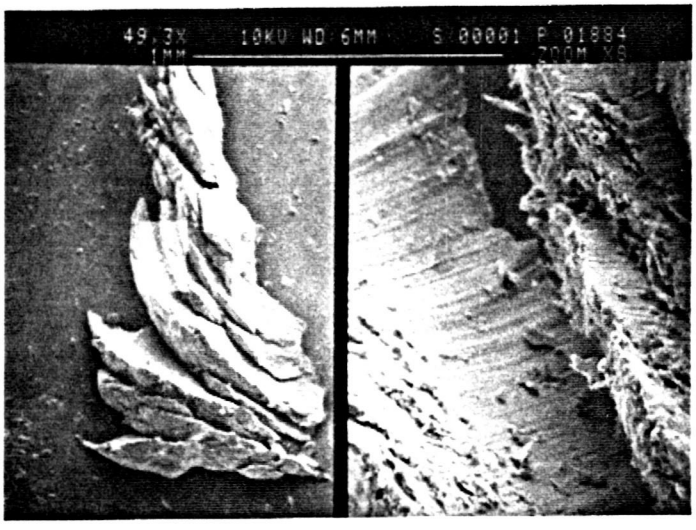
49.3X
1MM
10KV WD 6MM
S 00001 P 01884
ZOOM X8

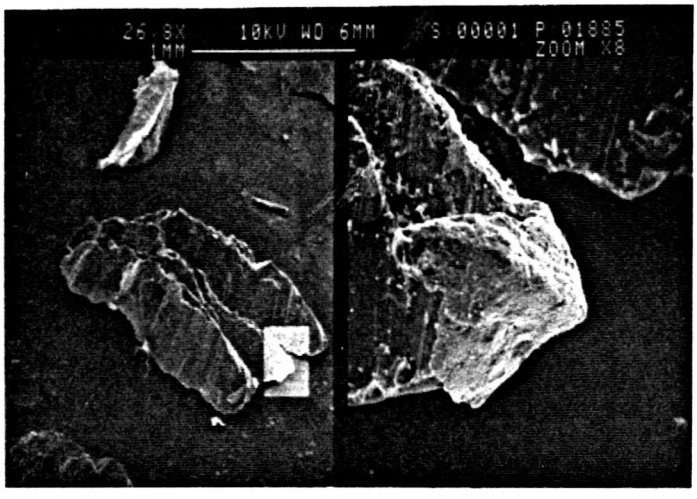
26.8X
1MM
10KV WD 6MM
S 00001 P 01885
ZOOM X8

hammered edges (Figure 13c). Many grains of this type exhibit a shingled appearance (Figure 13b) which is probably due to crystalization or slippage along weaker crystal plains. Each layer or shingle is delicately connected to its adjacent shingle.

The second morphological type represents the majority of the gold found in the Payan placer deposits and generally accounts for more than 90 percent of the gold by weight. This type of gold does not show signs of primary crystalline structure and is here referred to as highly deformed gold (Figure 14a-c). The most characteristic features of this gold type are its well-rounded flakiness and lack of jagged edges and angular proturbances. The shapes of this gold type range from near perfect disks (Figure 14a) to more elongate irregular flakes (Figure 14c). Bent and hammered edges are common. The degree of bending and hammering varies from single proturbances which were folded to meet the main body of the grain and doubly folded or refolded edges (Figure 14b) to grains that suffered continual bending and hammering to the point where only the plastic flow lines that resulted from this action are discernable (Figure 14a). The gold particles of this type have a general dough-like texture with numerous randomly oriented scratches and crater-like depressions (Figure 14b).

The outer surface of the bent and hammered edge of the

Figure 14. Scanning Electron Photomicrographs of the highly deformed type of gold grains. Scale is indicated at the top of each photograph. (A) Detrital gold particle which has suffered continuous bending and hammering resulting in its well-rounded platy shape. The plastic flow lines from folded and refolded edges can be seen. (B) Detrital gold particle showing randomly oriented scratches and crater-like depressions. (C) Gold particles illustrating how bending and folding of edges results in the well-rounded shape shown in photograph A.

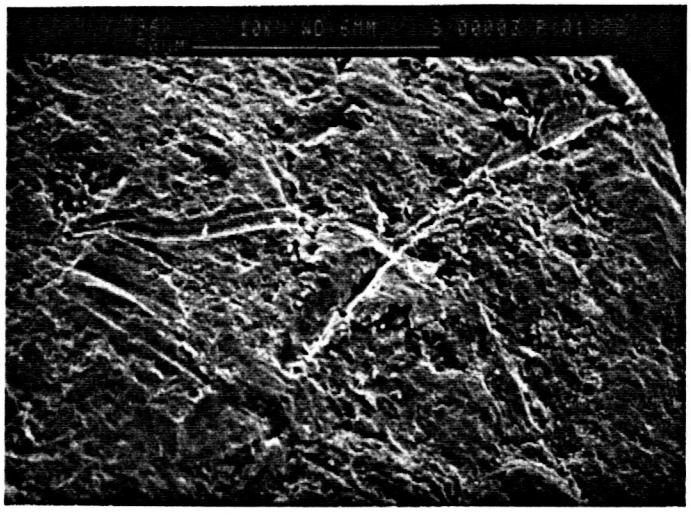

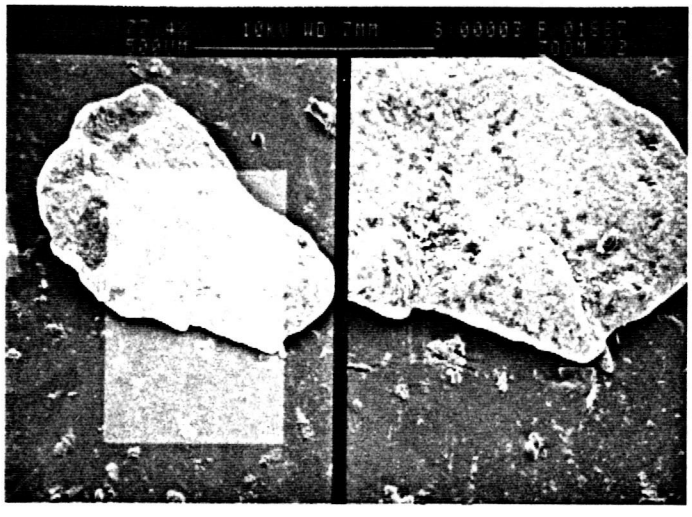

crystaline type grain in Figure 13c appears to be developing the dough-like surface texture that is common in the highly deformed gold type. This suggests that with increased transport and abrasion the crystaline type gold would eventually aquire the characteristics of the highly deformed type gold. Thus, the morphological characteristics observed in these two types is probably related genetically to the amount of fluvial transport and abrasion imposed on each grain. Hallbauer and Utter (1977) observed similar characteristics on gold grains in their study of the paleo-placers of the Witwatersrand, South Africa.

CHAPTER 4

DISCUSSION OF RESULTS

One of the main objectives of this research was to use size analyses of the gold grains and their associated black sands in order to determine if these mineral populations were deposited in hydraulic equilibrium. The concept of hydraulic equivalence and the associated data on settling velocities have important applications to placer exploration. For example, if the gold is deposited in hydraulic equalibrium with the black sand, then depositional conditions such as this might be related to a given black sand texture or depositional environment within the paleo-fan. That is, sand bars, sieve deposits, etc. might be related to higher gold concentrations.

Hydraulic Equivalence of Gold and Black Sands

Tourtelot and Riley (1977) used size distributions, based on sieve data, of gold and black sand grains to determine if the two populations were deposited in hydraulic equilibrium. Their results showed that the general parallelism between cumulative size curves of

the gold and black sands in their samples, combined with the fact that the median size of the denser gold was finer than that of the black sand, indicated that the two materials were in virtual hydraulic equilibrium. The difference in median size between gold and black sand size distributions was greater in some samples than in others. Tourtelot and Riley were able to account for this difference by calculating the Corey shape factor for the gold grains. Tourtelot (1968) determined that a Corey shape factor of 0.3 reduced the settling velocity of a quartz sphere (0.2 mm in diameter) from 25.8 mm/sec to 18.6 mm/sec at 24°C, a reduction of 28 percent.

As mentioned earlier, the cumulative size curves (sieve analysis) for the gold and black sands in my study showed surprising results (Appendix B). The median size of the gold distributions was always coarser than the median size for the black sands despite the much higher density of gold. This relationship has not been discussed in the published literature, and suggests an extreme deviation from hydraulic equivalence. Since these size distributions were based on sieve sizes and not hydraulic equivalent settling sizes, there is a possibility that the shape of the gold grains could account for this deviation. For this reason Corey shape factors were calculated for gold grain populations (Appendix C). Results showed that the gold grains were extremely flakey and only grains less than 3

phi in diameter approach sphericity. These relationships are probably not sufficient to account for the difference between median sizes of the gold and black sand populations in this study (Figure 15). Consequently, since the effect of shape on settling velocity is not clearly understood, a direct measurement of settling velocites (RSA) was employed. Translating gold and black sand settling velocities to fall equivalent quartz sphere sizes would be more diagnostic for determinations of hydraulic equivalence. The results of RSA analyses confirmed that the gold populations are indeed coarser than their associated black sand populations and, thus, these two populations are not hydraulically equivalent.

Could this mean that the gold in the Payan terrace deposits was not deposited under the same hydraulic conditions as the associated black sands? Previous explanations for deviations in hydraulic equivalence have followed two lines of reasoning: (1) hydraulic inequivalence is the result of differentially inherited size restrictions from the source rocks, or (2) hydraulic inequivalence is the result of differential transport of various minerals (Rittenhouse, 1943; Shanov, 1964; Briggs, 1965). However, subsequent work by Lowright et al. (1972) has shown that differential transport and not source restrictions better explain deviations from hydraulic equivalence. Von Engelhart (1940) determined from 14

Figure 15. Relationship among Corey shape factor, sieve diameter, and standard settling diameter. (From American Society of Civil Engineers, 1962).

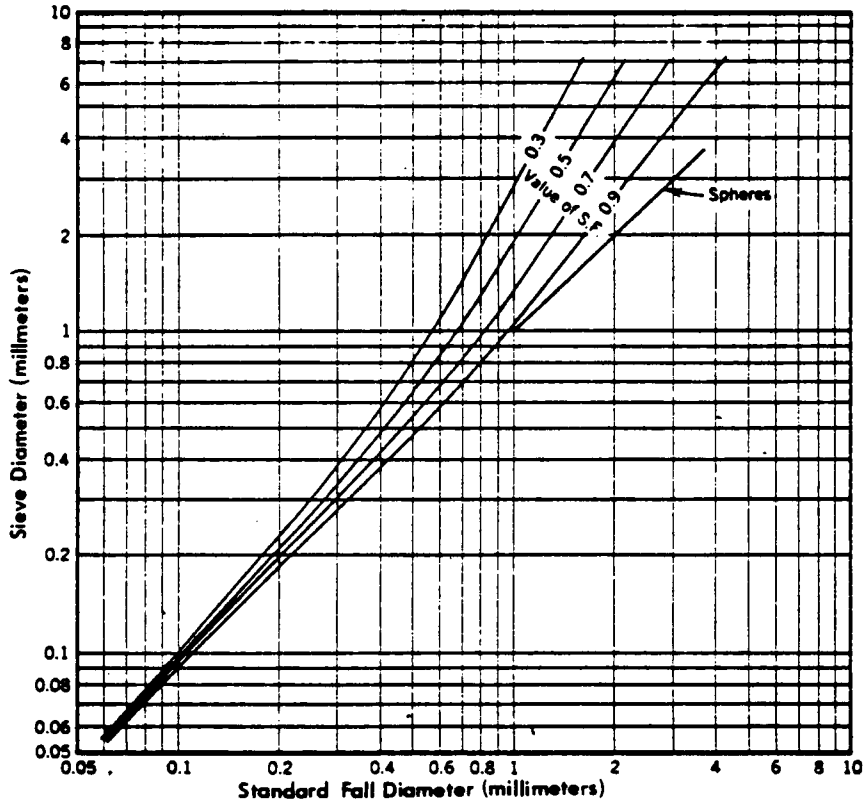
Sieve Diameter (millimeters)
Standard Fall Diameter (millimeters)
Value of S_F
0.3
0.5
0.7
0.9
Spheres
10
8
6
4
2
1
0.8
0.6
0.4
0.2
0.1
0.08
0.06
0.05
0.05
0.1
0.2
0.4
0.6
0.8
1
2
4
6
8
10

modern dune and beach sands that size distributions were explainable by a "process model" and that the influence of source grain size restrictions was slight. He also demonstrated that hydraulically equivalent quartz and magnetite in suspensison would be different from hydraulic equivalent materials that were transported by rolling. Hand (1967) extended this idea to explain why heavy minerals in quartz laminae on three New Jersey beaches had lower settling velocities than than those of the associated quartz predicted for hydraulic equalibrium. He concluded that because the heavy minerals were smaller than the light minerals they would be shielded by the larger grains and also not protrude into zones of higher velocity in the flow. Thus the larger light grains would be preferentially removed. Grigg and Rathbun (1969) also showed that grains which settle together will not necessarily be entrained together.

Thus, deviations from hydraulic equivalence of light and heavy minerals have been interpreted as due to differential entrainment. Slingerland (1984) discussed the role of differential entrainment in the formation of fluvial placers. The results of his work have a direct application for explaining the occurance of Payan gold in sizes larger than those of the associated black sand. Slingerland observed that flows commonly enrich deposits by entraining or depositing size fractions of the original

deposit such that the heavy minerals become more nearly the same size or larger than the light minerals. This conclusion was based on his observations of the swashface on Assateaque Beach, Virginia. Here the processes of transportation, deposition, and reentrainment occur over each swash advance and retreat, simulating the longer term flow variability in streams. Samples of the upper grain layers taken at the time of maximum swash advance and maximum retreat show a trend of increasing heavy mineral percent with increasing mean heavy-to-light size ratios. This was explained to be the result of alternately settling grains of heavy and light minerals and preferential reentrainment of only the larger light grains (quartz). By analogy, differential entrainment was probably a significant factor in creating the size relationships observed between gold and black sand in the Payan terrace deposits.

Results of shape analysis also support this hypothesis of differential entrainment for gold accumulation in the Payan area. Although flakey grains are more easily transported relative to similar sizes of spherical grains with similar densities, the flakes are more difficult to entrain once deposited. Middleton and Southard (1978) considered the case of a thin plate inclined at an angle to the downstream direction. Such a plate is theoretically similar to a flakey grain. The resultant pressure force in

this case is directed downstream and towards the bed. In general therefore, the flow tends to press the imbricated flat grains down onto the bed, rather than lifting them off as it does most other grains (Figure 16). Consequently, flat flakey gold grains found in the Payan deposits should be more difficult to dislodge than the larger more spherical grains of magnetite.

Results of this research, interpreted in light of previous work, indicates entrainment sorting was a major process responsible for the concentration of placer gold, as well as the ultimate size distributions of Payan gold and black sand populations. Entrainment sorting seems to best explain the deviation from hydraulic equivalence found between the gold grains and their associated heavy minerals contained in the sands and gravels of the Payan terrace deposits. The flakey shape of heavy minerals such as gold has been shown to enhance the effects of entrainment sorting (Middleton and Southard, 1978).

Although entrainment sorting has recieved much attention in the published literature (Sundborg, 1968; Brady and Jobson, 1973; Grigg and Rathbun, 1969; Ljunggren and Sunborg, 1958; Saks and Gavshina, 1976) it only explains the characteristics of lag deposits. Transport sorting, defined as the fractionation of grains due to differential transport (Slingerland, 1984) must also be considered in terms of the depositional origin of the Payan

Figure 16. Flow patterns and hypothetical pressure distributions for plates and spheres: (a) flow pattern and pressure distribution for plates similar to gold grains (b) flow pattern and pressure distribution for spheres similar to magnetite grains (from Middleton and Southard, 1978)

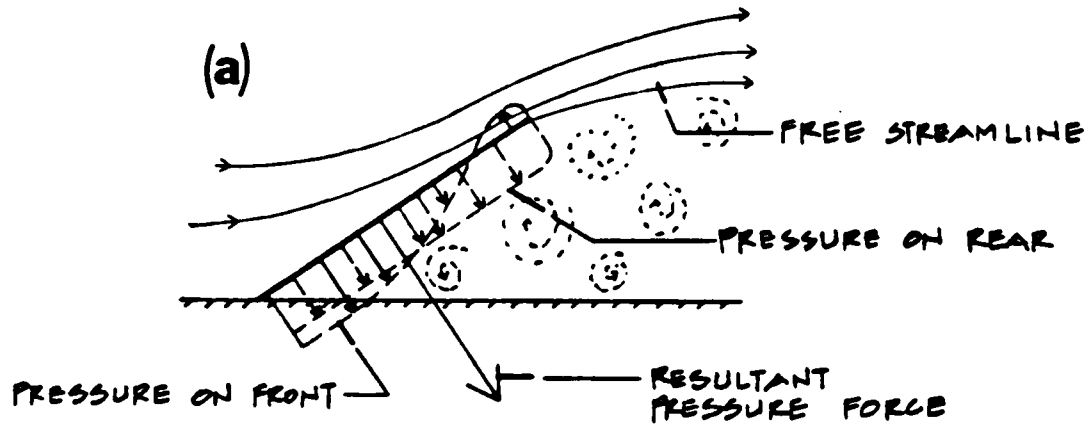
(a)
FREE STREAMLINE
PRESSURE ON REAR
PRESSURE ON FRONT
RESULTANT
PRESSURE FORCE

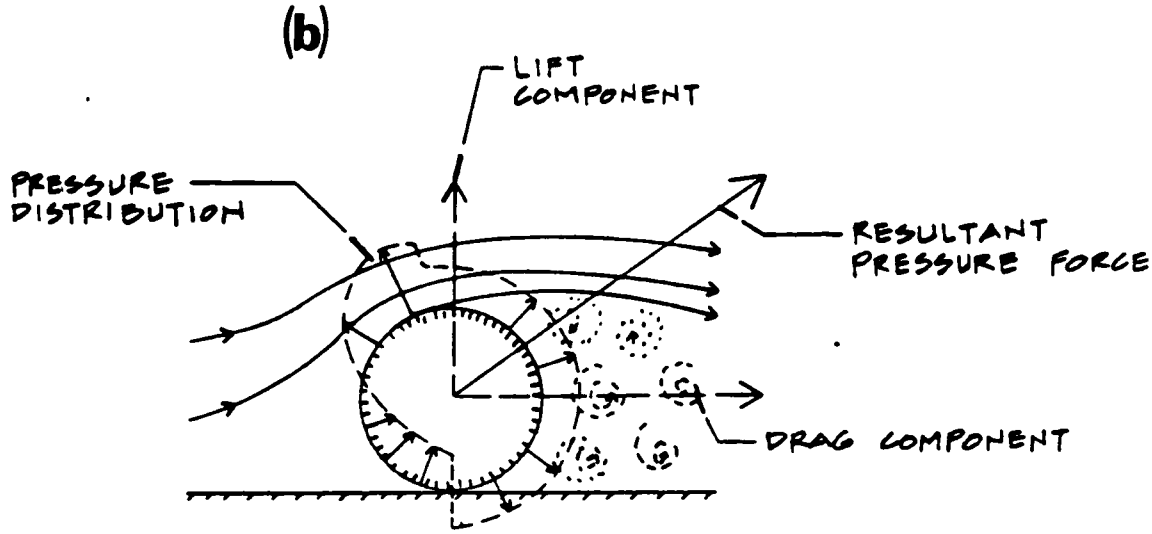
(b)
LIFT
COMPONENT
PRESSURE
DISTRIBUTION
RESULTANT
PRESSURE FORCE
DRAG COMPONENT

placers. Differential transport is defined here as differences between the unit sediment transport rates of black sands and gold grains. Since these differences are due to varations in the probability of entrainment as well as the mean velocity of a grain already moving in the flow, transport sorting includes entrainment sorting and sorting by differential settling velocities.

Slingerland (1984) used the Einstein bed load function to calculate the transport rates of quartz and magnetite under conditions of interest. He choose this equation because it accounts for smaller grains hiding among larger grains. Slingerland's flume experiments demonstrated stream energy slope and bottom roughness are the major variables that determine total unit transport rates and the ultimate enrichment of magnetite with respect to quartz. He calculated quartz and magnetite transport rates for different energy slopes (0.001, 0.01, 0.1) and bed roughness values. Results showed that for any one energy slope, the transport rates for all sizes of gold and magnetite in the initial distribution decrease with increasing bed roughness due to the hiding factor determined by the roughness elements. Therefore the mean size of the lag deposit increased. The opposite is true for increasing the energy slope at any one roughness. Slingerland's data showed that there is a point where roughness and stream energy slope are optimum for maximum

enrichment of magnetite to occur. At a stream energy slope of 0.01 and a bed roughness of 5 millimeters, no magnetite was transported, only quartz was entrained. Some of the smaller grains of quartz might be left as lag because they are hidden by magnetite grains. Maximum enrichment occured at this point and the mean size of the magnetite became larger than the mean size of the quartz. From this flume experiment, Slingerland concluded that it is reasonable for a band of placer enrichment to form at a certain position perpendicular to the regional slope on an alluvial fan system, where bed roughness and stream energy slope are conducive for maximum transport fractionation to occur.

Although these flume observations compared populations of quartz and magnetite with specific gravities of 2.65 and 5.18 respectively, the same relationships should apply when comparing magnetite to gold (sg.=15.0-19.3). In fact, owing to the greater density difference, hydrauluc responses should be even more pronounced.

Darby and Whittecar (1985) were able to calculate the paleo-fan slope of the Antigua Formation sediments in the Payan Mining District, based on elevations of unweathered gravel/volcanic ash contacts (Figure 17). Apparently the ash buried an active depositional surface. The calculated slope of 0.01 is similar to that described by Slingerland for maximum enrichment to occur.

Figure 17. Paleo-fan slope of Payan area based on elevations of gravel-ash contacts. Sites marked with an "e" are exposures where the top of the gravel has been eroded by post-fan stream incision (after Darby and Whittecar, 1985).

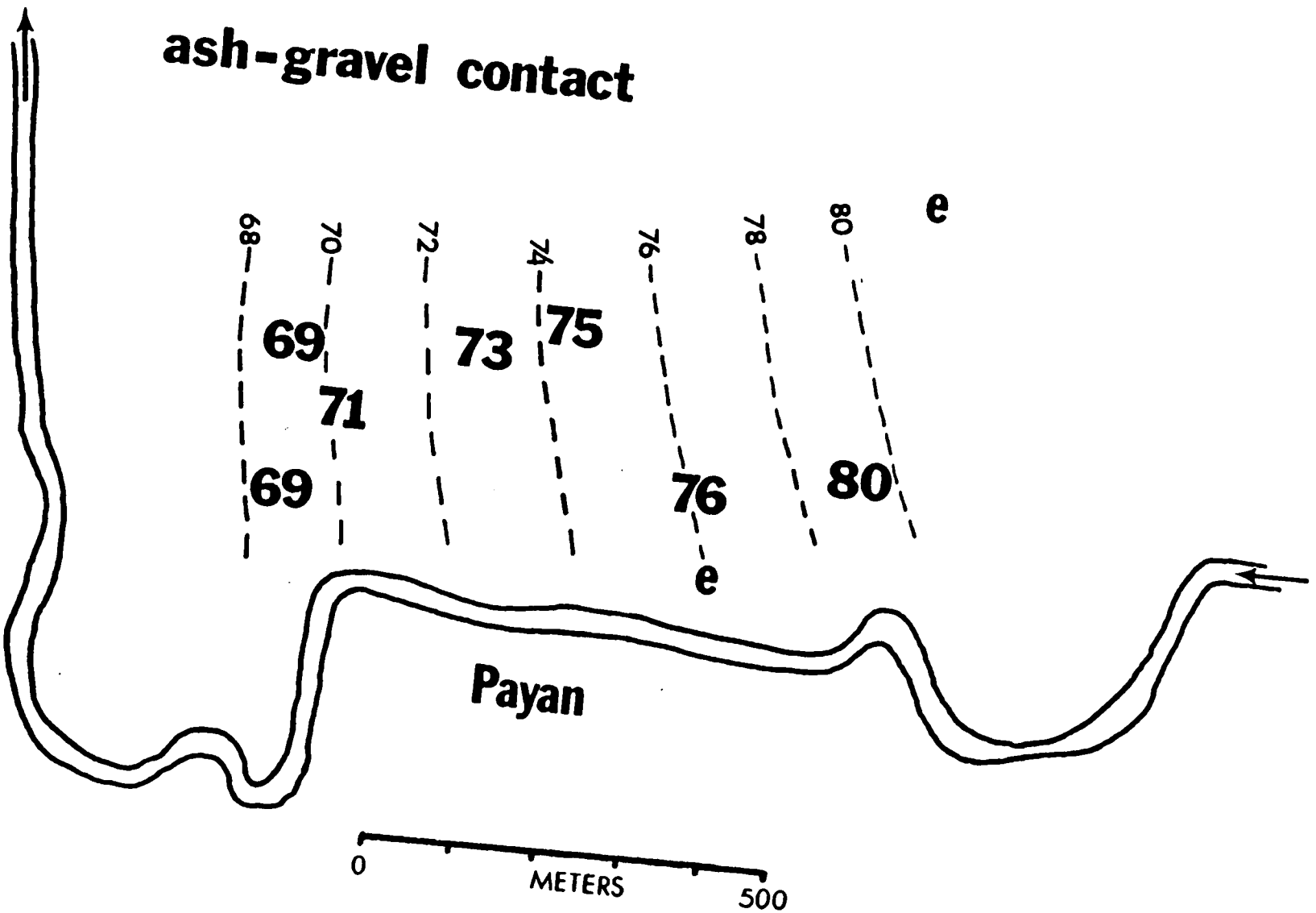
ash-gravel contact
68
70
72
74
76
78
80
e
69
71
69
73
75
76
e
80
Payan
0
METERS
500

The fact that the mean gold size in all samples was coarser than the mean size of magnetite (Appendix B and D), implies that conditions in the Payan area were favorable for high gold enrichment. Samples analyzed in this study also showed a general increase in the mean size of the gold with higher gold concentration values (Table 2) which is consistent with the above findings. The flakey shape of most of the Payan gold grains also enhances the effects of transport sorting. These grains are as easily transported as larger spherical magnetite grains, especially in turbulent flows (Willmarth, 1964). This would allow both larger flakes and smaller spheres of gold to be deposited with even larger magnetite grains. Because these magnetite grains protrude into the flow, they are quickly re-entrained leaving the gold behind. At lower flow velocities, smaller magnetite is deposited with the gold thus explaining the anomalous size relationship between gold and magnetite (Figure 18).

Several lines of evidence have been presented to explain the deviations from hydraulic equivalance observed between gold and black sand in the Payan Mining District. Hydraulic equivalance and theoretical sorting mechanisms probably cannot fully explain the origin of the Payan placer deposits, because of local variations of stream geometry or input from tributaries. Nevertheless, the concept of hydraulic equivalance is important to the

Figure 18. The effects of the entrainment sorting process under waning flood conditions. U arrows indicate direction and magnitude of stream flow. Oval shapes are gold grains, solid circles are magnetite grains, and circles with an X are quartz grains. Facing arrows delineate the boundary layer (δ). The first case (1) represents conditions during high flow velocities. Small magnetite and quartz grains are carried in suspension. All gold grains are deposited due to their high specfic gravity. Large magnetite grains and even larger (hydraulically equivalent) quartz grains are deposited, however, they protrude above the boundary layer and are quickly re-entrained and carried in suspension or by saltation further downstream, thereby increasing the mean size ratio of gold to black sand. The second case (2) represents lower flow conditions. All of the gold has already been deposited and its flakey shape acts to hold it to the bed. Medium sized magnetite and quartz grains are now deposited and those which protrude above the now larger boundry layer are re-entrained and carried downstream. During lowest flow velocities, case (3), large grains are no longer being transported. Small magnetite and quartz are deposited with the larger gold grains and are not re-entrained because of the decreased velocity of the flow. This results in a final lag deposit in which the mean size of gold is ½ the mean size of quartz, which is ½ the mean size of magnetite.

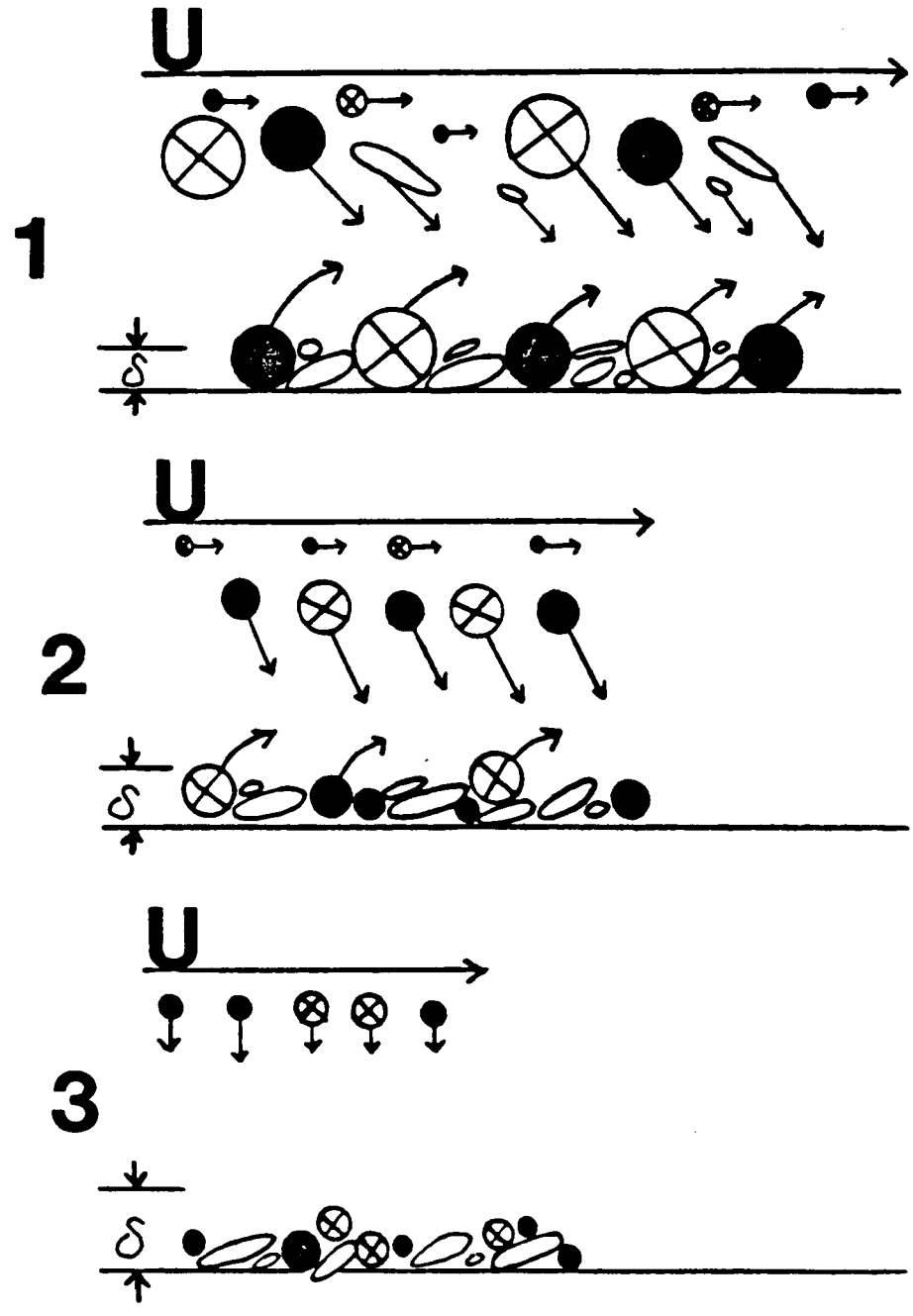
U
1
δ
U
2
δ
U
3
δ

dynamic processes which formed these auriferous deposits.

Proposed Depositional Processes and History

Climate must have been a major factor controlling the local deposition and concentration of the auriferous sands and gravels in the Payan Mining District. Most previous studies have involved placer deposits in arid to semi-arid alluvial fans. Nicholas (1897) was the first to recognize the peculiarities of tropical auriferous gravels deposited at the base of alluvial fans subject to intense rainfall and flooding. Nicholas examined several placer deposits in the Pacific Lowlands of central Colombia just north of the present study area. As in the Payan area, he found large vertical and lateral variations of gold concentration in the same horizon within a small area. Nicholas attributed these extremely localized concentrations of gold to excessive floods and heavy rains which caused local mass movements in the gravel deposit. These local movements juxtaposed gravels of different values and they were not always apparent in outcrop. He further postulated that the rains continuing after a flood had subsided were sufficient to cause local erosion and winnowing that was much different from that which took place under lower flow conditions prior to the flood. This winnowing resembles the action of waves on a beach sand, resulting in modified

concentrations of gold.

Flooding most likely was also an important process controlling gold deposition in the Payan terrace gravels. Assuming that the gold-bearing sandy matrix was not deposited under the same hydraulic conditions as the larger pebbles and cobbles, a flood event most likely deposited the open-fabric gravel bars typical of the Payan area. As the flood subsided and during subsequent lower flow conditions, sand-sized material was deposited and kinetically sieved down into the open-fabric gravel. During the early phases of this matrix infilling, transport sorting was the dominant proccess controlling the deposited size distributions of the gold and black sand. The flakey shape of the gold grains, which served to increase their transportability, allowed longer suspension transport and thus deposition with finer black sand grains despite the large difference in density. In the early infilling stage, entrainment sorting and reconcentration of gold had little effect on the deposited size distributions of gold and magnetite, because as the deposited grains settled within the bed roughness elements they probably vibrated into the open-fabric gravel and were shielded from the flow. Therefore, high gold concentrations would not be expected at this stage. However, as matrix infilling continued to the surface of the gravel bar, conditions became more favorable for concentration of gold. This is because the

matrix had now reached a level from which it was susceptible to reworking and entrainment sorting by the flow (Schumm, 1977). Based on Slingerland's work, there should be a stage when this matrix infilling process changes the bed roughness with respect to the flow velocity and paleo-slope for maximum placer enrichment to occur.

After this relatively thin zone of high gold concentration had formed atop a flood deposited gravel, two situations were possible: (1) low or fluctuating flow conditions may continue, resulting in continued deposition of sand-sized material or (2) a successive flood event could deposit another layer of open-fabric gravels before lower flow conditions allowed the accumulation of a sand layer. Under the first possibility, additional reworking and entrainment sorting might further enrich the deposit tending to increase the mean size of the gold relative to the black sands. Results of size analysis have shown gold to be better sorted towards the coarse end in samples where gold concentration values were relatively high. This sequence of events is postulated as being responsible for the highest gold concentrations found in the Payan area. That is, hydraulic conditions were optimum for gold enrichment in the Payan sands and gravels just above and below the contact of a matrix filled gravel and its overlying sand unit (Figure 19). Gold concentration values

Figure 19. Gold concentration across gravel-sand contact (after Darby and Whittecar, 1985).

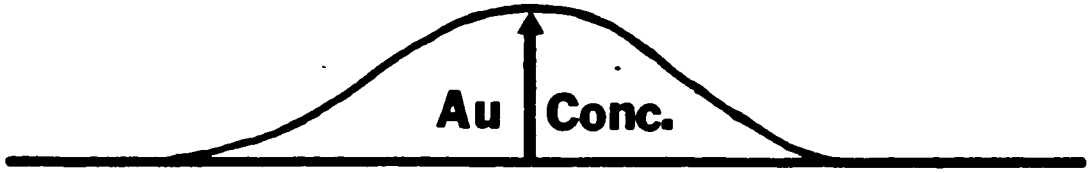
Au
Conc.

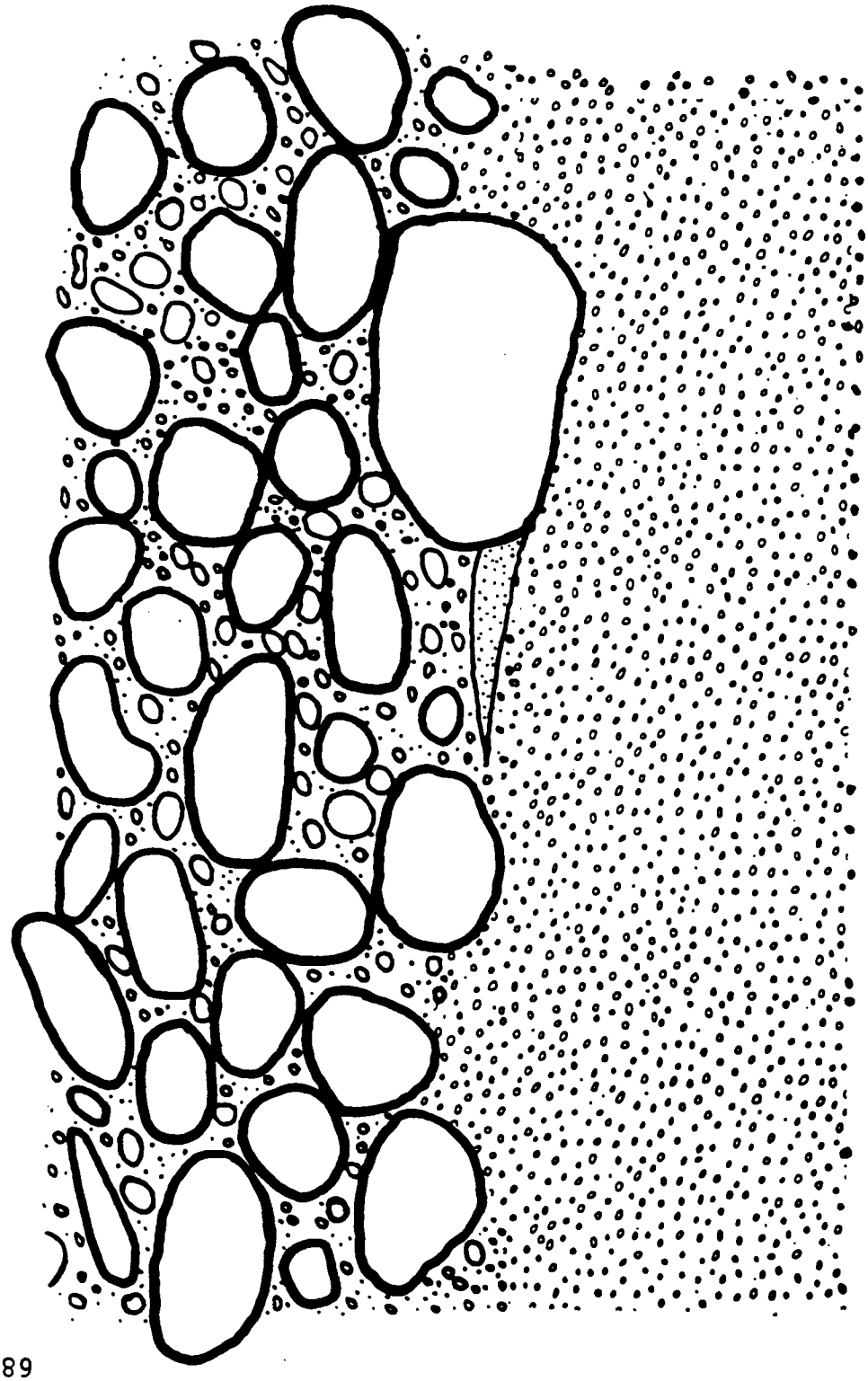

generally support this hypothesis (Table 2 and Appendix A). However, it should be noted that although hydraulic conditions are optimum for gold enrichment, small scale local conditions such as channel morphology or obstructions may cause variations in the distribution and concentration of gold within short distances.

In the second case of further gravel deposition without a sand layer, two flood events might result in a seemingly uninterrupted vertical sequece of gravel. Such events account for the thick sequence of gravels observed in the Payan area. Depending on how much matrix infilling occured between flood events, a relatively high zone of gold concentration is possible between the gravels associated with each event. However, this zone should not be as rich as the one formed in the first case, where entrainment sorting can work longer and the preservation potential is higher than in the case of another flood event. A second flood event shortly after the first might wash away part or all of a previously concentrated enriched zone. Such erosion could occur in case one, where the sand might be even more susceptable to erosion.

To summarize, two types of stratigraphic zones of relatively high placer concentration occur in the Payan Mining District. The formation of these zones is controlled by paleo-flood events and periods of lower flow between these events. The most important of these zones

occurs when sustained lower flow conditions allow complete matrix infilling of a flood-deposited gravel, eventually leading to the deposition of a sand layer. A more minor zone of high gold concentration is likely to be preserved between succesive flood gravels which undergo some winnowing but no sand layer is deposited. Measured gold values in stratigraphic sequences indicate that these major and minor placer concentration processes occurred periodically at many locations studied within the Payan area.

Modes of Placer Gold Occurence

Gold concentration processes in the Payan Mining District operated on three scales. The ultimate richness of any particular location was determined by the combined effects of fluvial processes operating on the drainage system planimetric scale (10^4 m), the bar scale (10^2 m) and the generally discontinuous bed scale (≤1 m).

Placer concentration processes associated with the drainage system scale have been discussed by several authors (McGowen and Groat, 1971; Smith and Minter, 1980; Slingerland, 1984). The most common sites of placer concentration at this scale are in bands parallel to the depositional strike and at the heads of wet alluvial fans (Schumm, 1977). Darby and Whittecar (1985) determined

that the Antigua Formation sediments were deposited on a wet alluvial fan with a paleo-slope of 0.01 (55 ft/mi). The regional trend of placer deposits in Colombia occurs in a north-south band approximately 20 kilometers in width (Figure 3). If a straight line were drawn between the two samples (this study) which had the highest gold concentration values (Marta Mine and Panambisito Mine) (Plates 1 and 2) it would also form a line parallel to the depositional strike. This might be a coincidence with only two data points or it could be a reflection of the regional trend observed by other workers. If this is the case, low concentration values found west of this line, indicate higher values may be encountered further to the east (upstream). Future exploration of these upstream terraces needs to be undertaken to determine this.

Size relationships between gold and black sands have been shown to have the hydraulic properties that are characteristic of deposits occuring in bands parallel to the depositional strike of alluvial fans. These deposits occur where bed roughness and stream energy slope are optimum for placer enrichment. The fact that gold was found in every sample also indicates placer concentration occurs on a drainage system scale. At this scale it can be said that regional conditions near Payan are optimum for placer concentrations, provided that local or smaller scale concentration processes are adequate.

Sites of heavy mineral enrichment on the bar scale were

observed in recent Rio Magui deposits and older terrace deposits. Black sand concentrations were observed on convex banks of meanders along with deposition of wood debris. In the older terrace deposits there seemed to be a relationship between wood debris and gold concentration values. Nearly always when high gold concentration values were found, wood debris was present. However, the presence of wood debris was not always associated with high gold concentrations. Along the present Rio Magui heavy mineral concentrations were also observed on the heads of mid-channel bars, point bars with suction eddies, and concave sides of sharp bends although no gold analyses were performed at these sites (Babuin, 1985).

Concentration processes acting on the bed scale were also observed in the Payan sediments. These include shadow deposits on the leeward side of obstacles such as large boulders where high concentrations of heavy minerals were observed. Also, bedform concentrations of heavy mineral-rich forset laminae were observed at the San Juan Mine; at the Travesia Mine, plane-parallel laminae of mostly magnetite were found. Field panning of these laminated sands showed relatively high gold concentrations (qualitatively). Scour-fills were present at the Luis Mine associated with a sand lense which was moderately rich near its lower gravel contact. In the present Rio Magui system, winnowed tops of gravel bars are common, and many of these

other erosional and depositional features are also found (Babuin, 1985).

Thus gold concentration processes operate on different scales in the Payan Mining District, ranging from small scale eddy winnowing to regional concentration on a paleo-fan system. The interrelationship of these processes is the controlling factor in the distribution of gold in the Payan area. An insufficient number of gold samples exists thus far to resolve the exact nature of this interrelationship.

Provenance Considerations for Gold

Scanning Electron Microscope (SEM) analysis of the surface texture and morphology of gold grains from the Payan terrace deposits has revealed certain characteristics which reflect the distance of transport for the Payan gold. As discussed earlier, the SEM observations confirmed that two types of gold were present. The first type of gold (crystalline gold) is characterized by jagged irregular shapes which reflect its primary crystalline structure (Figure 13). These characteristics suggest a relatively short distance of transport. Textural and morphological features of the second type (highly deformed gold) (Figure 14), such as complete destruction of crystalline morphology, rounded flat shapes, bent and hammered edges and abrasion scratches and craters, indicate

a much longer distance of transport.

This simultaneous occurence of two morphological types of gold suggests two different supply areas. Thus, two sources of gold are proposed for placer deposits in the Payan Mining District. Darby (1981) observed both rounded and angular zircon grains in an examination of heavy minerals in the Payan terrace gravels. Because of the difficulty in rounding zircon this observation supports a dual source for zircon also. Approximations regarding the distance to each of these sources can be made based on the work of Hallbauer and Utter (1977). They studied the morphological features of gold grains of recent placers with known source locations; thus, they were able to semi-quantitatively relate the distance travelled by gold grains to morphological features observed under SEM (Table 4).

According to Hallbauer and Utter, gold particles reflecting primary crystalline structure and exibiting only slight deformation in the form of occasional bent and hammered edges probably travelled no more than 20 kilometers. Whereas, the more deformed platy gold showing many bent and hammered edges, plastic flow deformation, and randomly oriented scratches (Figure 14), probably traveled distances of 80 to 100 kilometers.

At distances of 80 to 100 kilometers upstream (on the Rio Patia or Rio Telembi) from the Payan Mining District

TABLE 4. Morphological characterisics of gold grains observed under SEM related to distance of fluvial transport. (Based on Halbauer and Utter, 1977).

MORPHOLOGICAL CHARACTERISTICS OF GOLD GRAINS	DISTANCE TRAVELLED
1. Very angular and jagged edges 2. Primary crystalline structure visible 3. Occasional bent and hammered edges	1-25 kilometers
1. Dough-like micro-texture 2. Slightly angular and jagged edges 3. Signs of primary crystalline structure rarely visible 4. Numerous scratches and abrasions	30-80 kilometers
1. Grains are rounded and have flakey shapes 2. Bent and hammered edges and refolded edges are common 3. Abrasion scratches and crater-like depressions	80 -100 kilometers
1. Grains are hammered into thin sheets 2. Few abrasion scratches because associated pebbles and cobbles are now rounded 3. Repeated bending and folding gives grains appearance of several thin layers	½150 kilometers

are several lode mines which have been described by Gamba, 1912; Miller and Singewald, 1919; and Radelli, 1965. According to Miller and Singewald these ore bodies occur along and near the contact of a large body of "granite" on the west and schists on the east. The location of this mineralized belt appears to correspond to the mapped contact between several quartz-diorite Tertiary intrusive stocks and the surrounding metamorphosed Diabase and Dagua Group rocks of Cretaceous age. The metals associated with this diorite are gold, silver, lead, zinc, copper, iron, and mercury which are commonly dispersed into the basic volcanic rocks (Radelli, 1965).

The mining areas of Piedrancha, Mallama, Samaniego, and Tambo have yielded significant quantities of primary gold and probably constitute a continuous mineralized belt (Figure 20). The ore bodies in these areas generally occur along the contact of a large area of granite and schists cut by and overlain by younger eruptives to the east. At Samaniego the gold veins occur in both the granite and the schists. The weathering of the granite is so intense that this material may often be mined by eluvial methods. This granite also contains auriferous aplitic dikes. To the northeast of Samaniego is the Tambo mining area. Miller and Singewald (1919) observed these ore bodies and found them to consist of a stockwork of quartz veinlets containing gold and auriferous pyrite in dacite intrusions

Figure 20. Geologic map of the Department of Narino, Colombia showing location of known lode mines and possible source areas for Payan placer gold (Tertiary Intrusions)(based on Arango and Ponce, 1982).

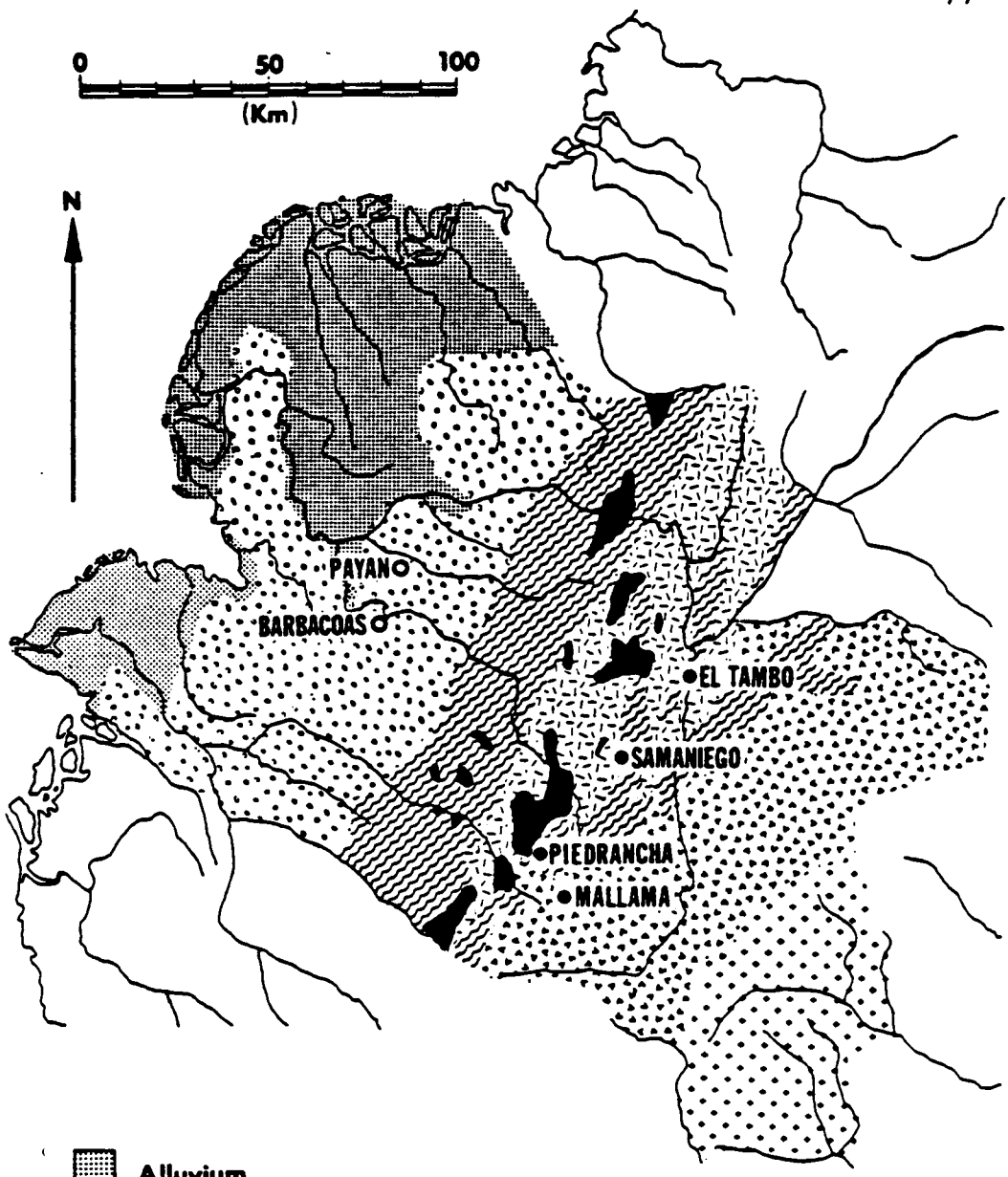

Quaternary
- Alluvium
- Undifferentiated Sediments of Fluvio-Volcanic Origin

Tertiary
- Intrusive Bodies
- Volcanic Rocks: Lavas, Ash, Lapilli

Cretaceous
- Diabase Group
- Dagua Group

Paleozoic
- Cajamarca Group

- ● Lode Mining Areas
- ○ Placer Mining Areas

of slates and schists. The dacite is overlain by completely altered rhyolite with coarse bi-pyrimidal quartz crystals. These deposits are also strongly decomposed and can be worked as eluvium. Thus these deposits are easily eroded and transported downstream.

Based on the gold transport distances determined in this study, any of these areas could have supplied the bulk of the gold to the Payan terrace deposits depending on the paleo-drainage patterns that existed in Plio-Pleistocene time. Presently much of this area drains into the Rio Patia System. It should be noted that this mountainous and heavily vegetated region is poorly explored and the true extent of Tertiary intrusives and associated mineralized belts is not known. Therefore, the real source of Payan gold could be related to unmapped Tertiary intrusions of the Diabase and Dagua Groups in the Western Cordillera of the Andes Mountains.

At distances of 20 kilometers or less from Payan no known lode mines have been reported which could account for the short transport gold type. The rocks within these distances are mapped as Lower to Middle Tertiary continental and marine sediments (Arango and Ponce, 1982). Intrusive igneous rocks have not been observed within these distances; however, gold transport distances indicate they may exist or have existed and have been cut by old rivers that once drained into the Payan area. Although this type

of gold only accounts for less than 20 percent of the gold in the Payan terrace deposits, exploration for its lode source may prove worthwhile.

Studies of abrasion rates of gold in a simulated high energy environment showed that the velocity of the particle appears to be a more important factor in the abrasion of gold than the distance of travel. Yeend (1975) found that a fourfold increase in velocity produced a tenfold increase in the rate of gold abrasion. Thus while near and far distance sources for the Payan gold can be assumed, actual distance determinations based on Hallbauer and Utter's (1977) work should be considered with some caution.

CHAPTER 5

CONCLUSIONS

Gold concentration values calculated from 0.5 to 1.0 cubic meter assay samples, taken throughout the Payan terrace deposits, have shown the distribution of gold to be extremely variable over short lateral and vertical distances. Sieve and RSA size distributions of gold and black sand concentrates facilitated determination of hydraulic equivalence between the two mineral populations. Because the mean size of black sand populations was consistently smaller than the mean size of the denser gold, I concluded that the gold and black sand are not hydraulically equivalent and were not deposited under the same flow conditions. Deviations from hydraulic equivalence, observed in the Payan placer deposits can be explained by two previously published hydraulic sorting mechanisms: (1) entrainment sorting and (2) transport sorting. Both of these mechanisms served to increase the mean size of the gold grains relative to the black sands. Entrainment sorting increased the mean size ratio of gold grains to black sands because the smaller original size of

the denser gold grains allowed them to be shieled by the larger less dense minerals keeping them from protruding into zones of higher velocity in the flow. Thus the larger lighter minerals were preferentially removed.

Shape analysis of the gold grains has shown most of them (especially the larger grains) to be extremely flakey (very low Corey shape factors). The flakey shape of the gold grains enhanced the effects of entrainment sorting because flakes are theoretically much harder to lift off the bed than coarser spherical magnetite grains. However, once the flakey gold grains were entrained, they were more easily transported than their associated black sands, allowing them to be transported further downstream with the finer more spherical magnetite grains.

Flood events and the time interval between flood events are proposed to be the major factors controlling the deposition of gold in the Payan Mining District. The ultimate richness of these sediments is affected by concentration processes operating on three linear scales: a drainage system scale, a sand bar scale, and a discontinous bed scale.

Finally, scanning electron microscopy was successful in identifying textural and morphological characteristics of gold grains applicable to provenance considerations. Two distinct morphological types of gold were identified as well as two populations of zircon grains (rounded and

angular). This simultaneous ocurrence of two morphological types of gold is interpreted to be a result of two auriferous source areas. The first gold type, which shows signs of its primary crystalline structure and comprises less than 20 percent of the Payan gold, probably traveled less than 20 kilometers. The largely unknown geolgy within this distance leaves the source for this gold type unknown. Future exploration for this source should include a search for presently undiscovered Tertiary intrusives within 20 kilometers east of Payan. The highly deformed gold type traveled much greater distances, possibly 80 to 100 kilometers. Retracing these distances upstream, the probable source is the Mallama-Samaniego- Tambo mineralized zone or any of the Tertiary intrusives of the western versant of the Western Cordillera of south-central Narino.

Because the modern Rio Magui is eroding older auriferous terraces as well as possible auriferous intrusives to the east, exploration along this river might be of value. Assuming the same relationship between gold grains and zones of concentration for the older terraces at paleo-slopes of about 0.01, exploration in the Modern Rio Magui should center upon areas further to the east (upstream) because river gradients in the Payan area are only about 0.003.

Results of this research indicate that future exploration for placer gold in the Payan Mining District

should be conducted in the terraces east of the north-south line connecting the Marta Mine and the Panambesito Mine. This conclusion is based on gold concentration values determined in this study and the regional trend of placer concentrations in a north-south band perpendicular to the depositional strike. Size analysis of gold and black sand grains should be useful in guiding this exploration as well as designing efficient recovery techniques.

REFERENCES CITED

American Society of Civil Engineers, 1962, Task Committee on Preperation of Sedimentation Manual, Introduction and properties of sediments, Amer. Soc. of Civil Eng. Proc., v.88, no.HY4, pp. 77-107.

Arango, J.L. and Ponce, A.N., 1982, Mapa Geologico Generalizado de Departemento de Narino, Inst. Nat. de Invest. Gelogio-Mineras, Bogata.

Babuin, M.L., 1985, Fluvial depositional processes of a tropical river, Colombia, South America, unpub. Masters Thesis, Old Dominion University, Norfolk, Virginia, 139 pp.

Brady , L.L. and Jobson, H.E., 1973, An experimental study of heavy mineral segregation under alluvial flow Conditions, U.S. Geol. Surv. Prof. Paper 562-K, 38 pp.

Briggs, L.I., 1965, Heavy mineral correlations and provenances, Jour. Sed. Petrology, v.35, pp. 939-955.

Bueno, R.S. and Govea, C.R., 1976, Potential for exploration and development of hydrocarbons in Atrato Valley and Pacific Coastal and Shelf Basins of Colombia, In: Circum-Pacific Energy and Mineral Resources, Amer. Assoc. Pet. Geol., Memoir 25, Tulsa, pp. 318-327.

Bureau of Land Management (BLM), 1970, Placer Examination: Principles and Practice, U.S. Department of the Interior, 209 pp.

Case, J.E., 1974, Major basins along the continental margin of northern South America, In: The Geology of Continental Margins, Burk C.A. and Drake C.L. (eds.), Springer-Verlag, N.Y., pp. 733-741.

Corey, A.T., 1949, Influence of shape on the fall velocity of sand grains, Colorado State University, Fort Collins, unpup. Masters Thesis, 102 pp.

Crampton, F.A., 1937, Occurence of gold in stream placers, Mining Journal, v.20, pp. 3-34.

Darby, D.A., 1981, Geology and sedimentology of the Rio Magui terraces near Payan, Colombia, South America, Tech. Rept. GSTR-83-1, Old Dominion University, Norfolk, 23 pp.

Darby, D.A. and Whittecar, G.R., 1984, Geology and gold evaluation of the Payan Mining District, Narino, Colombia, Tech. Rept. GSTR-84-11, 95 pp.

Darby, D.A. and Whittecar, G.R., 1985, A model of placer deposition in tropical alluvial fans lacking bedrock control, Geol. Soc. Amer. Abstracts with Program, v.17(2), p. 87.

Duque Caro, H., 1972, Relaciones entre la bioestratigraphia y la cronoestratigraphia en la llamado geosinclina de Bolivar, Colombia, Serv. Geol. Nac. Bol. Geol., v.19(3), pp. 25-68.

Folk, R.T., 1974, Petrology of Sedimentary Rocks, Hemphill Publishing Company, Austin, p. 25.

Frost, I.C., 1959, Elutriating tube for the specfic gravity separation of minerals, Amer. Mineralogist, v.44(78), pp. 886-890.

Gamba, F.P., 1912, Porvenier Mine in the district of Mallama, Min. and Sci. Press, v.105, p. 598.

Grigg, N.S. and Rathbun, R.E., 1969, Hydraulic equivalence of minerals with a consideration of the reentrainment process, U.S. Geol. Surv. Prof. Paper, no.650-B, pp. B77-B80.

Hallbauer, D.K. and Utter, T., 1977, Geochemical and morphological characteristics of gold particles from recent river deposits and the fossil placers of the Witwatersrand, Mineralium Deposita, v.12, pp. 293-306.

Hand, B.M., 1967, Differentiation of beach and dune sands using settling velocities of light and heavy minerals, Jour. Sed. Petrology, v.37, pp. 514-521.

Heywood, H., 1933, Calculation of a specific surface of a powder, Inst. Mech. Eng. Proc., v.125, pp. 383-459.

Inter-Agency Committe on Water Resources, (1957), A study of methods used in measurement and analysis of sediment load in streams, Rept.12, Washington, U.S. Govt. Printing Office, 55 pp.

Kartashov, I.P., 1971, Geological features of alluvial placers, Econ. Geol., v.66, pp. 879-885.

Krumbien, W.C., 1942, Settling velocity and flume-behavior of non-spherical particles, Am. Geophys. Union Trans., v.23(2), pp. 621-633.

Ljunggren, P. and Sundborg, A., 1968, Some aspects on fluvial sediments and fluvial morphology, Geografisk Annaler, v.50(A), pp. 121-135.

Lowright, R., Williams, E.G., and Dachille, F., 1972, Analyses of factors controlling deviations in the hydraulic equivalence in some modern sands, Jour. Sed. Pet., v.42, pp. 635-645.

Mackie, W., 1923, The principles that regulate the distributions of heavy minerals in sedimentary rocks as illustrated by the sandstones of northeast Scottland, Edinburg Geol. Soc. Trans., v.11(2), pp. 138-164.

McGowen, J.H. and Groat, C.G., 1971, Van Horne Sandstone West Texas: An alluvial fan model for mineral exploration, Univ. of Texas., Bureau of Econ. Geol., no.72, 38 pp.

Middleton, G.V. and Southard, J.B., 1977, Mechanics of Sediment Movement, SEPM Short Course, no.3, Binghamtom, sec. 4-6.

Miller, J.N. and Singewald A.P., 1919, Mineral deposits of South America, McGraw-Hill Book Co., Inc., New York, 598 pp.

Nicholas, C.F., 1897, Explorations in the gold fields of western Colombia, The School of Mines Quarterly, v.18, pp. 259-256.

Nygren, W.E., 1950, Bolivar geosyncline of northwestern South America, AAPG. Bull. 34, pp. 1998-2005.

Ortiz, H., 1982, Projecto Payan: reconocimiento geologico de depositos de placer, Progress Rept. No. 1, Compania Minera de Colombia y Texas, S.A., Inc., 13 pp.

Peele, R. and Church, J., Mining Engineers Handbook, John Riley and Sons, Inc., New York, pp. 33-102.

Radelli, L., 1965, Metallogenic belts and igneous rocks of the Colombian Andes, Traux du Laboratoire de Geologie de la Faculte des Sciences de Greoble, tome 41, pp. 219-228.

Ramirez, J.E., 1977, Geological and Geophysical setting of Colombia, pp. 25-29, In: The Ocean-Continent Transition in southwest Colombia, Instituto Geofisco Universidad Javeriana, Bogata.

Rittenhouse, G., 1943, Transportation and deposition of heavy minerals, Geol. Soc. Amer. Bull., v.54(12), pp. 1725-1780.

Rossiter, R.W., 1973, Silver and Gold: The mining and metalurgical industry of the United States, J.B. Ford Co., New York, pp. 221-241.

Rubey, W.W., 1933, The size distribution of heavy minerals within a water-laid sandstone, Jour. Sed. Pet., v.3(1), pp. 3-29.

Saks, S.E. and Gavshina, A.N., 1976, Stream transport of casseterite, Litologiya Poleznye Iskopaemye, pp. 129-134.

Schultz, E.F., Wilde, R.H., Albertson, M.L., 1954, Influence of shape on the fall velocity of sedimentary particles, Omaha, U.S. Army Corps. of Engineers, Missouri River Div., MRD Sediment Ser., no.5, 161 pp.

Shanov, V.N., 1964, The distribution of minerals in the size fractions of sand deposited by water, Universitat Vestinik, v.6, pp. 155-163.

Schumm, S.A., 1977, The Fluvial System, John Wiley Sons, New York pp. 221-241.

Slingerland, R., 1977, The effects of entrainment on the hydraulic equivalence of light and heavy minerals in sands, Jour. Sed. Pet., v.47(2), pp. 753-770.

Slingerland, R., 1984, The role of hydraulic sorting in the orgin of fluvial placers, Jour. Sed. Pet., v.54(1), pp. 137-150.

Smith, N.P. and Minter, W.L., 1980, Sedimentological controls of gold and uranium in two Witwatersrand paleo-placers, Econ. Geol., v.75, pp. 1-44.

Sneed, E.D. and Folk, R.L., 1958, Pebbles in the lower Colorado River, Texas, Jour. Geol., v.66(2), pp. 114-150.

Sundborg, A., 1956, The River Klaralveni: a study in fluvial processes, Geografiska Annaler, A., no.115, pp. 125-316.

Tourtelot, H.A., 1968, Hydraulic equivalence of grains of quartz and heavier minerals, and implications for the study of placers, G.S.A. Prof. Paper 594-F, 13 pp.

Tourtelot, H.A. and Riley, L.B., 1973, Size and shape of gold and platinum grains, In: Ores in Sediments, Amstutz, G. and Bernard, A. (eds.), pp. 307-318.

Tyrell, J.B., 1912, The law of the pay streak, Inst. Mining and Metallurgy Trans., v.21, pp. 593-605.

Utter, T., 1979, The morphology and silver content of gold from the upper Witwatersrand and Ventersdorp systems of the Klerksdorp Gold Field, South Africa, Econ. Geol., v.74, pp. 27-44.

von Engelhardt, W., 1940, The distinction of water and wind sorted sands on the basis of the grain-size distribution of their light and heavy components, Chemie der Erde, v.12, pp. 445-465.

Wadell, H.A., 1936, Some practical sedimentation formulas, Geol. Foren. Stockholm Forh., v.58(3), pp. 397-408.

West, R.C., 1957, The Pacific Lowlands of Colombia, L.S.U. Press, Baton Rouge, La., 278 pp.

Willmarth, W.W., (1964), Steady and unsteady motions and wakes of free falling disks, Phys. Fluids, v.7, pp. 197-208.

Yeend, W., 1975, Experimental abrasion of detrital gold, Jour. Research U.S. Geol. Survey 3, pp. 203-212.

APPENDIX A

Stratigraphic Descriptions of Individual Mine Sites Showing Sample Locations and Gold Concentration Values

APPENDIX A. STRATIGRAPHIC DESCRIPTIONS OF MINES, PAYAN MINING DISTRICT

EXPLANATION OF SYMBOLS


volcanic ash, both pyroclastic and reworked


highly weathered volcanic ash (clay)


volcanic gravel or volcanic conglomerate


laminated volcanic ash


mud or mudstone


cobble to boulder gravel with sandy matrix


pebble to cobble gravel with sandy matrix


sand


wood debris


cross-bedding


cobble imprication


grab sample


$0.25m^3$ sample for Au content


$0.5\ m^3$ sample for Au content


$1.0\ m^3$ sample for Au content

TYPED DESCRIPTIONS

σ	sorting
Mz	average size of matrix
Max	maximum clast size in matrix
V	volcanic fragment or aggregate
Q	quartz
Q′	bipyramidal quartz
M	mica (mostly leached biotite)
B	biotite
Mag	magnetite and other opaques
H	hematite (coating)
L	lithic fragment (mostly volcanic)
G	garnet
Py	pyrite
H	hornblende
( )	minerals in order of abundance

DISTANCE AND DIRECTION TO MINE SITE BASED UPON BRASS MARKER IN FRONT OF PAYAN CHURCH.

ALCOSE (1000 meters, N22W)

DESCRIPTIONS OF STRATIGRAPHIC SECTIONS

GOLD CONTENT (oz/yd^3)

-cobble to boulder gravel with red-brown to gray sand matrix (0.25-2mm) mostly weathered to clay; average clast is 8-10cm; maximum clast is 45 cm.

-sand lense with laminae of gray, brown or red sand (0.2-2mm), mostly weathered to clay; convolute bedding & liesegang rings; laminations dip N30°W at 19°.

-? ash

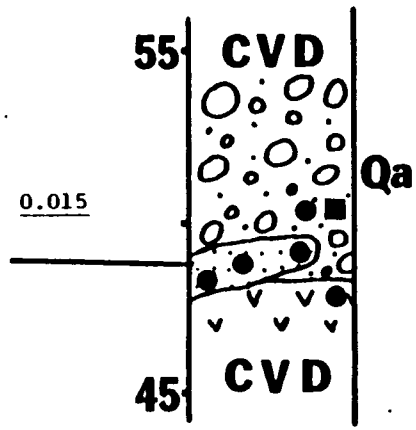

DESCRIPTIONS OF ANALYZED SAMPLES

ALC-3	Mz=0.2mm Max=0.8mm(Q,V,M)
ALC-4,2, and 1	Mz=0.14mm Max=2mm(V,Q/,L,M,B)
ALC-5	Mz=0.3mm Max=2mm σ=poor(V,Q,B,H)

ANANIAS (1400 meters, S51E)

DESCRIPTIONS OF STRATIGRAPHIC SECTIONS

GOLD CONTENT (oz/yd^3)

-red ash and fine-grained volcanic gravel mostly weathered to clay.

-white ash, very blocky with iron concretions, laminated at the base; pyroclastic debris is finer than 0.08mm. Sharp contact with sand below dips to south (7°).

-dark gray fine sand (0.13-0.25mm)

-cobble to boulder gravel with fine to coarse sand matrix (0.12-1mm); charred wood debris in upper meter; average clast is 12cm and largest boulder is 35cm.

-buff colored volcanic sand, fine conglomerate & ash, well indurated.

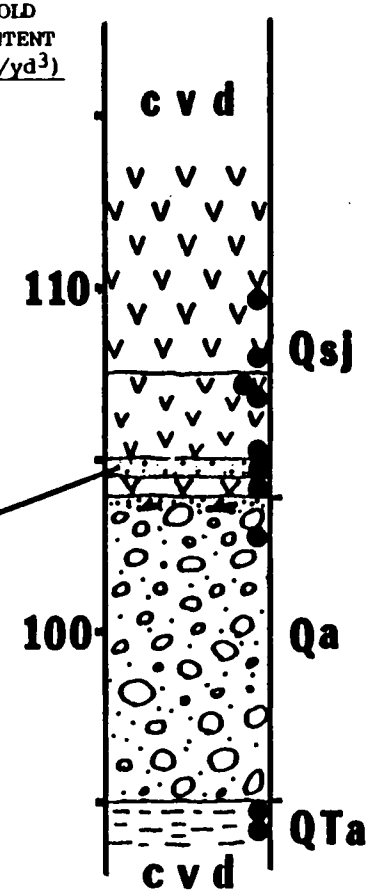

DESCRIPTIONS OF ANALYZED SAMPLES

ANA-4	Mz=0.21mm Max=2.1mm σ=good(V,L,Mag,Q,B)
ANA-8	Mz=0.25mm Max=1.2mm σ=mod.(Q,V,Mag,M)
ANA-2	
ANA-3	Mz=0.33mm Max=4.3mm σ=poor(H,Basalt,Q,B)
ANA-6	Mz=0.2mm Max=0.7mm σ=good(Mag,V,Q)
ANA-7	Mz=0.1mm Max=0.9mm σ=good(V,Q,B,Mag)
ANA-5	Mz=0.3mm Max=1.6mm σ=mod.(V,Q,Mag,B)
ANA-1	MZ=0.18mm Max=0.5mm(V,Q,M,H,L)
ANA-9	Mz=0.3mm Max=0.9mm(V,Q,M)
ANA-10	MZ=0.1mm Max=0.6mm(V,Q,Mag,L)

ANGUIÑO (280 meters, S51E)

DESCRIPTIONS OF STRATIGRAPHIC SECTIONS

GOLD CONTENT (oz/yd^3)

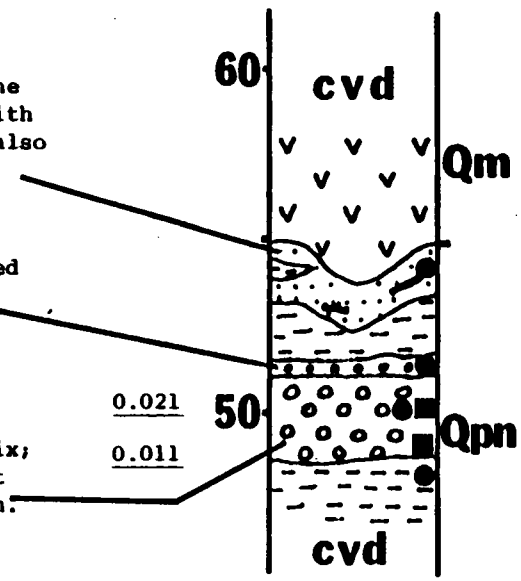

-ash

-interbedded light gray mudstone lenses & brown or gray sand with wood debris in both. Sand is also lense-shaped with irregular contacts with mudstone.

-pebble gravel with gray, fine sandy matrix, moderately sorted & lacking wood debris. Chert pebbles abundant. Iron-rich concretions along contact between gravels.

0.021

-pebble gravel with red-brown, very fine to coarse sand matrix; no wood debris; abundant chert cobbles; many coated with iron.

0.011

-light gray massive mudstone exposed in sluice.

DESCRIPTIONS OF ANALYZED SAMPLES

ANG-1	Mz=0.18mm Max=2mm(L,Q',L,M)
ANG-2	Mz=0.1mm Max=0.37mm(Q,V,G,L)
ANG-3	Mz=0.5mm Max=2mm(Q,V,Mag)
ANG-4	Mz=0.4mm Max=0.7mm(Q,V,L,M)

BLANDITO (850 meters, S17E)

DESCRIPTIONS OF STRATIGRAPHIC SECTIONS

GOLD CONTENT (oz/yd^3)

-red ash & fine-grained volcanic gravel. very clayey with many 3-5cm clases weathered to clay. Irregular indistinct boundary.

0.012

-pebble to boulder gravel with white-to-red clayey matrix. Nearly all clasts weathered to clay. No wood observed. Contains one-meter-thick lens of thorougly weathered fine-to-coarse sand. Average clasts are 6cm, maximum clasts are 35 cm. Matrix contains 0.5-2mm grains weathered to clay.

-fine red ash, reworked.

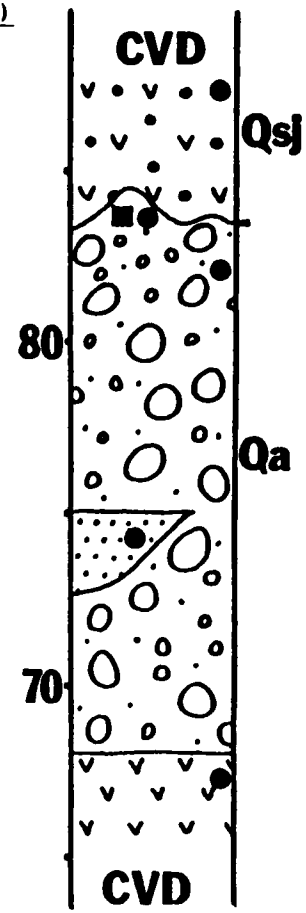

DESCRIPTIONS OF ANALYZED SAMPLES

BLA-5 Mz=0.2mm Max=0.9mm σ=good(Q,Mag,V,H,M)

BLA-4

BLA-3 Mz=0.12mm Max=35cm(V,Q,M)

BLA-2 Mz=0.12mm Max=2mm(V,Q,M,Mag)

BLA-1 Mz=0.13mm Max-0.6mm σ=good(Q,Mag,V,M)

CLARISA (890 meters, N32E)

DESCRIPTIONS OF STRATIGRAPHIC SECTIONS

GOLD CONTENT (oz/yd^3)

-ash

-pebble gravel with fine sandy matrix poorly sorted (CLA-2). Firm chert pebbles abundant.

-UNCONFORMITY

-red medium to coarse sand, entirely weathered to clay.

-brown & red cobble-to-pebble gravel with sandy matrix. Thoroughly weathered to clay: Lens of medium-coarse contains wavy laminations and cross-bedding dipping S30E, N70E, & N55E.

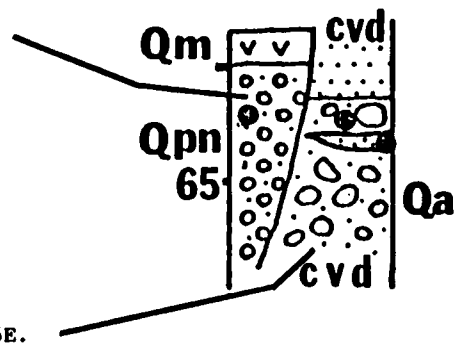

DESCRIPTIONS OF ANALYZED SAMPLES

CLA-2	Mz=0.25mm Max-2.0mm(V,Q/)
CLA-1	Mz=0.25mm Max-1.0mm(V,Q,M)
CLA-3	Mz=0.12mm Max-2.0mm(V,L,Q,M)

EPIMENIO (530 meters, N13W)

DESCRIPTIONS OF STRATIGRAPHIC SECTIONS

GOLD CONTENT (oz/yd^3)

-red to white ash weathered to clay.

-intercalated medium sand & mudstone with occasional wood debris especially concentrated at base of unit.

-cobble to boulder gravel with light gray, medium sand (0.35mm) matrix; average clast is 6cm & maximum clast is 30cm; varying degrees of weathering in cobbles.

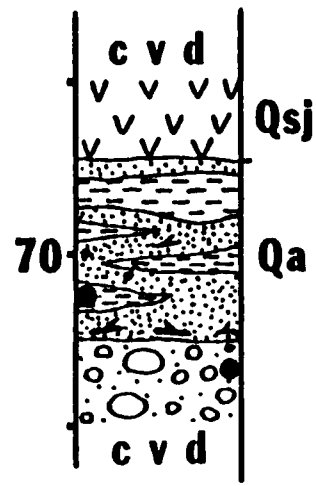

DESCRIPTIONS OF ANALYZED SAMPLES

EPI-2 Mz=0.2mm Max=0.3mm(V,Q,Mag,L)

EPI-1 Mz=0.35mm Max=0.5mm(Q,V,L,M,H,B)

HIPOLITO (440 meters, N40E)

DESCRIPTIONS OF STRATIGRAPHIC SECTIONS

	GOLD CONTENT (oz/yd^3)
-red & white mottled ash & fine-grained volcanic gravel. Many banded rock fragments weathered to clay.	
-very fine-grained mudstone. Blocky and massive.	
-cobble gravel with blue-gray matrix interbedded with sand lenses. Cobbles well-rounded with moderately thick weathering rinds. Some imbrication visible. Lowest blue-gray sand lens contains poorly sorted coarse sand with some thin cobble beds and no wood.	0.010
	0.008
Middle sand lens deposited behind 2-meter boulder & contains medium-to-coarse sand with weathered pebble ghosts & no sedimentary structures. The upper sand lens contains medium-to-coarse sand with abundant wood debris & no sedimentary structures. All sand lenses partly weathered to clay.	0.002
-fine-grained compact mudstone & medium sand.	

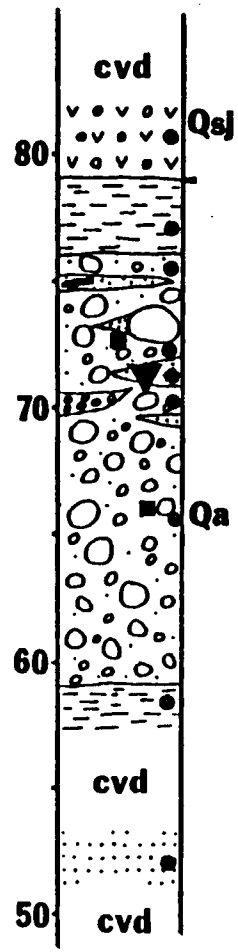

DESCRIPTIONS OF ANALYZED SAMPLES

HIP-10	Mz=0.1mm Max=1.7mm(Q,V,Mag,M)
HIP-2	Mz=0.18mm Max=0.4mm(Q,V,Mag,B)
HIP-4	Mz=0.1mm Max=0.37mm(V,Q,L,M)
HIP-5	Mz=0.1mm Max=2mm(Q/,V,Mag,M,L)
HIP-7	Mz=0.09mm Max=2mm(Q,V,M,Mag,L.)
HIP-3	Mz=0.2mm Max=0.8mm(Q,V,L,M)
HIP-8	Mz=0.09mm Max=1mm(Q/,V,Mag,L)
HIP-9	Mz=0.2mm Max=2mm(V,Q/,Mag,L,Py)
HIP-6	Mz=0.37mm Max=2mm(V,Q,Mag,B,G,Py)
HIP-1	Mz=0.2mm Max=0.9mm(Q,V,Mag,L)
MAG-3	Mz=0.3mm Max=0.4mm(Q,Mag,V,M,L)

LA JUNTA (540 meters, N45W)

DESCRIPTIONS OF STRATIGRAPHIC SECTIONS

DESCRIPTIONS OF ANALYZED SAMPLES

GOLD CONTENT (oz/yd^3)

-red to red-gray, highly weathered ash; some laminae 5m above the base of unit.

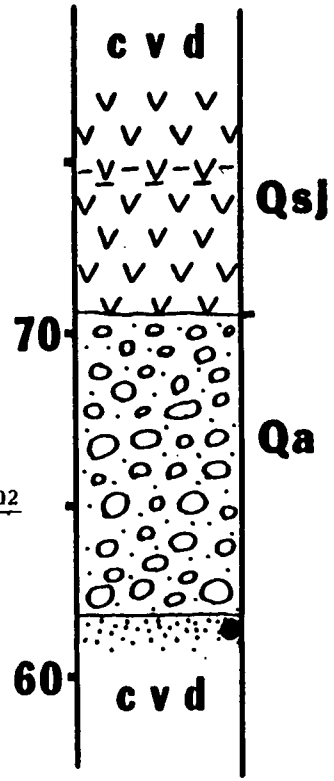

-greenish, gray cobble gravel (average clast is 10cm, maximum size is 20cm) with coarse sand (.8-1mm) matrix; mostly weathered to clay except for cobbles.

0,00002
0,002
0.008
0.009

LAJ-1 Mz=0.13mm Max=0.7mm(V,L,Q,M,Mag)

-gray, compact, fine sand mostly weathered to clay.

0.010

0.013 Average value (±0,082) from 50-55 level.
in nearby drill hole (Ortiz, 1983).
0.082 49m level (Ortiz, 1983).
0.029 48m level (Ortiz, 1983).
0.005 Average (±0.005) from 40-47m level).

LUIS (430 meters, N51W)

DESCRIPTIONS OF STRATIGRAPHIC SECTIONS

GOLD CONTENT (oz/yd^3)

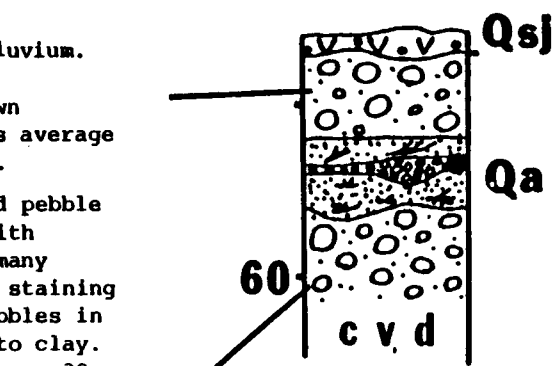

-red-brown volcanic ash; colluvium. Irregular contact.

-cobble gravel with grey-brown coarse sandy matrix. Cobbles average 8cm diameter, maximum 15 cm.

-coarse sand with interbedded pebble lens. Sand is bluish-gray with scattered wood fragments & many pyrite grains visible. Iron staining present along fractures. Pebbles in lens are 3-5cm & weathered to clay. Troughs filled with pebbles are 30 to 70cm long. Carbonized wood & no pebbles lie in sand below pebble lens. Sharp undulatory contact at base of sand.

-cobble gravel with grayish-brown sand matrix.

DESCRIPTIONS OF ANALYZED SAMPLES

LUI-1 Mz=0.13mm Max=3-5cm(V,Q,M,L,Mag,B,Py)

MAGDALENA (340 meters, N46E)

DESCRIPTIONS OF STRATIGRAPHIC SECTIONS

GOLD CONTENT (oz/yd^3)

-tan -to-orange volcanic ash, clayey. Many liesegang rings 1 to 3mm thick.

-orange-to-white volcanic ash & volcanic sand with black-to-rust iron concretionary layers. Clasts in volcanic gravel are medium-to-coarse sand.

-cobble to boulder gravel with coarse, poorly-sorted sand matrix. Clasts average 15cm in outcrop, maximum 36cm. 60cm boulder seen in tailings. Many cobbles in contact with cobbles while others float in matrix. Cobbles fine upwards & have notable imbrication. Minor amounts of wood present. Matrix well-weathered to clay, bottled from white-to-red.

-compact gray mudstone, exposed in sluice.

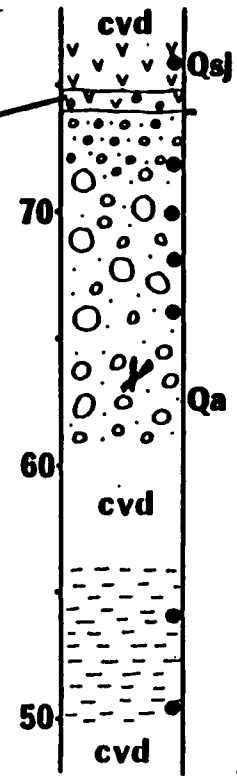

DESCRIPTIONS OF ANALYZED SAMPLES

MAG-9	Mz=0.12mm Max=1.1mm(Q,V,Mag,M)
MAG-6	Mz=0.25mm Max=3mm(V,Q,Mag,B)
MAG-7	Mz=0.25mm Max=0.5mm(V,Q,M)
MAG-2	Mz=0.25mm Max=0.5mm(V,Q,M)
MAG-1	Mz=0.25mm Max=1mm(V,Q,M)
MAG-5	Mz=0.2mm Max=0.5mm(V,Q,B)
MAG-4	Mz=0.1mm Max=0.4mm(Q,L,Mag,V,M)
MAG-8	Mz=0.3mm Max=1.9mm(Q,V,L,M,H)

MARIANNA (470 meters, N47E)

DESCRIPTIONS OF STRATIGRAPHIC SECTIONS

GOLD CONTENT (oz/yd^3)

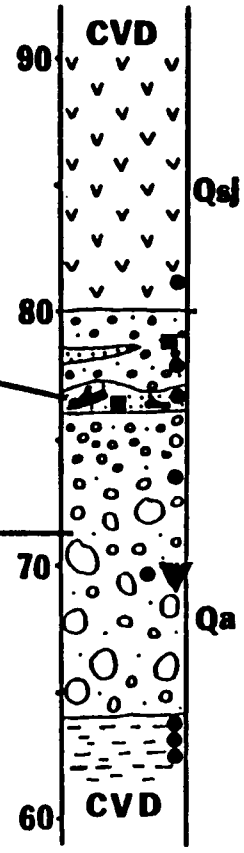

-red ash & volcanic sand, highly weathered.

-cobble to boulder gravel (average size of clasts is 10cm, maximum size is 35cm) with red & gray, mottled, coarse sand (0.5-0.8mm) matrix & lenses of mud & sand; mostly weathered to clay.

-gray, coarse sand (0.5-0.8mm) with wood debris (up to 0.8m) especially concentrated near top of unit; weathered to sticky clay; alternating coarse & fine-grained laminae & trough cross-bedding dipping 8° to west (N86°W).

-cobble to boulder gravel (average clast is 20cm, maximum clast is 80 cm) with blue-gray, weathered coarse to medium sand matrix; cobbles fine upward.

-compact, gray to brown mudstone with small amount of medium to coarse sand.

DESCRIPTIONS OF ANALYZED SAMPLES

MAR-1 Mz=0.2mm Max=1.4mm σ =mod.(Q,V,Mag)

MAR-8 Mz=0.25mm Max=0.5mm(V,Q,M)

MAR-5 Mz=0.09mm Max=0.5mm(L,Q,M,Mag)

MAR-3 Mz=0.25mm Max=0.5mm(V,Q,M,L)

MAR-4 Mz=0.25mm Max=0.5mm(Q,V,M,H)

MAR-6 Mz=0.06mm Max=0.7mm(Q,V,L,Mag)

MAR-2 Mz=0.1mm Max=1.3mm(V,Q,M,L,Mag)

MAR-7 Mz=0.1mm Max=0.7mm(Q,V,M,Mag,L)

MARTA (880 meters, N31E)

DESCRIPTIONS OF STRATIGRAPHIC SECTIONS

GOLD CONTENT (oz/yd^3)

-red volcanic ash.

-red-brown to gray coarse sand; many weathered ghost grains. Scattered wood debris. No sedimentary structures visible. Contains poorly sorted pebble gravel lens with wood debris.

0.012

0.040

-cobble-to-boulder gravel with sandy matrix. Cobbles average 10 cm in outcrop, maximum 45 cm. Many weathered clay ghosts of pebbles.

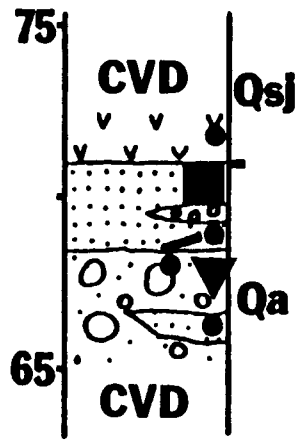

DESCRIPTIONS OF ANALYZED SAMPLES

MAT-1 Mz=0.2mm Max=1.6mm(Q,V,Mag)

MAT-2 Mz=0.1mm Max=5mm(Q,L,M,Mag)

MAT-3 Mz=0.2mm Max=0.8mm(L,Q,M,H)

MAT-4 Mz=0.13mm Max=4mm(Q,L,Mag)

PAÑAMBISITO (690 meters, S58E)

DESCRIPTIONS OF STRATIGRAPHIC SECTIONS

GOLD CONTENT (oz/yd^3)

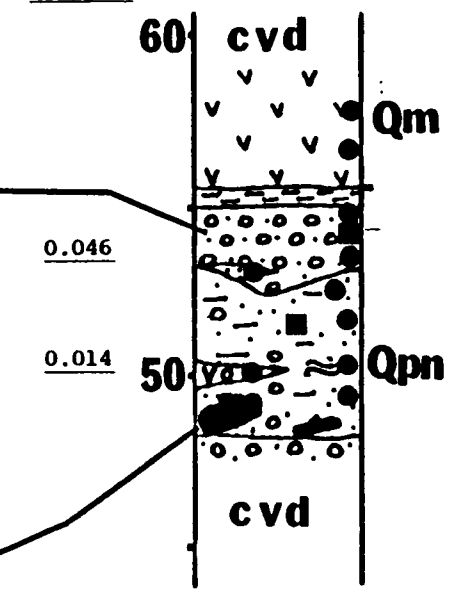

-red volcanic ash, very sticky.

-grey mudstone.

-pebble gravel with grey clayey matrix. Pebbles predominately white chert. Lens of coarse sand & gravel interbedded at base of unit; irregular abrupt contact.

-interbedded sands, mudstones, clays & pebbly gravel in extremely variable bedding pattern. Half-meter long logs & stumps, nuts & leaves present in organic-rich mudstone & medium sand. Agglomerate lens 25cm thick also interbedded.

-pebble conglomerate with very large basalt boulders visible in sluice.

DESCRIPTIONS OF ANALYZED SAMPLES

PAN-9	Mz=0.2mm Max=0.6mm(Q,V,Mag,M)
PAN-7	Mz=0.2mm Max=1.0mm(Q,V,Mag,M,B)
PAN-10	Mz=0.2mm Max=1.9mm(L,Q,M)
PAN-3	Mz=0.25mm Max=0.8mm(Q',V,L,M)
PAN-2	Mz=0.25mm Max=0.5mm(V,Q',L,H)
PAN-6	Mz=0.9mm Max=2mm(Q,L,Mag,M)
PAN-1	Mz=0.05mm Max=0.2mm(Q,V,Mag,L)
PAN-4	Mz=0.25mm Max=1.5cm(L,Q,Mag,M)
PAN-8	Mz=0.09mm Max=1.2cm(L,Q,Mag)
PAN-5	Mz=0.2mm Max=1.4mm(Q,V,Mag,B)
PAN-11	Mz=0.2mm Max=0.6mm(V,Q,H,wood debris)

PICCININI (580 meters, N44W)

DESCRIPTIONS OF STRATIGRAPHIC SECTIONS

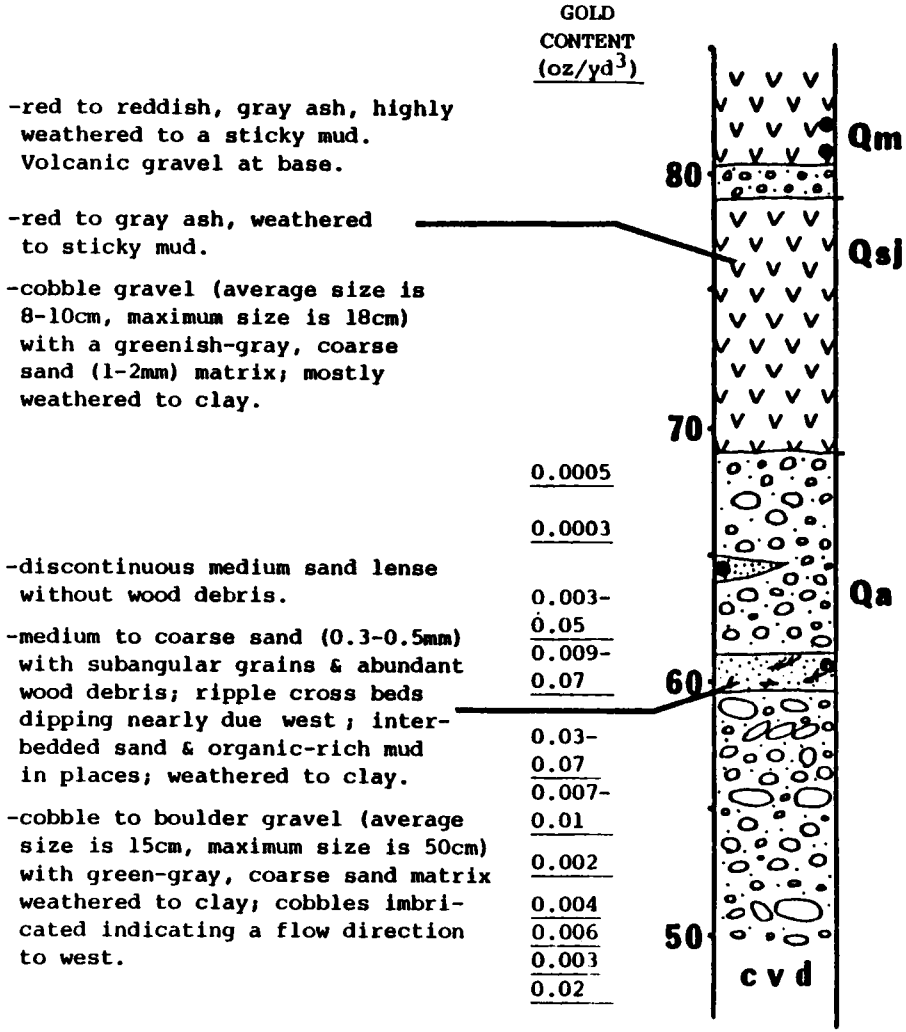

DESCRIPTIONS OF ANALYZED SAMPLES

PIC-2 Mz=0.12mm Max=1.9mm σ =mod./poor(Q,Fe,V,Mag,M)
PIC-3 Mz=0.2mm Max=0.3mm σ =good(Q,V,M,B,H,Mag)

PIC-4 Mz=0.18 mm Max=2.0mm(Q,L,M,Mag)

PIC-1 Mz=0.18mm Max=0.5mm(Q,L,Mag,B)

SAN JUAN (1220 meters, S50E)

DESCRIPTIONS OF STRATIGRAPHIC SECTIONS

GOLD CONTENT (oz/yd^3)

-red-brown volcanic ash & volcanic gravel; contains weathered pebbles & some cobbles. Sharp lower contact.

-dark red to white-&-purple volcanic ash & volcanic gravel; granules & pebbles up to 0.5cm present. Sharp lower contact.

-red medium sand with black sand laminae. Ripples up to 15cm amplitude present with dip directions at N20°W(21°) & S50°W(6°). Very little black sand present in upper 0.5 m of sand; some isolated 1cm pebbles present. Red clay laminations 5-8cm thick present throughout unit. Sand coarsens towards base. Sharp undulatory contact.

-pebble to cobble gravel with red-to-white sandy matrix. Clasts average 3cm at the top, 10cm at the base; maximum 35cm. Matrix & many cobbles extensively weathered to clay. Matrix ghost textures show medium-to-coarse sand.

-dark blue to buff colored volcanic sand, fine conglomerate & ash; well indurated.

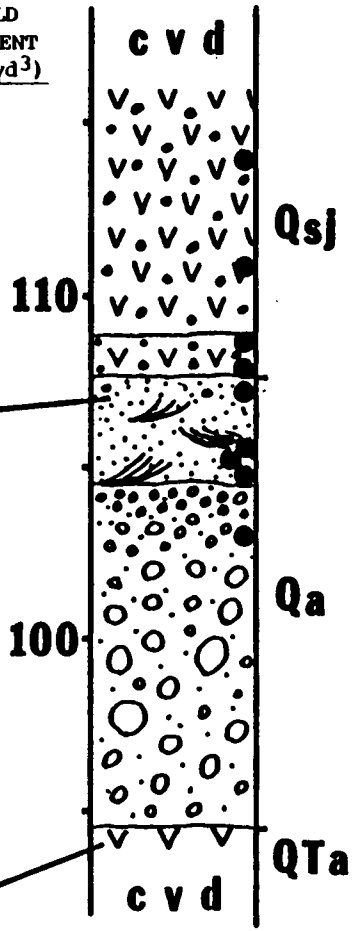

DESCRIPTIONS OF ANALYZED SAMPLES

SJU-6	Mz=0.15mm Max=0.7mm σ=mod.(Q,V,M)
SJU-9	Mz=0.12mm Max=1.0mm σ=mod.(V,Q,Mag,M)
SJU-8	Mz=0.3mm Max=1.0mm σ=mod.(V,Q,Mag,M)
SJU-7	Mz=0.1mm Max=0.9mm σ=good(Q,V,Mag,M)
SJU-10	Mz=0.13mm Max=4.0mm(L,Q,M,Mag)
SJU-2	Mz=0.09mm Max=2.0mm(L,Q,Mag,M,L,B)
SJU-3	Mz=0.09mm Max=2.0mm(L,Q,Mag,M,L,B)
SJU-11	Mz=0.13mm Max=2.0mm(L,Q,Mag,M)
SJU-3/4	Mz=0.13mm Max=0.5mm(Q,L,H,Mag,M)

SANTO DOMINGO I (480 meters, S9E)

DESCRIPTIONS OF STRATIGRAPHIC SECTIONS

GOLD CONTENT (oz/yd^3)

-red-brown ash & volcanic gravel (up to 10cm clasts) weathered to clay.

-red-brown, blocky ash, weathered to clay.

-white ash.

-lense of gray, medium sand (0.25-0.35mm) mostly weathered to clay.

0.003

-cobble to small boulder gravel (average clast is 10cm, maximum clast is 30cm) with brown to tan coarse sand matrix mostly weathered to clay. 1.5m boulders at 74m elevation.

-compact mudstone exposed in sluice.

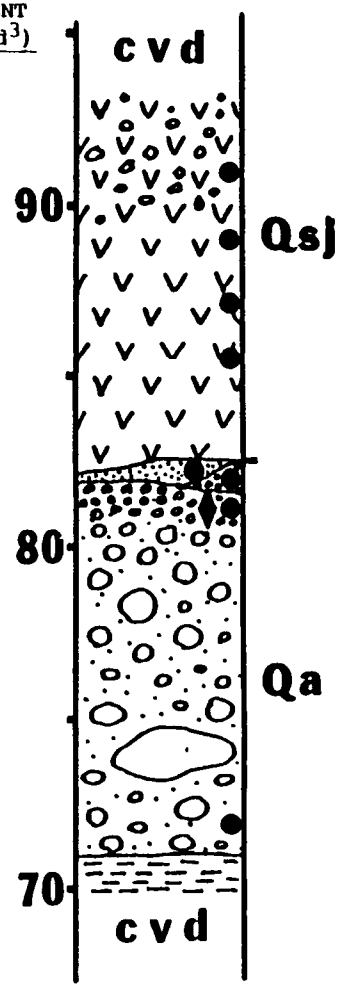

DESCRIPTIONS OF ANALYZED SAMPLES

SD1-1 Mz=0.25mm Max=0.7mm σ=good(V,Q,Mag,M)

SD1-8 Mz=0.14mm Max=2.0mm σ=poor(V,Q,Mag,M)

SD1-7 Mz=0.12mm Max=0.9mm σ=mod/good(V,Q,Mag,M)

SD1-4 Mz=0.13mm Max=1.4mm σ=mod/good(V,Q,Mag,M,H)

SD1-5 Mz=0.25mm Max=8.0mm(L,Q,M,B,Mag)

SD1-6 Mz=0.35mm Max=5.0mm(L,Q,M,Mag)

SD1-3 Mz=0.3mm Max=0.5mm(V,Q,L,M)

SD1-2 Mz=0.18mm Max=0.5mm(Q,V,M,H,L)

SANTO DOMINGO II (670 meters, S21E)

DESCRIPTIONS OF STRATIGRAPHIC SECTIONS

GOLD CONTENT (oz/yd^3)

-ash

-dark blue-gray, blocky, & massive mudstone, well-indurated with iron staining along fractures

-cobble to boulder gravel (avg. clast is 12cm, max.40cm) with gray, coarse sand matrix; pebble gravel at top of unit at contact with mudstone; medium to coarse sand lense with charred wood debris; fine pebble gravel at base of unit in contact with underlying mudstone.

0.027

-light grey, compact mudstone.

-cobble gravel, clasts fine upward; brown coarse sand matrix.

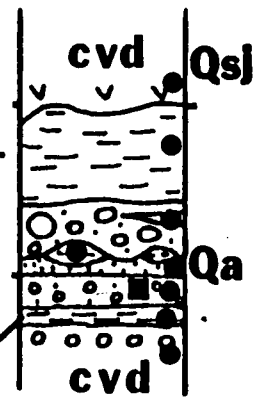

DESCRIPTIONS OF ANALYZED SAMPLES

SD2-5	Mz=0.1mm Max=1.1mm(V,Q,Mag,M)
SD2-4	Mz=0.3mm Max=0.4mm(V,M,H,Q)
SD2-3	Mz=0.24mm Max=0.7mm σ=good(Q,V,B,M,Mag,H)
SD2-1	Mz=0.3mm Max=1.7mm(V,Q,M,Mag)
SD2-2	Mz=0.22mm Max=3mm(L,Q,H,Mag,M,B,wood debris)
SD2-9	Mz=0.1mm Max=0.2mm(V,Q,B,M,H)
SD2-6	Mz=0.4mm Max=0.12mm(V,M,Q)
SD2-7	Mz=0.1mm Max=0.37mm(Q,V,H)

SANTA ANA TERRACE (ORTIZ) (300-600 meters west of Payan)

DESCRIPTIONS OF STRATIGRAPHIC SECTIONS

GOLD CONTENT (oz/yd^3)

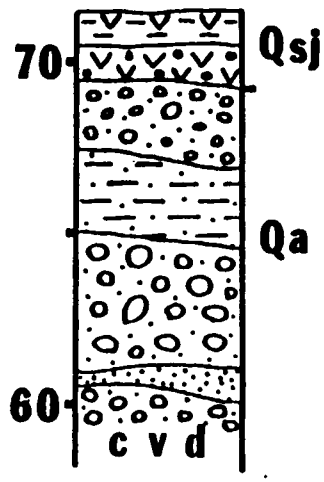

0.000025

0

0.0001
0.0015
0.0001
0.003
0.005
0.009

-weathered ash.
-weathered volcanic gravel & ash.

-cobble gravel (average clast is ∿6cm, with coarse sand matrix, mostly weathered to clay.
-blue-gray mudstone, finely laminated with leaf debris in places along laminae.

-cobble to boulder gravel (average clast is ∿10cm, maximum clast is 35cm) with coarse sand matrix, mostly weathered to clay.
-gray medium-coarse sand with minor wood debris, mostly weathered to clay.

-cobble to boulder gravel (average clast is ∿10cm, maximum clast is ∿30cm) with coarse sand matrix, mostly weathered to clay.

SAN JOAQUIN (1190 meters, S47E)

DESCRIPTIONS OF STRATIGRAPHIC SECTIONS

-brown-red, highly weathered ash.

-white, chalky ash (weathered), with occasional dark gray & white laminae; fining upward in laminae; small-scale slump faulting present in places.

-cobble to boulder gravel with coarse sand & pebble matrix; unweathered.

-white ash.

-cobble to boulder gravel with coarse sand & pebble matrix; unweathered.

GOLD CONTENT (oz/yd^3)

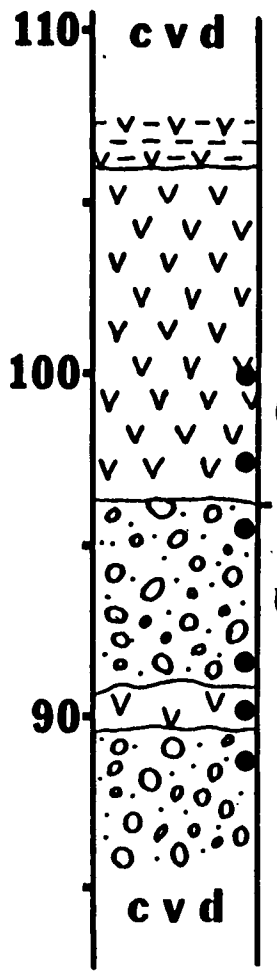

DESCRIPTIONS OF ANALYZED SAMPLES

SJO-1	Mz=0.07mm Max=0.8mm σ=mod.-good(V,Q,Mag,B)
SJO-2	Mz=0.2mm Max=2.0mm(V,Q,Mag)
SJO-5	Mz=0.25mm Max=1.0mm(Q,V,L,B,M)
SJO-4	Mz=0.8mm Max=0.5mm (V,Q,L,M,H)
SJO-6	Mz=0.25mm Max=2.5mm σ=mod.-good(Q,V,Mag,B)
SJO-3	Mz=0.25mm Max=0.7mm(V,Q,L,B)

SITE 6 (DARBY, 1976)(560 meters, S87E)

DESCRIPTIONS OF STRATIGRAPHIC SECTIONS

GOLD CONTENT (oz/yd^3)

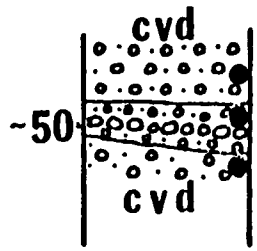

S6-2

S6-1

-pebble gravel with gray sandy matrix (Max: 10cm).

-gray fine pebble gravel (Max: 4cm) with fine sand matrix. Cobble lag interbedded in unit.

-red pebble gravel (Max: 3cm) with fine sand matrix.

TRAVESIA (560 meters, N3W)

DESCRIPTIONS OF STRATIGRAPHIC SECTIONS

GOLD CONTENT (oz/yd^3)

-pink and gray mottled ash.

-bluish-gray compact sand & mud lenses & interlaminae, fines upward; isolated cobbles, pebbles & wood debris; irregular ripple lamination & cut & fill troughs of coarse sand (0.25-0.35mm); weathers to red brown clay.

-basal coarse sand (0.25-0.5mm) with localized concentrations of black sand & large wood debris (up to 2m long); mostly weathered to clay.

-cobble to small boulder gravel with light gray, coarse sand (0.5-0.8mm) matrix; average clast is 6cm & maximum boulder size is 28cm; all degrees of cobble weathering.

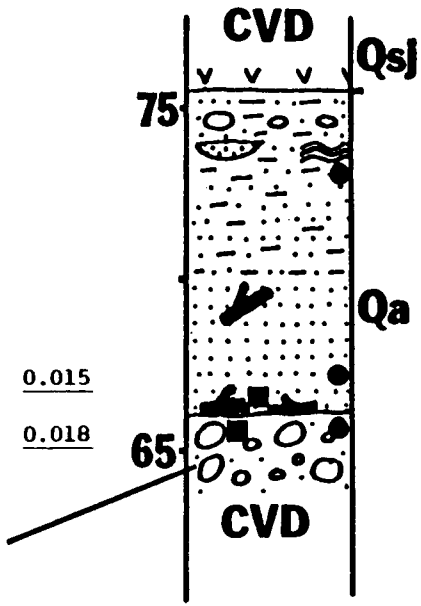

DESCRIPTIONS OF ANALYZED SAMPLES

TRA-1 Mz=0.3mm Max=0.6mm(V,Q,Mag,M,L)

TRA-2 Mz=0.1mm Max=2mm(L,Q,M,Mag,B)

TRA-3 Mz=0.1mm Max=0.8mm(V,Q,L)

APPENDIX B

Cummulative Percent Size Curves for Gold and Black Sand Populations Based on Sieve Analysis

(On each graph broken lines represent gold distributions and solid lines represent black sand distributions)

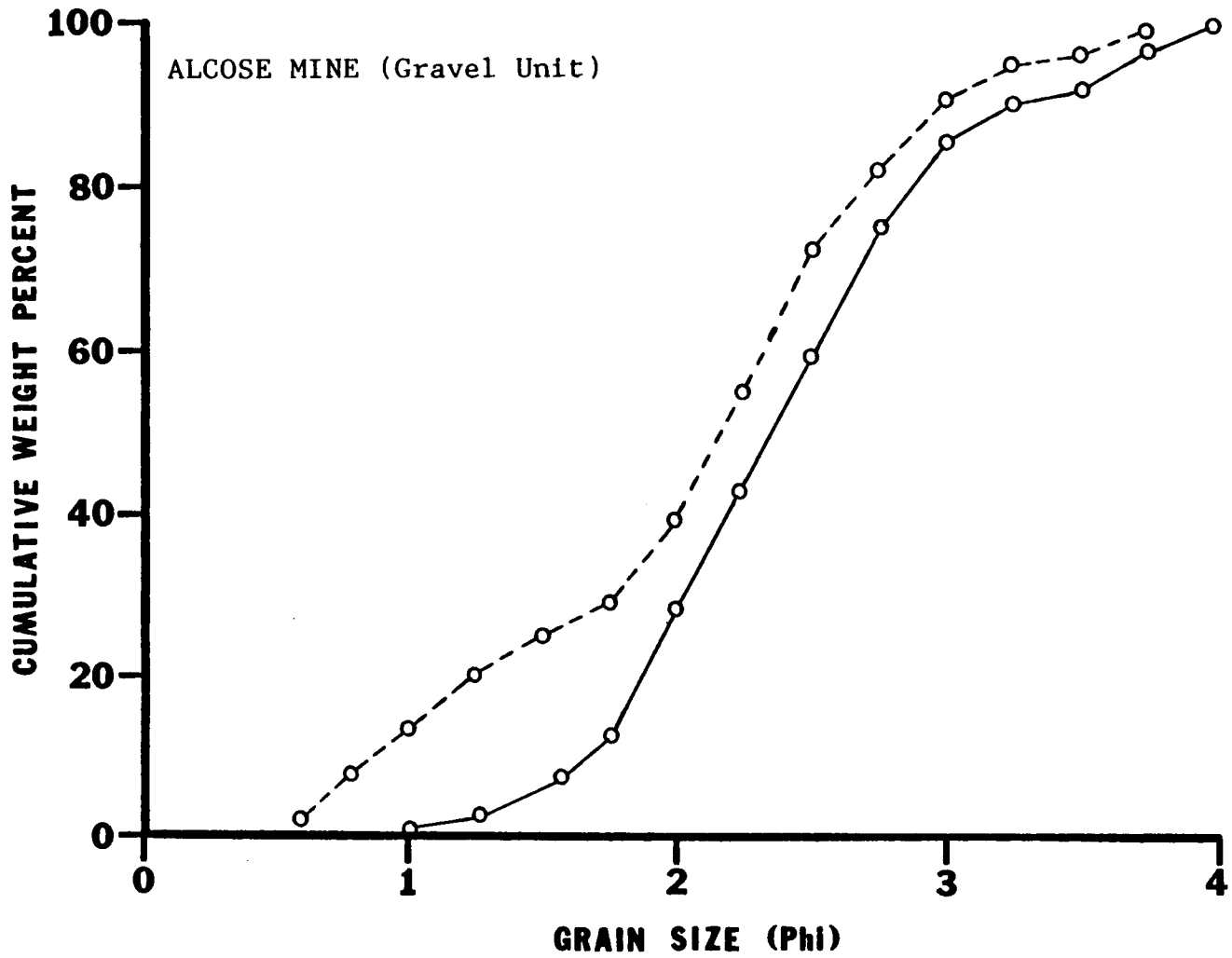
ALCOSE MINE (Gravel Unit)
CUMULATIVE WEIGHT PERCENT
100
80
60
40
20
0
0
1
2
3
4
GRAIN SIZE (Phi)

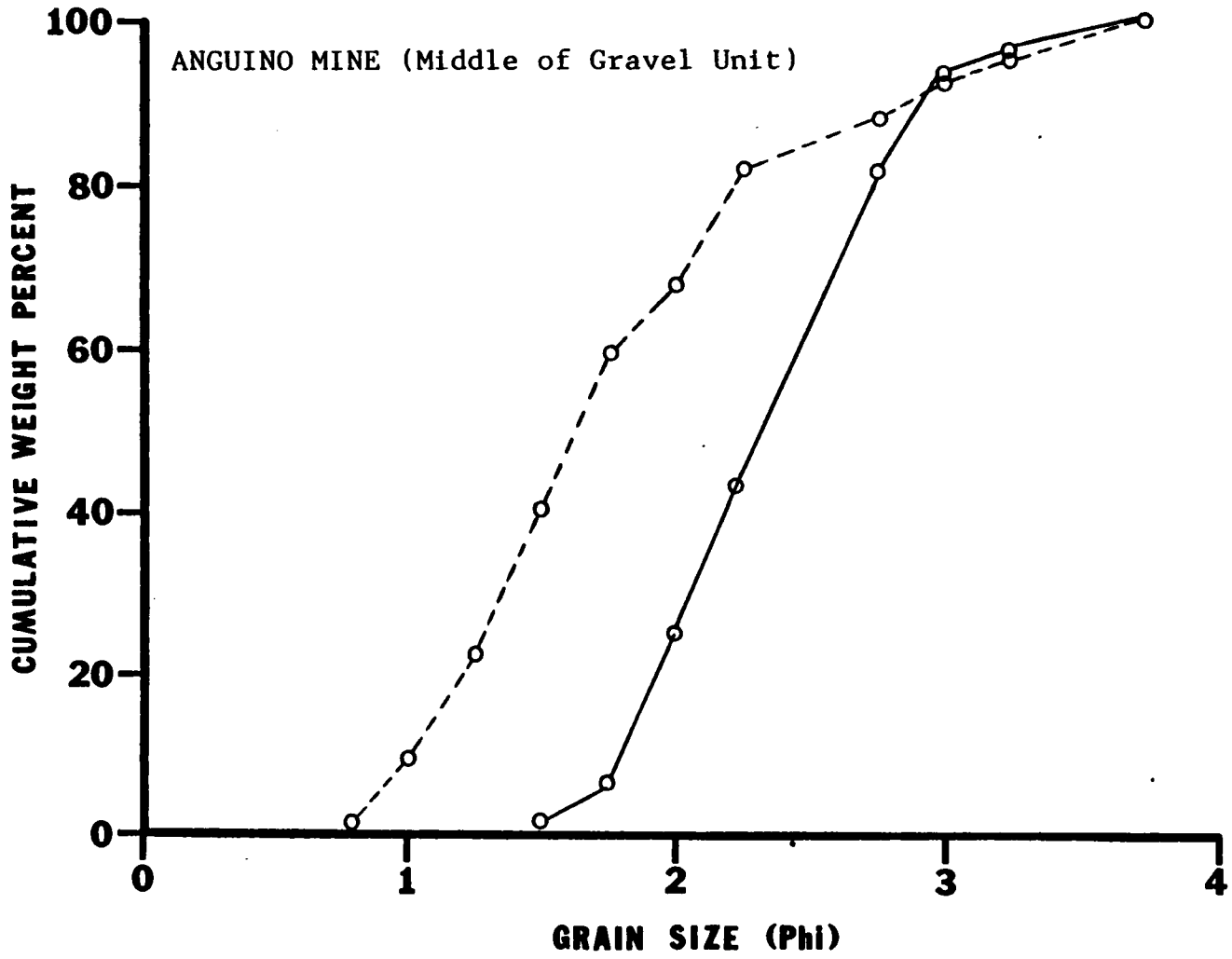
ANGUINO MINE (Middle of Gravel Unit)
CUMULATIVE WEIGHT PERCENT
100
80
60
40
20
0
0
1
2
3
4
GRAIN SIZE (Phi)

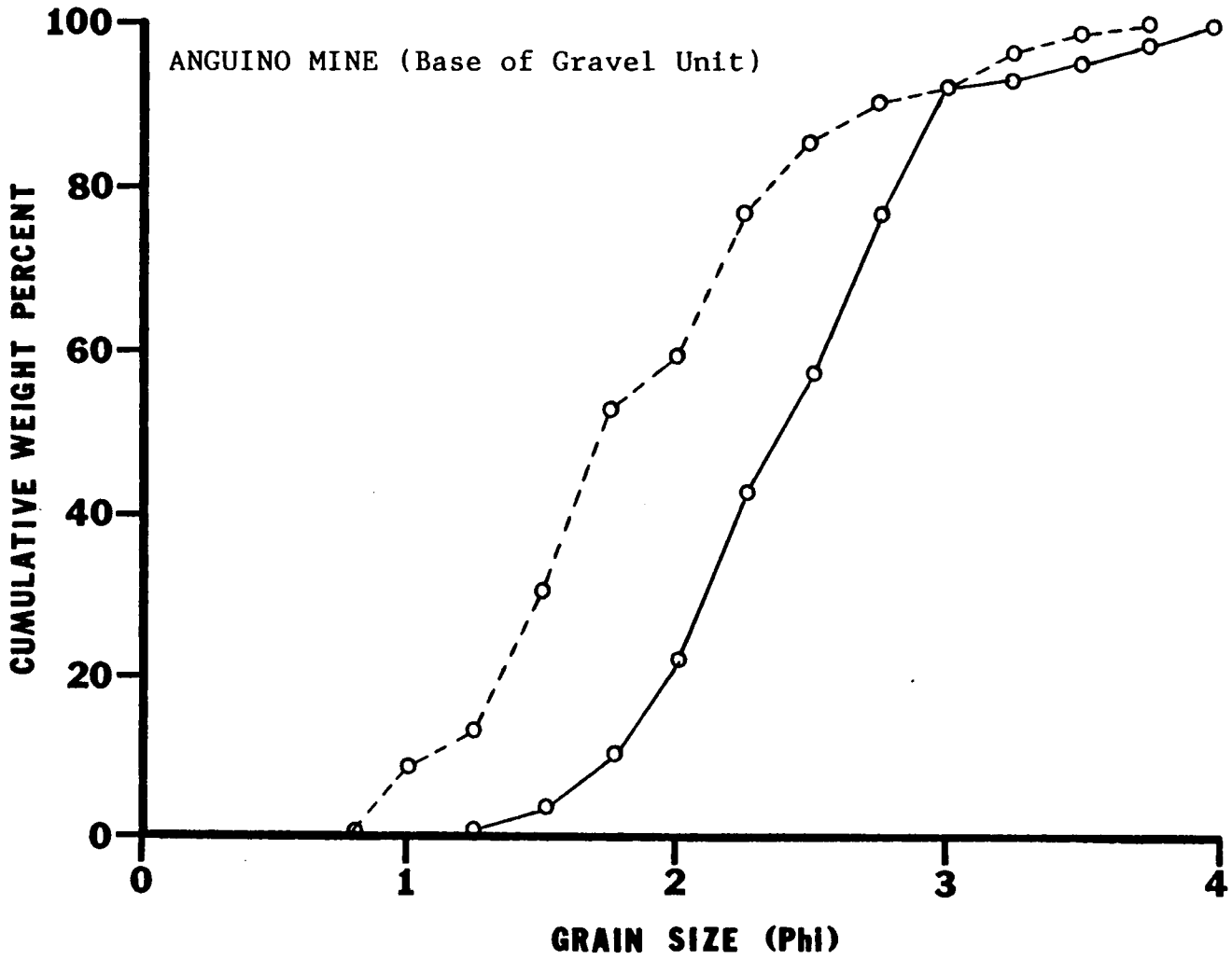
ANGUINO MINE (Base of Gravel Unit)
CUMULATIVE WEIGHT PERCENT
100
80
60
40
20
0
0
1
2
3
4
GRAIN SIZE (Phi)

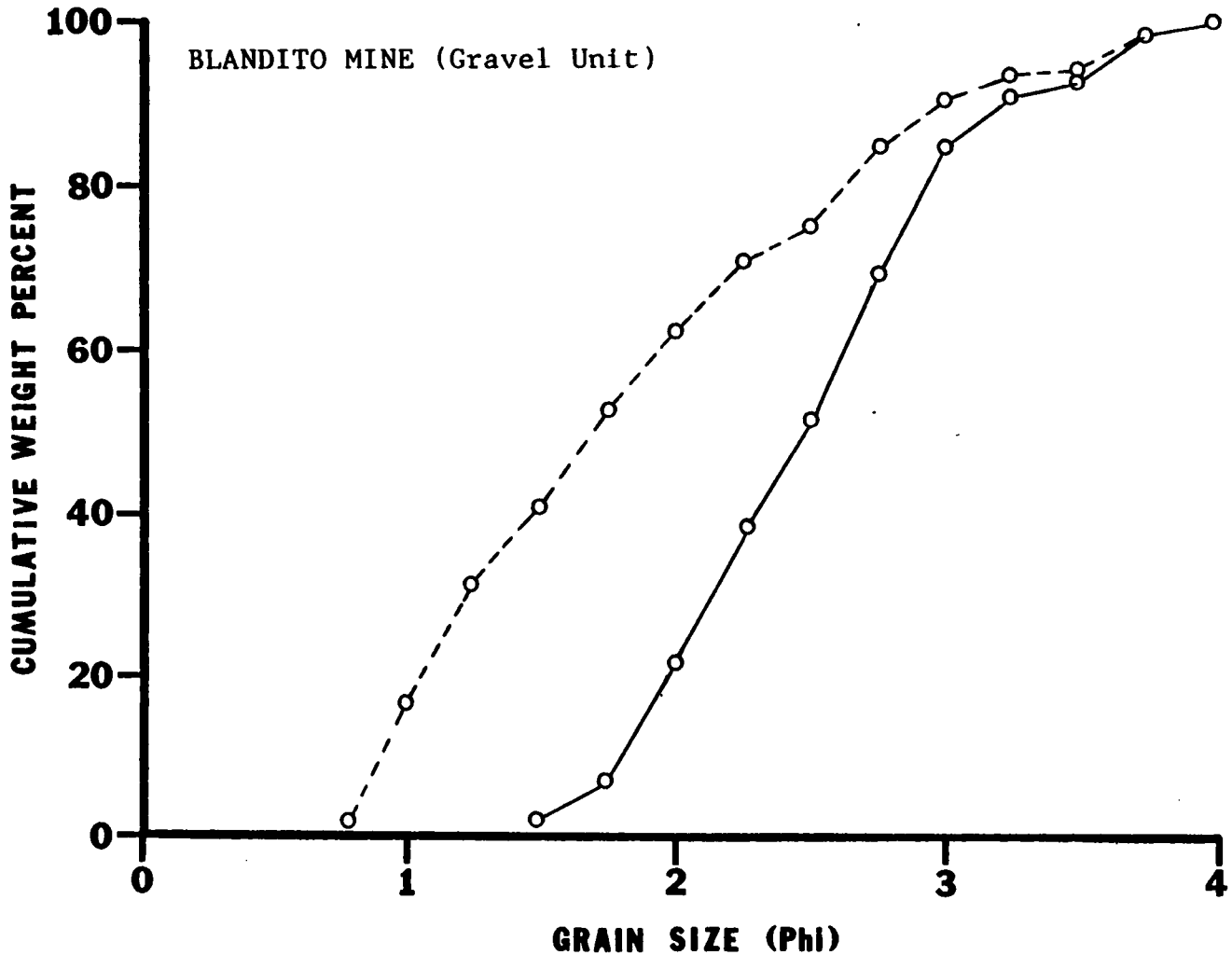
BLANDITO MINE (Gravel Unit)
CUMULATIVE WEIGHT PERCENT
100
80
60
40
20
0
0
1
2
3
4
GRAIN SIZE (Phi)

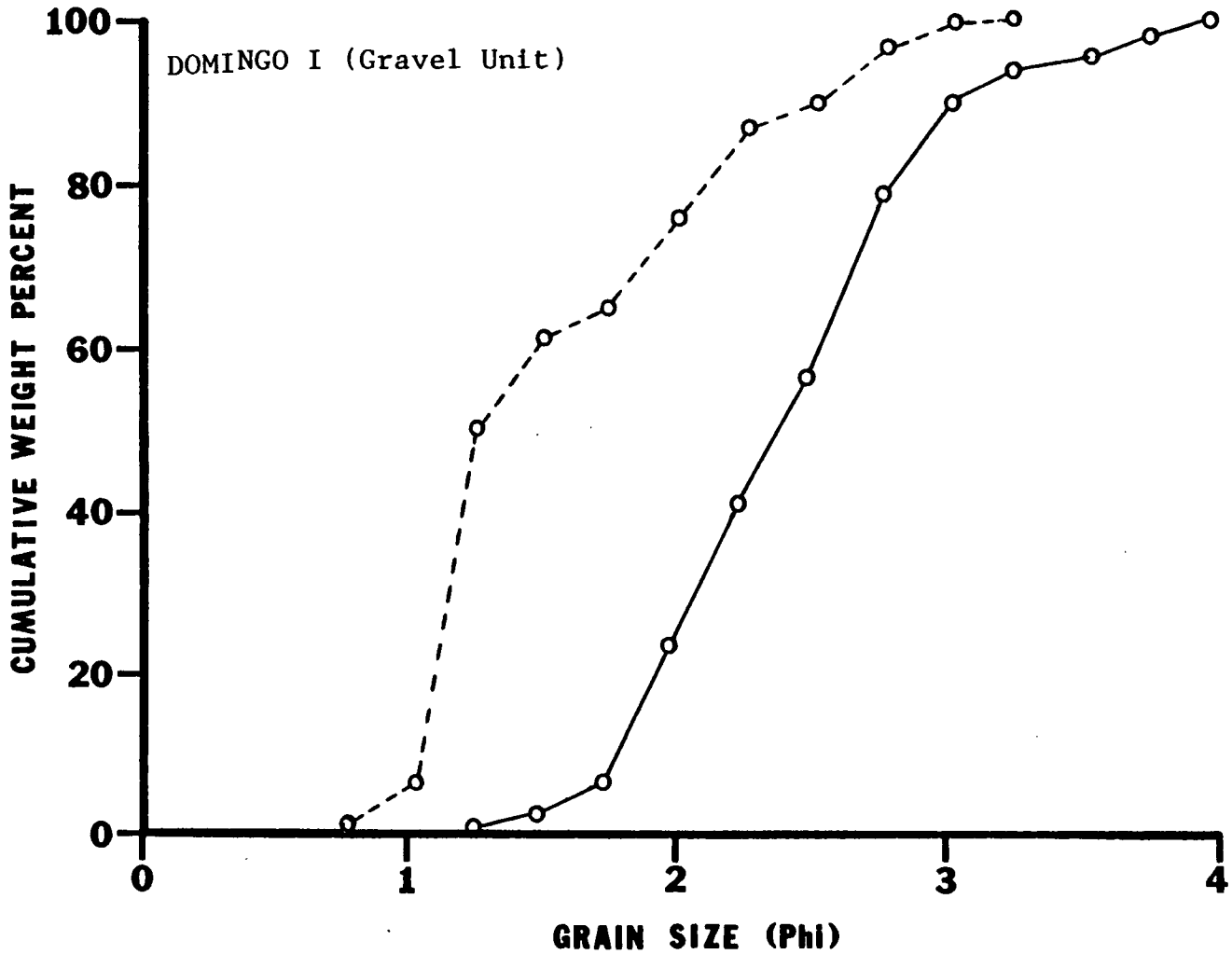
DOMINGO I (Gravel Unit)
CUMULATIVE WEIGHT PERCENT
100
80
60
40
20
0
0
1
2
3
4
GRAIN SIZE (Phi)

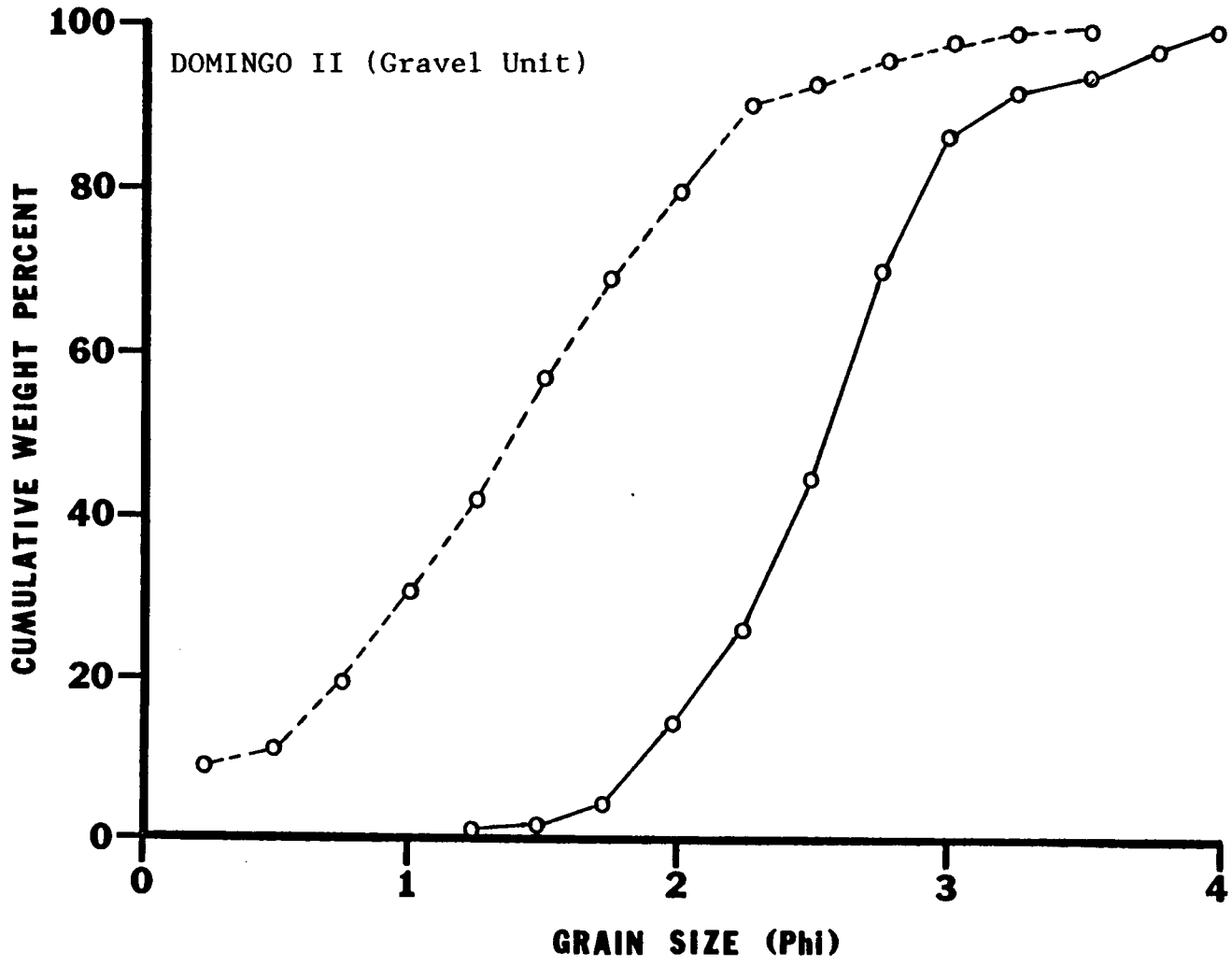
DOMINGO II (Gravel Unit)
CUMULATIVE WEIGHT PERCENT
100
80
60
40
20
0
0
1
2
3
4
GRAIN SIZE (Phi)

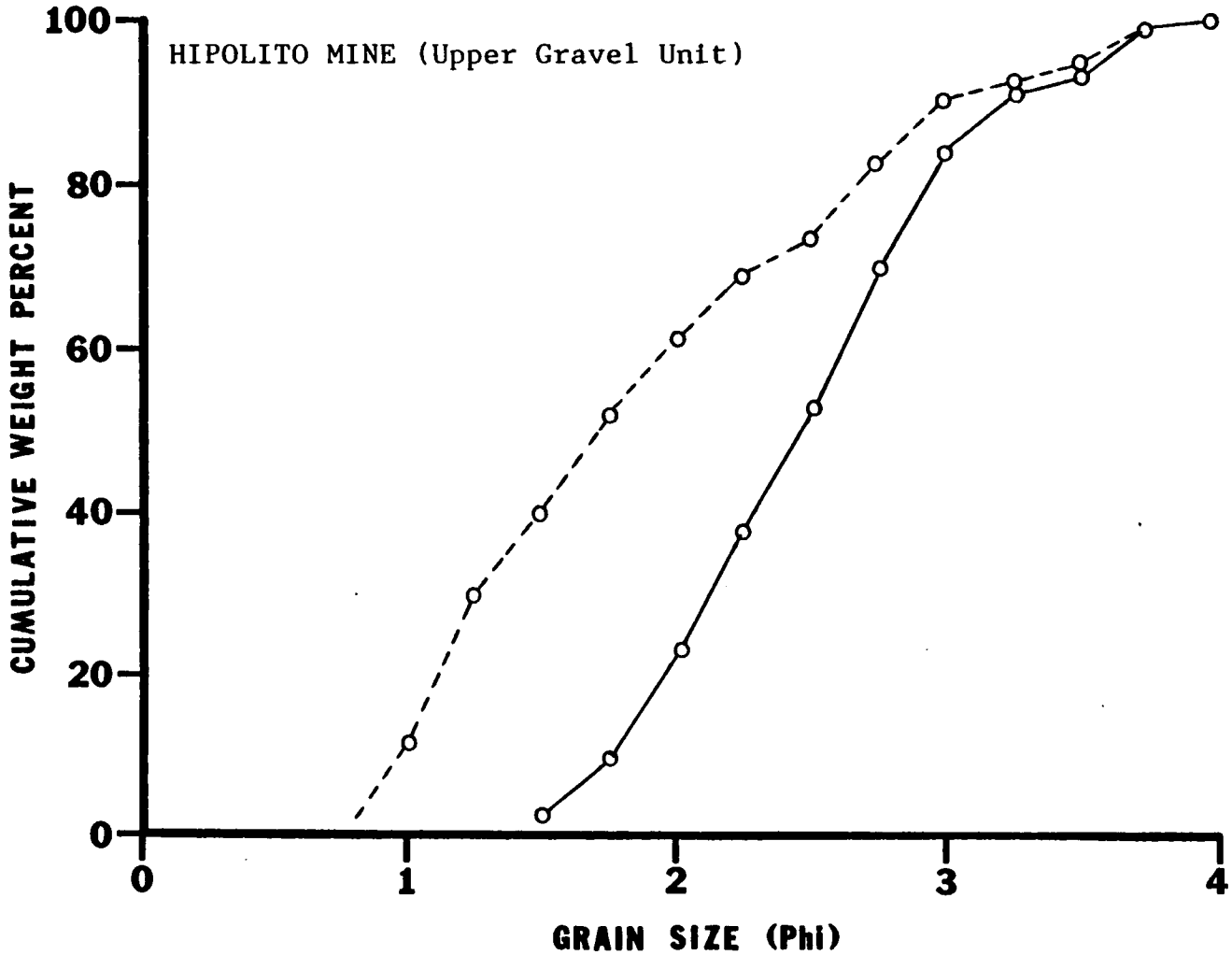
HIPOLITO MINE (Upper Gravel Unit)
CUMULATIVE WEIGHT PERCENT
100
80
60
40
20
0
0
1
2
3
4
GRAIN SIZE (Phi)

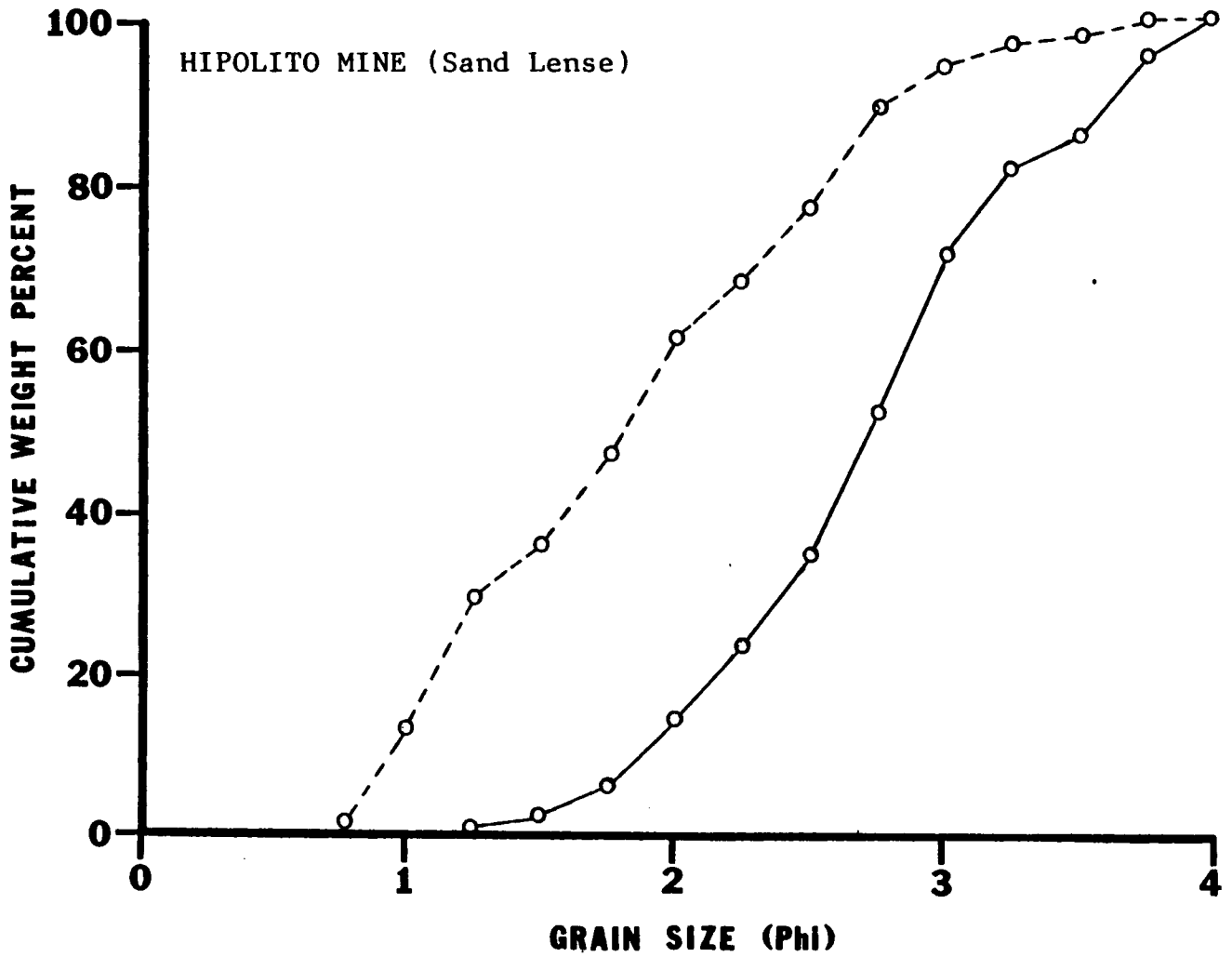
HIPOLITO MINE (Sand Lense)
CUMULATIVE WEIGHT PERCENT
100
80
60
40
20
0
0
1
2
3
4
GRAIN SIZE (Phi)

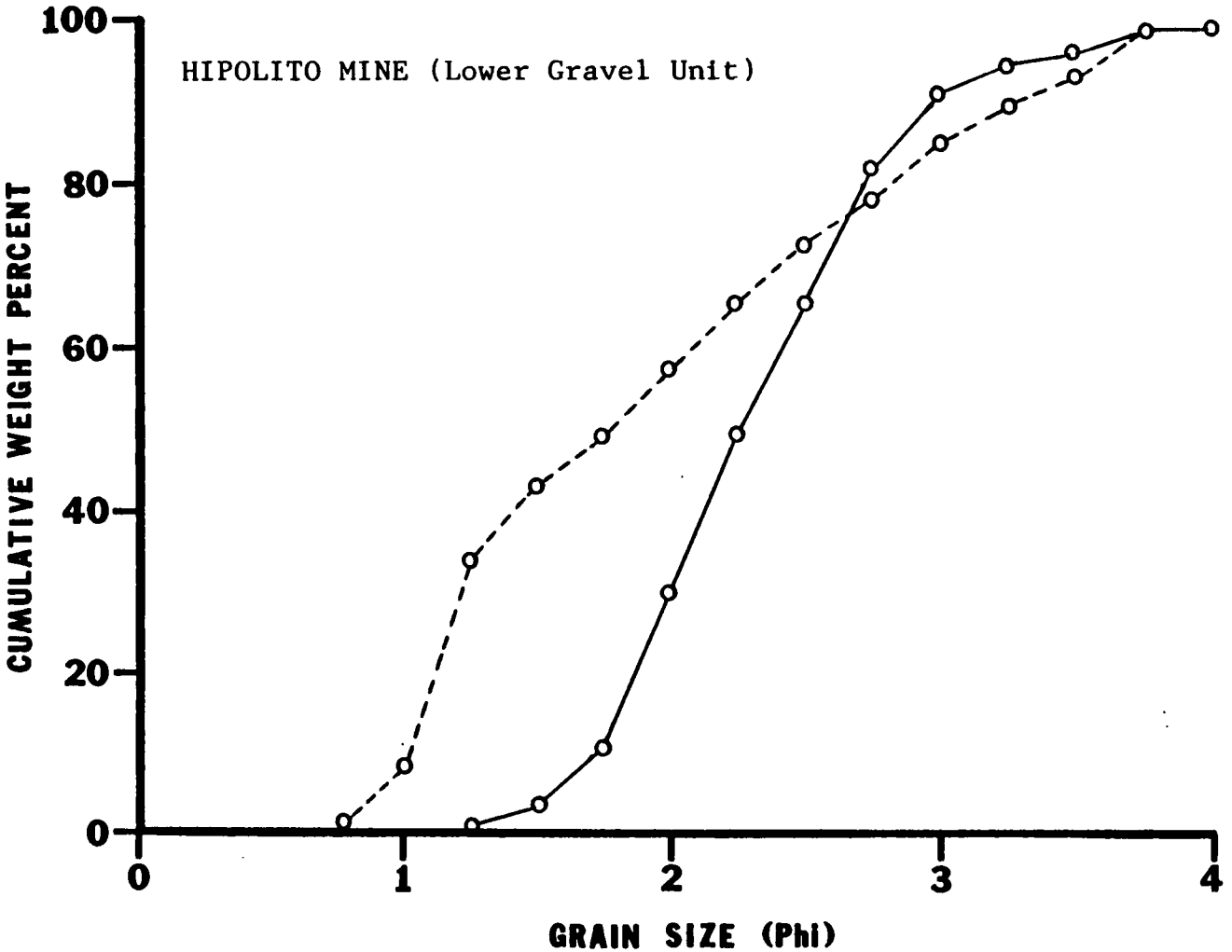
HIPOLITO MINE (Lower Gravel Unit)
CUMULATIVE WEIGHT PERCENT
100
80
60
40
20
0
0
1
2
3
4
GRAIN SIZE (Phi)

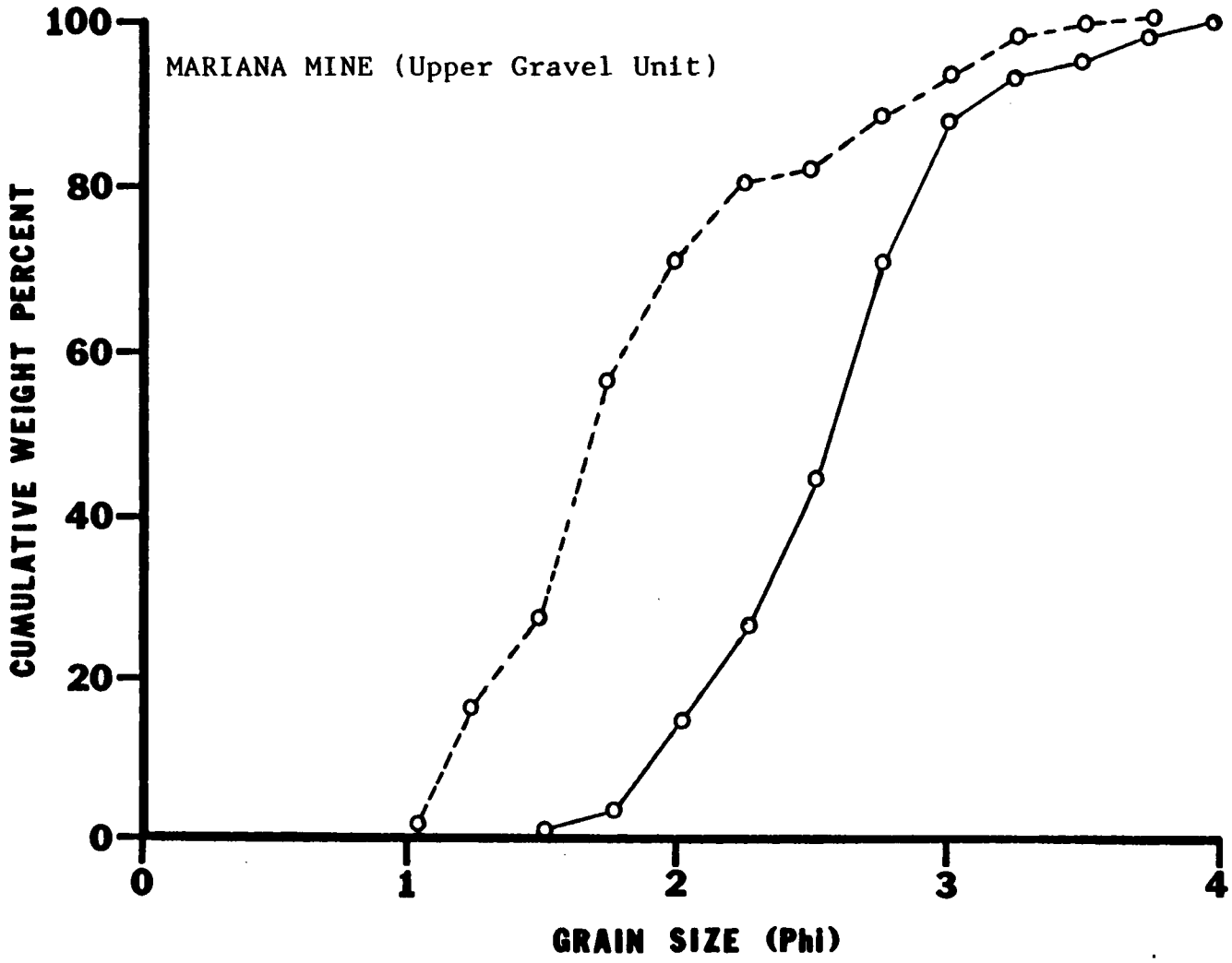
MARIANA MINE (Upper Gravel Unit)
CUMULATIVE WEIGHT PERCENT
100
80
60
40
20
0
0
1
2
3
4
GRAIN SIZE (Phi)

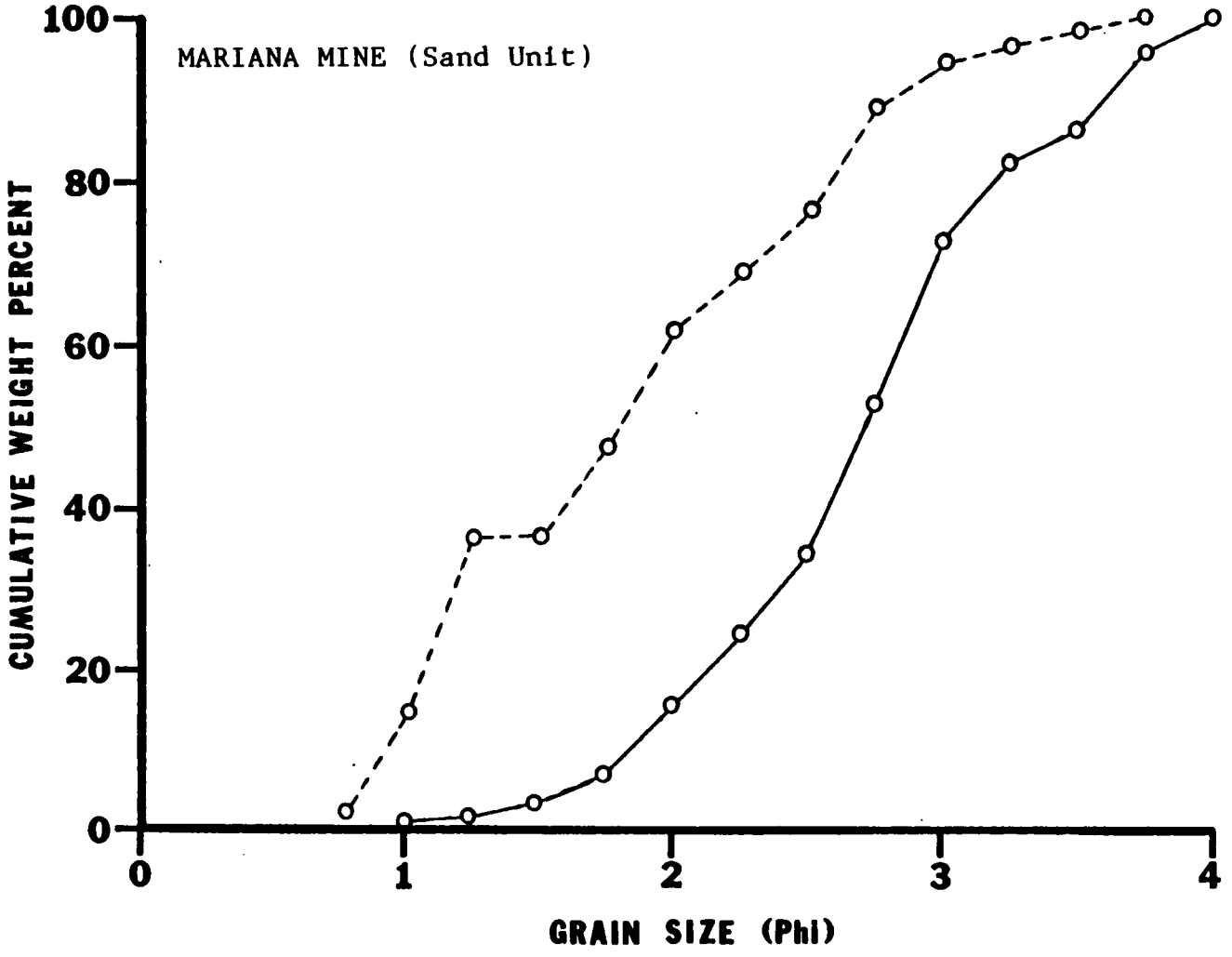
MARIANA MINE (Sand Unit)
CUMULATIVE WEIGHT PERCENT
100
80
60
40
20
0
0
1
2
3
4
GRAIN SIZE (Phi)

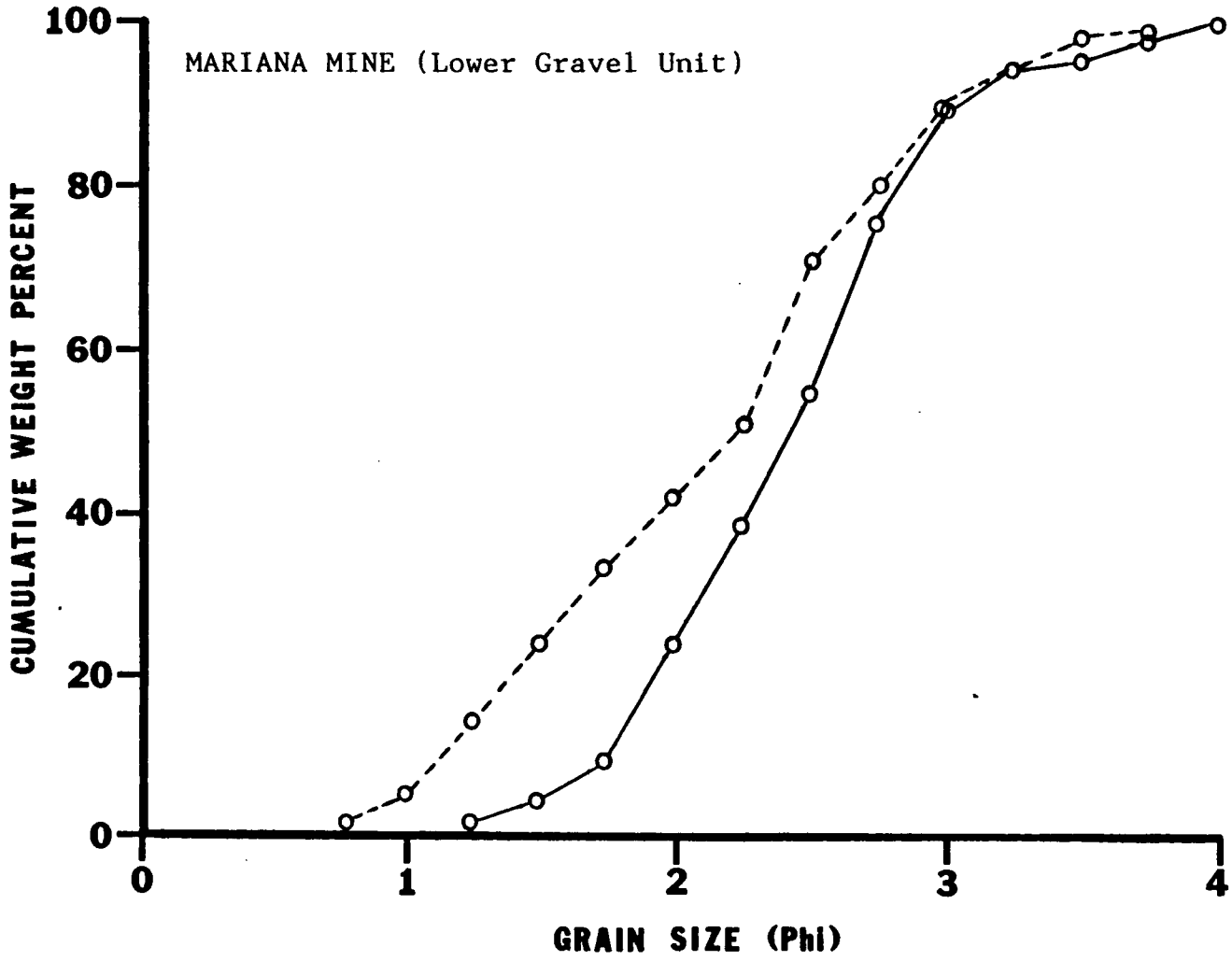
MARIANA MINE (Lower Gravel Unit)
CUMULATIVE WEIGHT PERCENT
100
80
60
40
20
0
0
1
2
3
4
GRAIN SIZE (Phi)

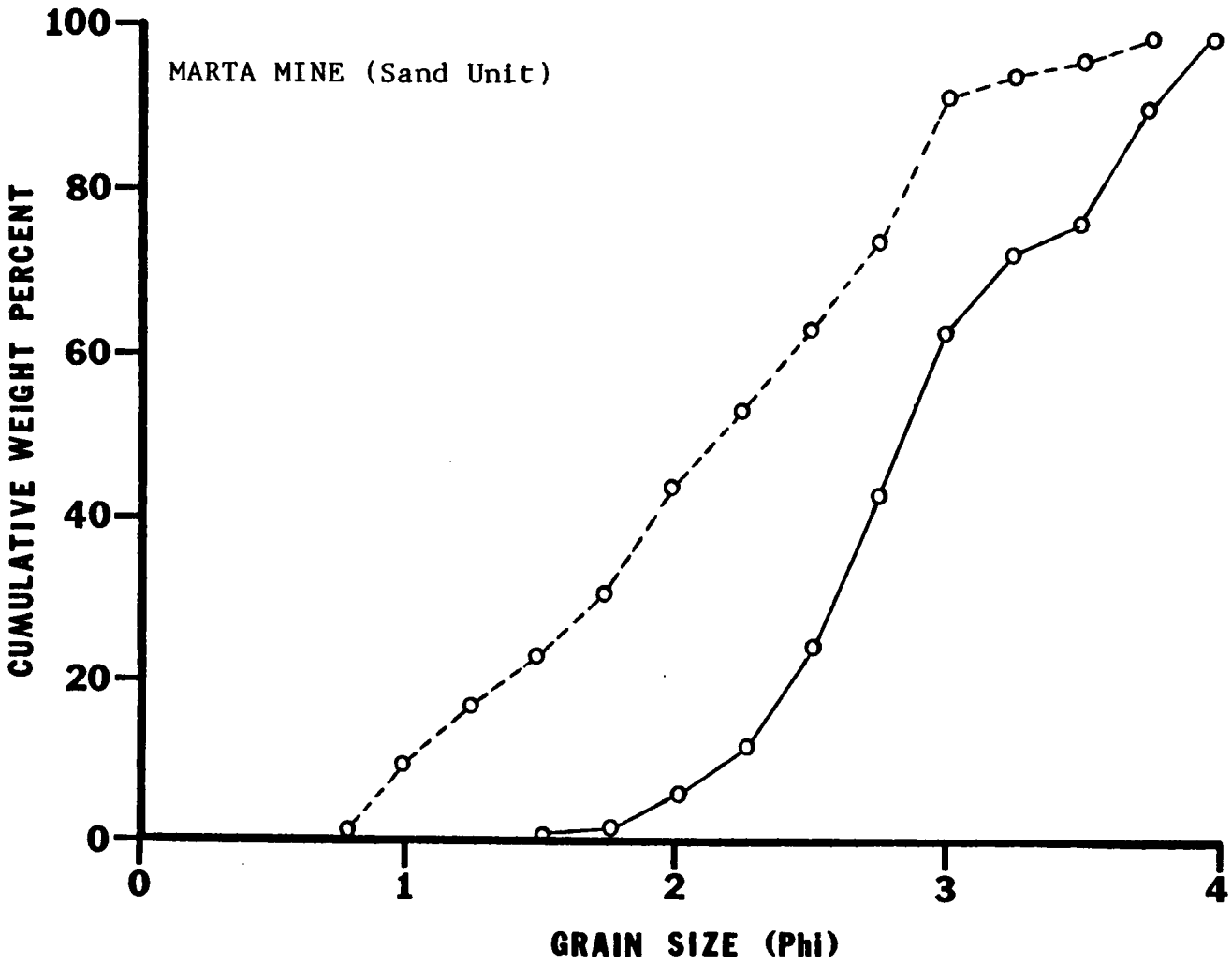
MARTA MINE (Sand Unit)
CUMULATIVE WEIGHT PERCENT
100
80
60
40
20
0
0
1
2
3
4
GRAIN SIZE (Phi)

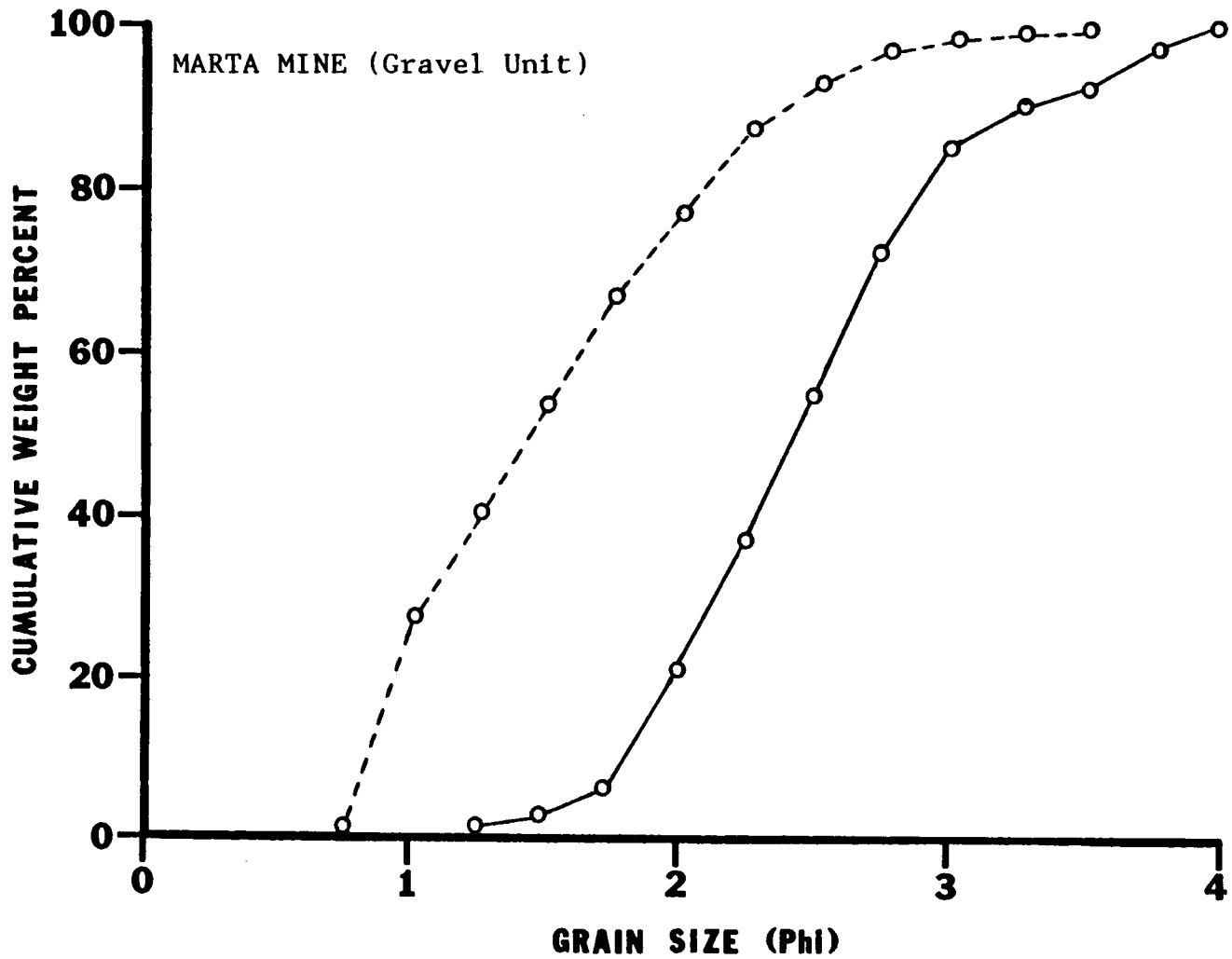
MARTA MINE (Gravel Unit)
CUMULATIVE WEIGHT PERCENT
100
80
60
40
20
0
0
1
2
3
4
GRAIN SIZE (Phi)

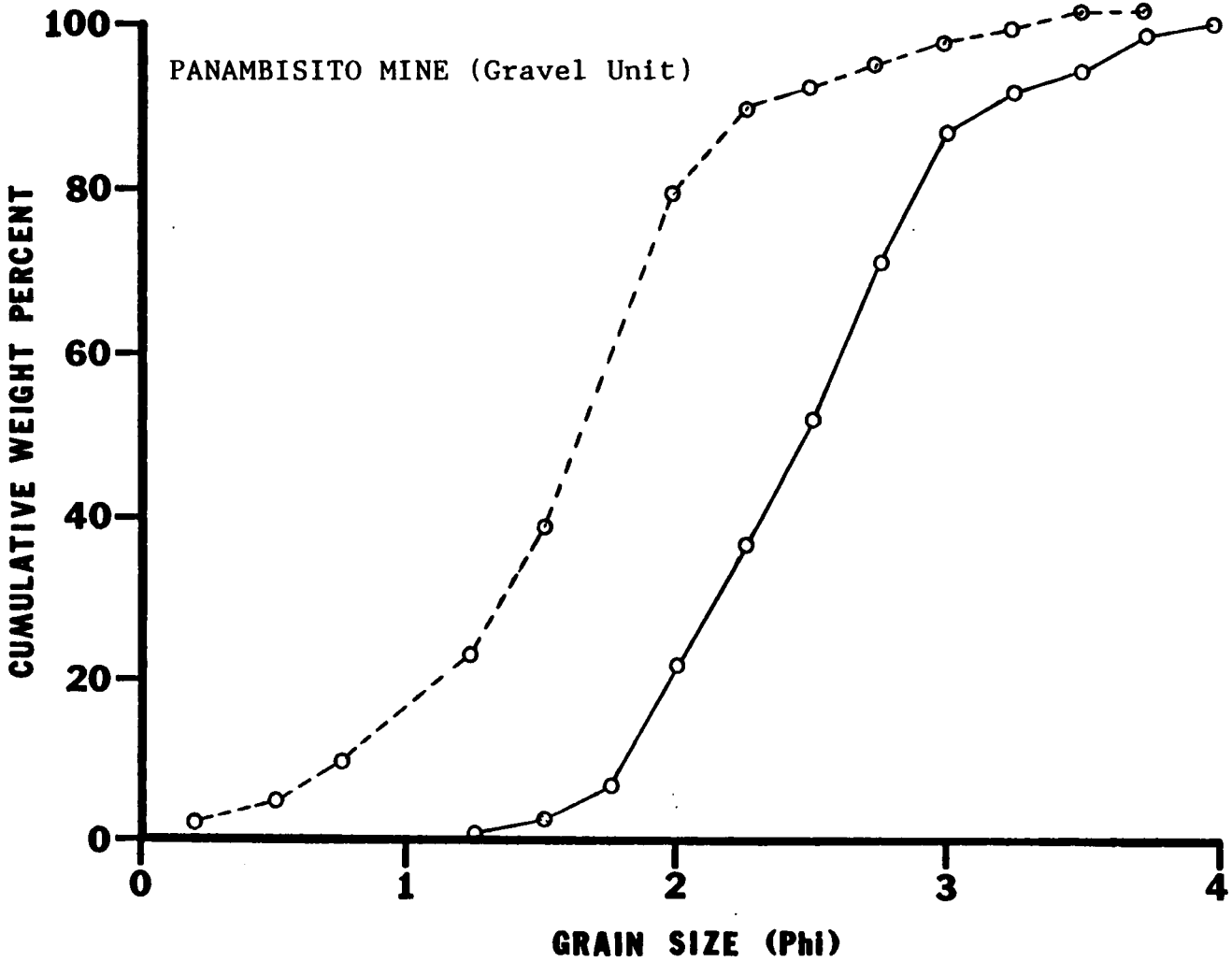
PANAMBISITO MINE (Gravel Unit)
CUMULATIVE WEIGHT PERCENT
100
80
60
40
20
0
0
1
2
3
4
GRAIN SIZE (Phi)

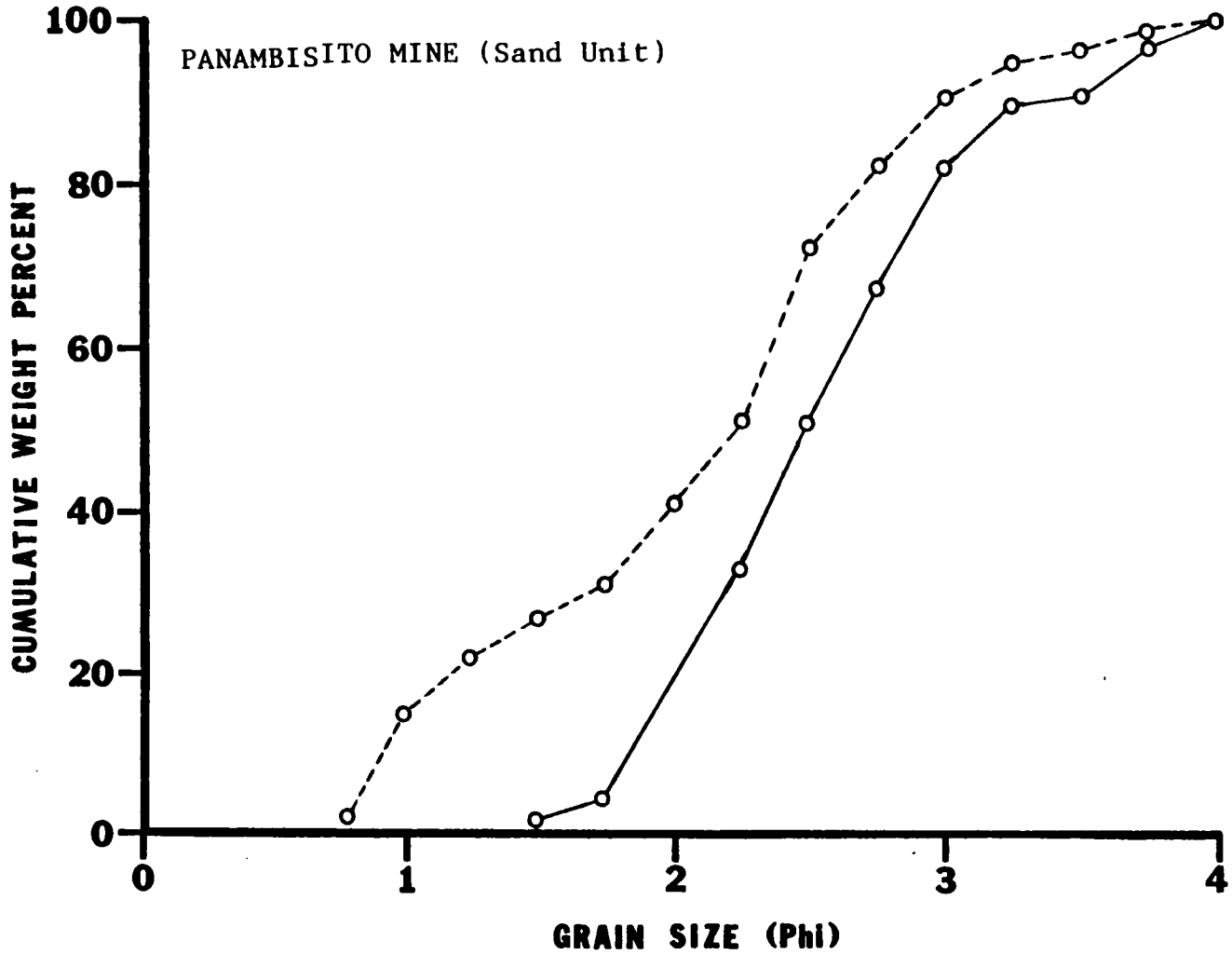
PANAMBISITO MINE (Sand Unit)
CUMULATIVE WEIGHT PERCENT
100
80
60
40
20
0
0
1
2
3
4
GRAIN SIZE (Phi)

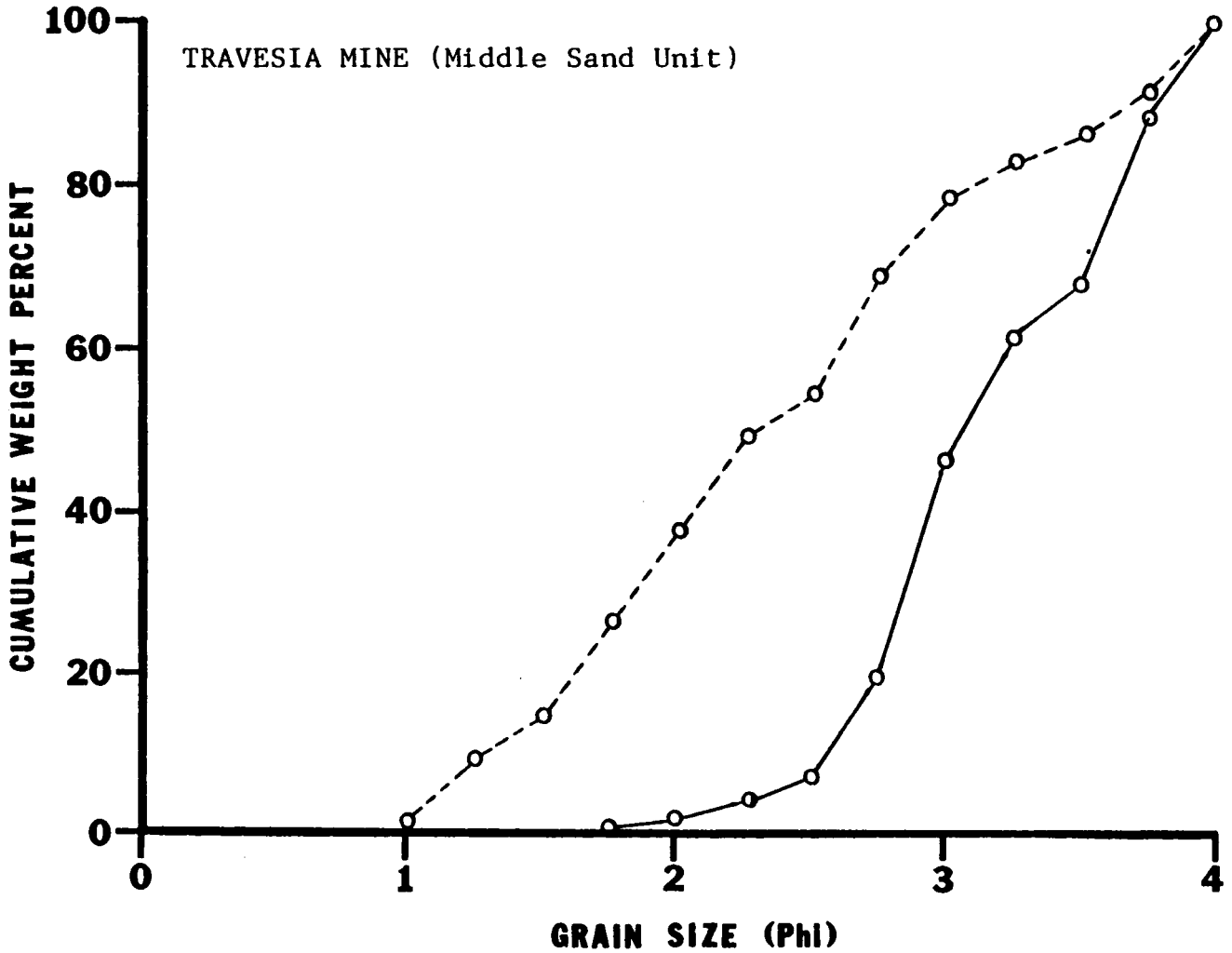
TRAVESIA MINE (Middle Sand Unit)
CUMULATIVE WEIGHT PERCENT
100
80
60
40
20
0
0
1
2
3
4
GRAIN SIZE (Phi)

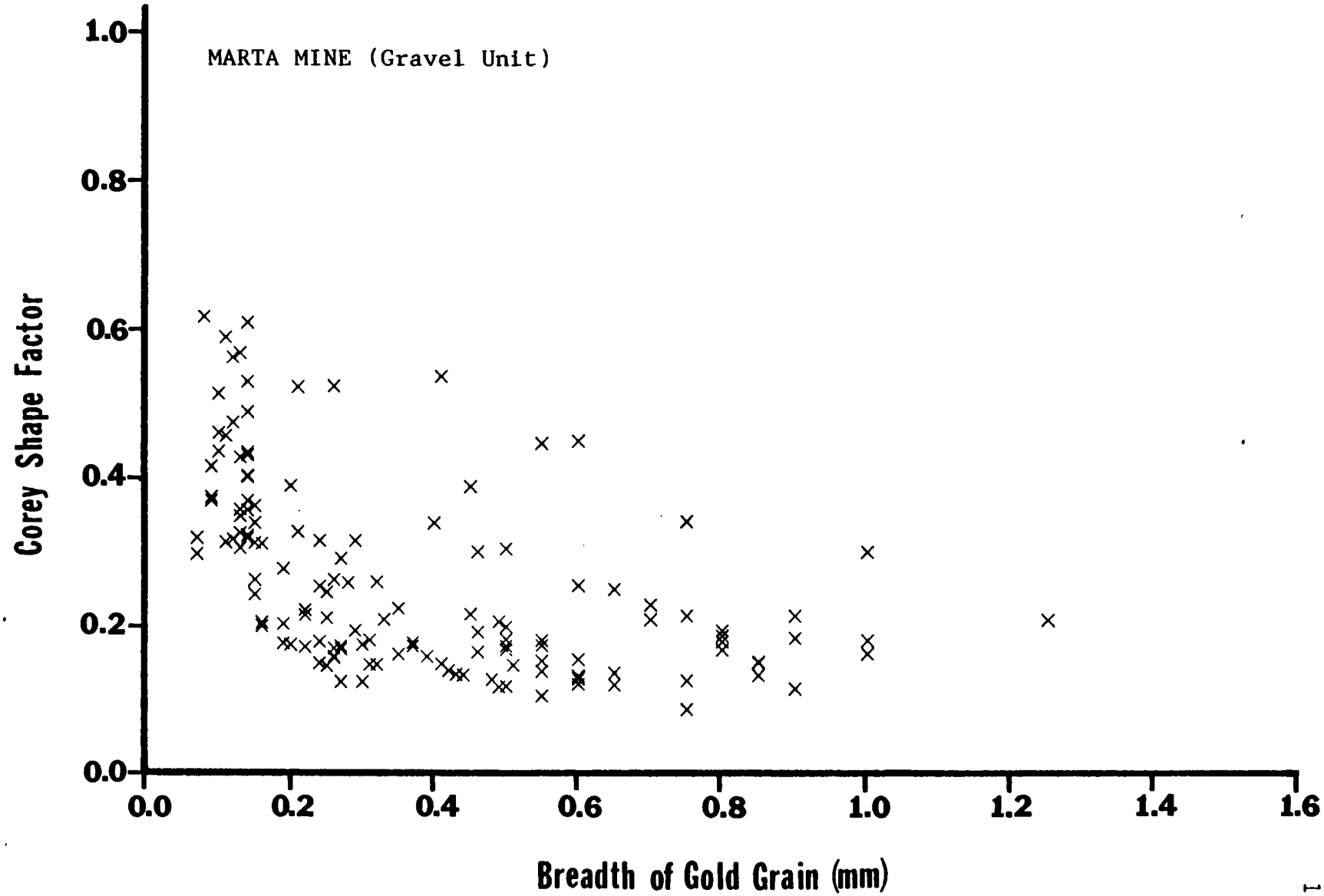
MARTA MINE (Gravel Unit)
Corey Shape Factor
1.0
0.8
0.6
0.4
0.2
0.0
0.0
0.2
0.4
0.6
0.8
1.0
1.2
1.4
1.6
Breadth of Gold Grain (mm)

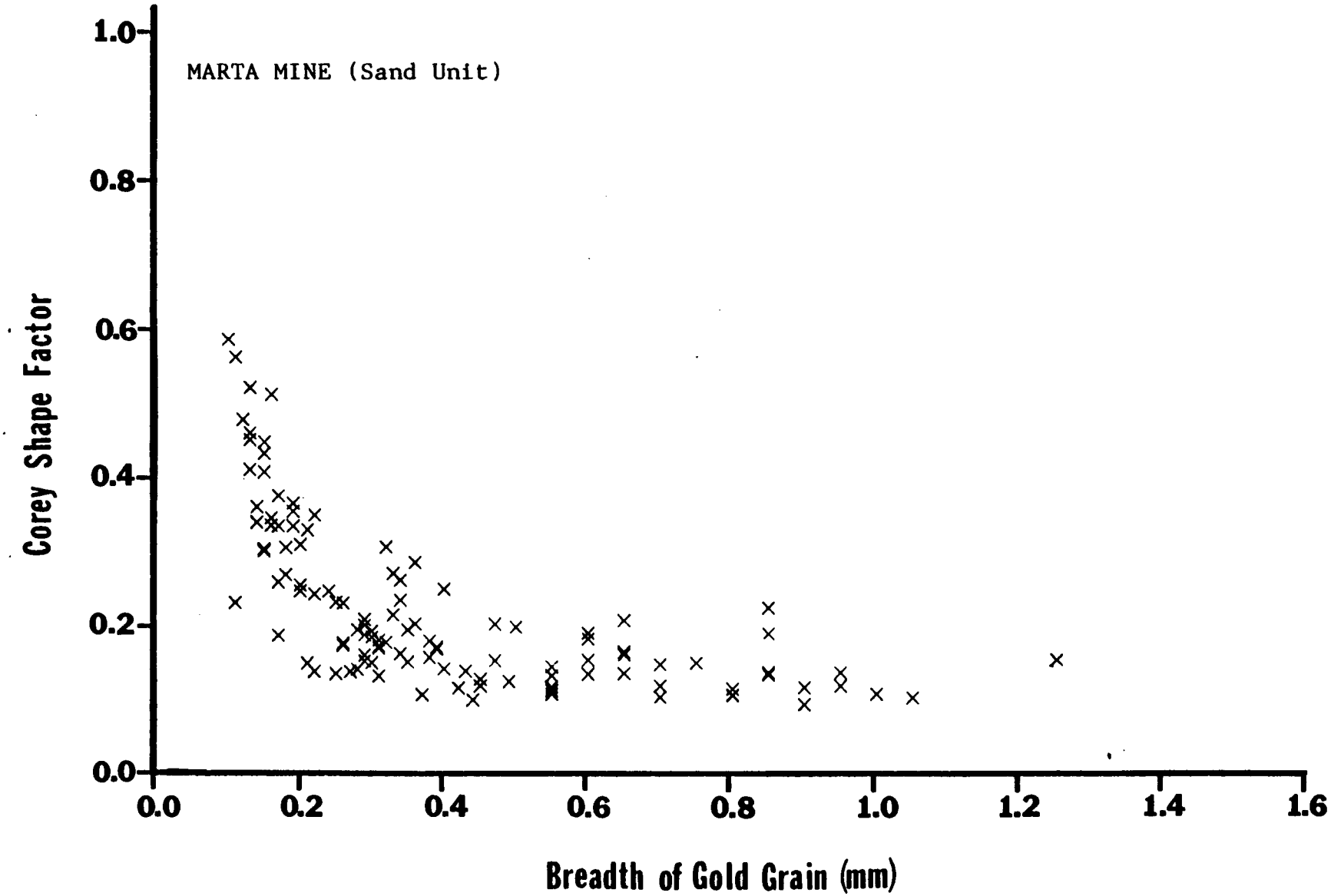
MARTA MINE (Sand Unit)
Corey Shape Factor
1.0
0.8
0.6
0.4
0.2
0.0
0.0
0.2
0.4
0.6
0.8
1.0
1.2
1.4
1.6
Breadth of Gold Grain (mm)

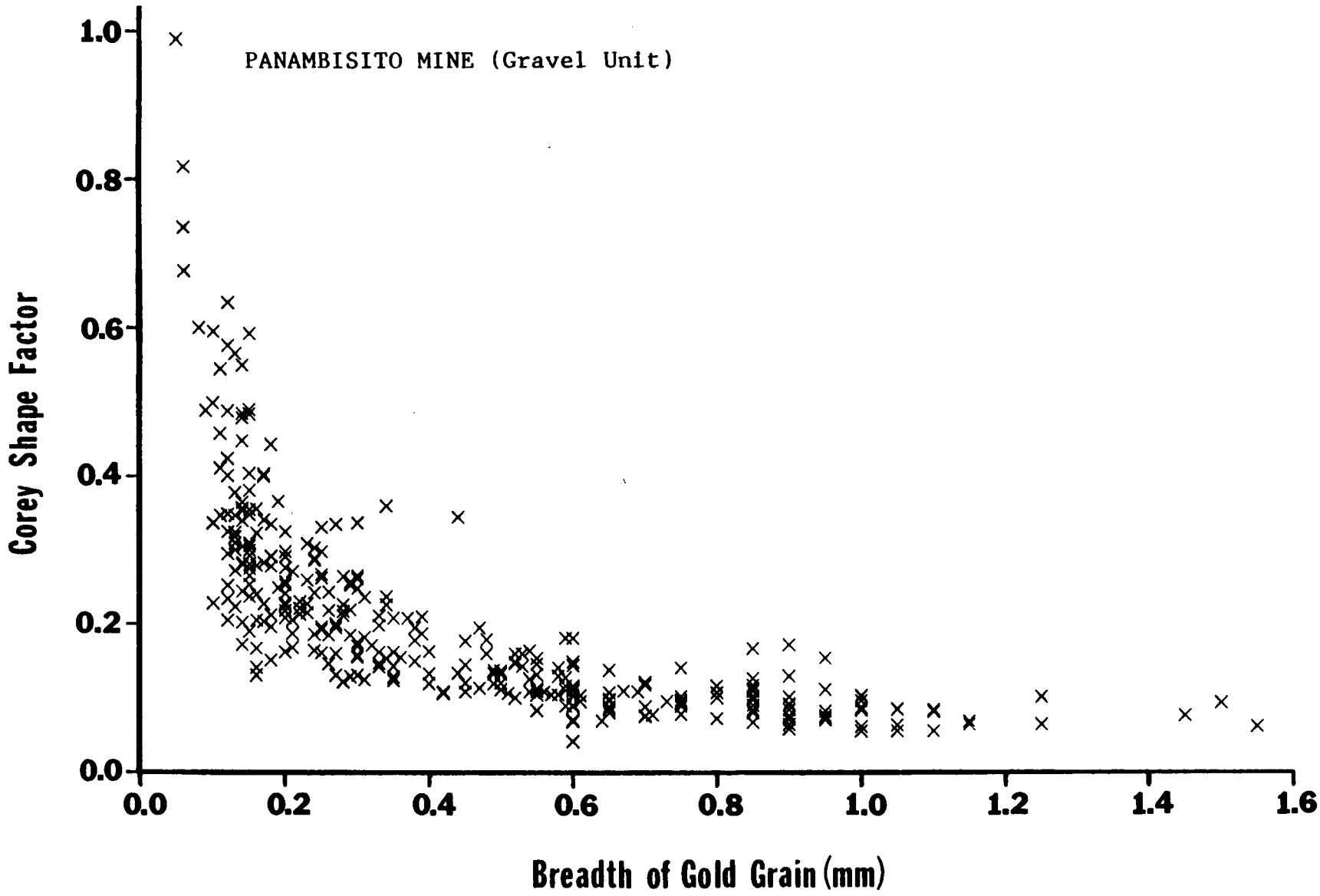
PANAMBISITO MINE (Gravel Unit)
Corey Shape Factor
1.0
0.8
0.6
0.4
0.2
0.0
0.0
0.2
0.4
0.6
0.8
1.0
1.2
1.4
1.6
Breadth of Gold Grain (mm)

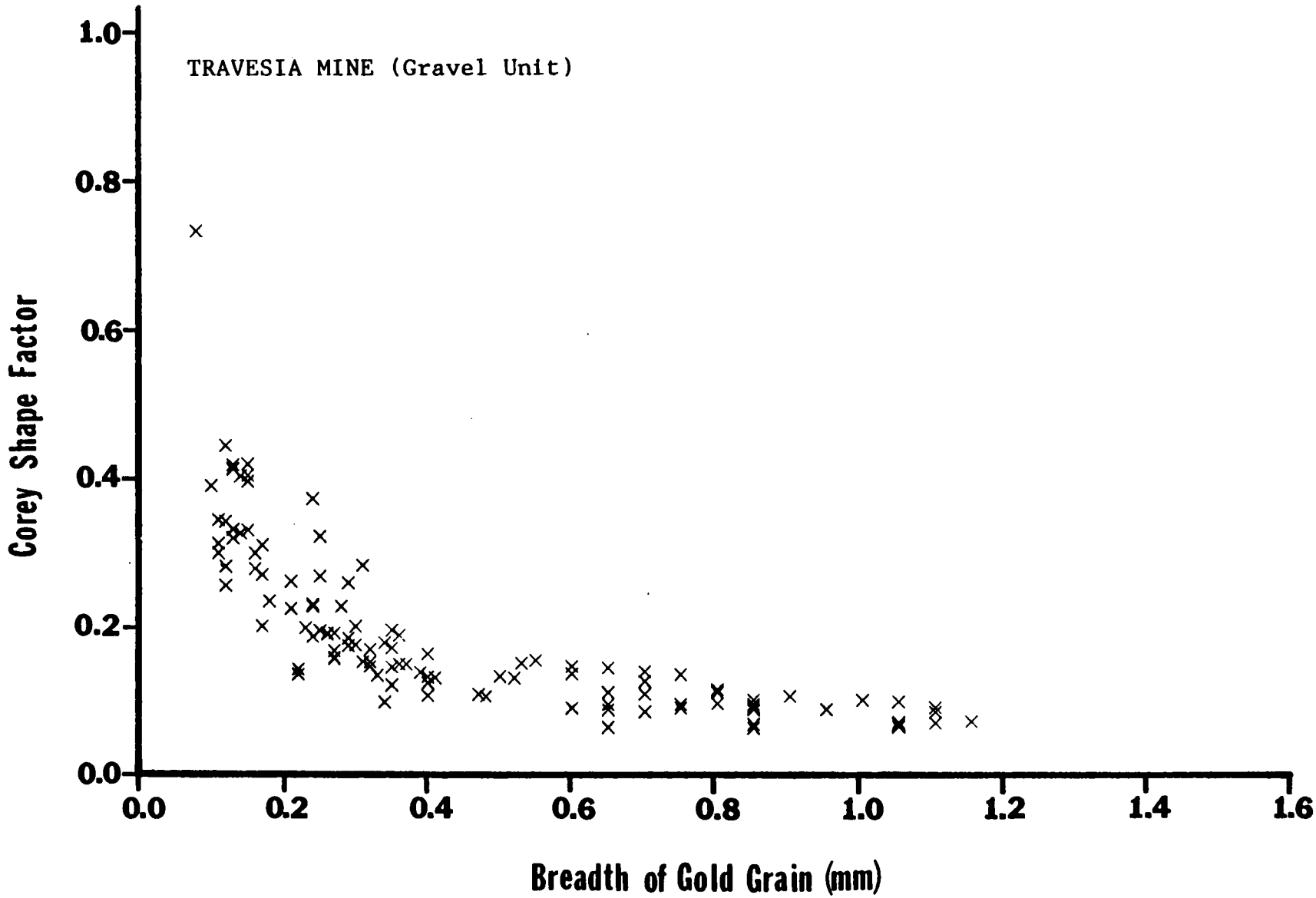
TRAVESIA MINE (Gravel Unit)
Corey Shape Factor
1.0
0.8
0.6
0.4
0.2
0.0
0.0
0.2
0.4
0.6
0.8
1.0
1.2
1.4
1.6
Breadth of Gold Grain (mm)

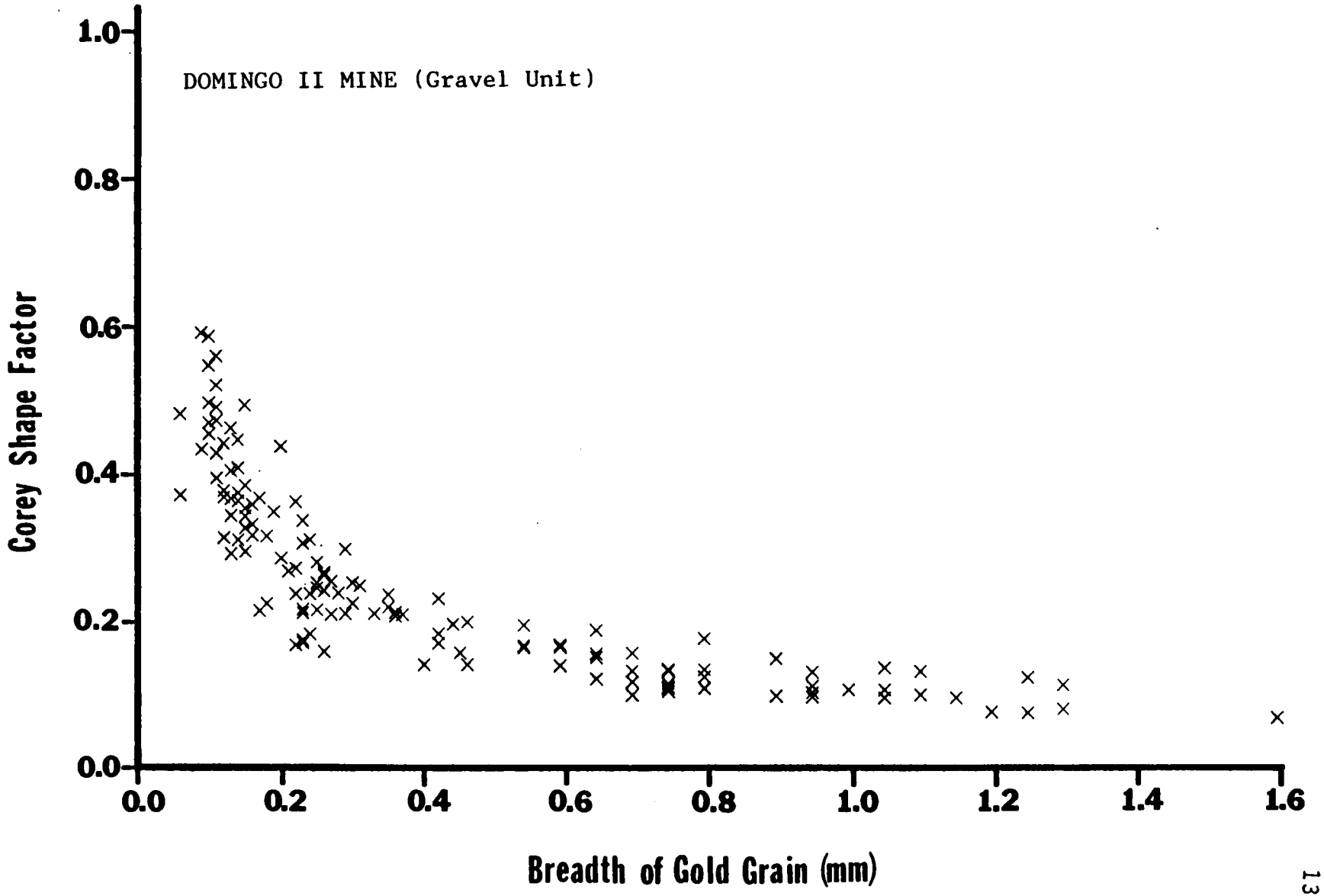
DOMINGO II MINE (Gravel Unit)
Corey Shape Factor
1.0
0.8
0.6
0.4
0.2
0.0
0.0
0.2
0.4
0.6
0.8
1.0
1.2
1.4
1.6
Breadth of Gold Grain (mm)

APPENDIX D

Cummulative Percent Size Curves for Gold and Black Sand Populations Based on Settling Velocities (RSA)

(On each graph broken lines represent gold populations solid lines represent black sand populations)

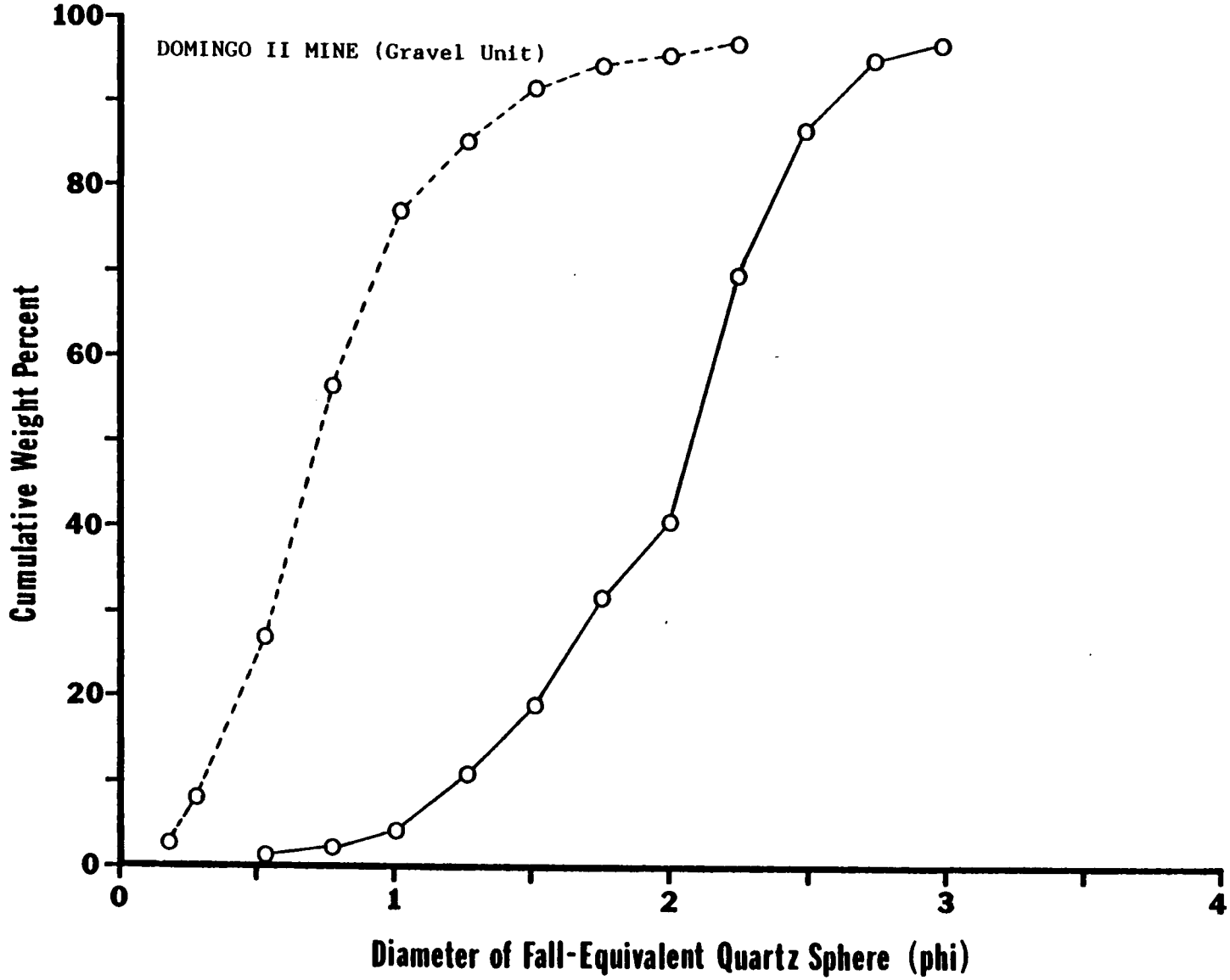
DOMINGO II MINE (Gravel Unit)
Cumulative Weight Percent
100
80
60
40
20
0
0
1
2
3
4
Diameter of Fall-Equivalent Quartz Sphere (phi)

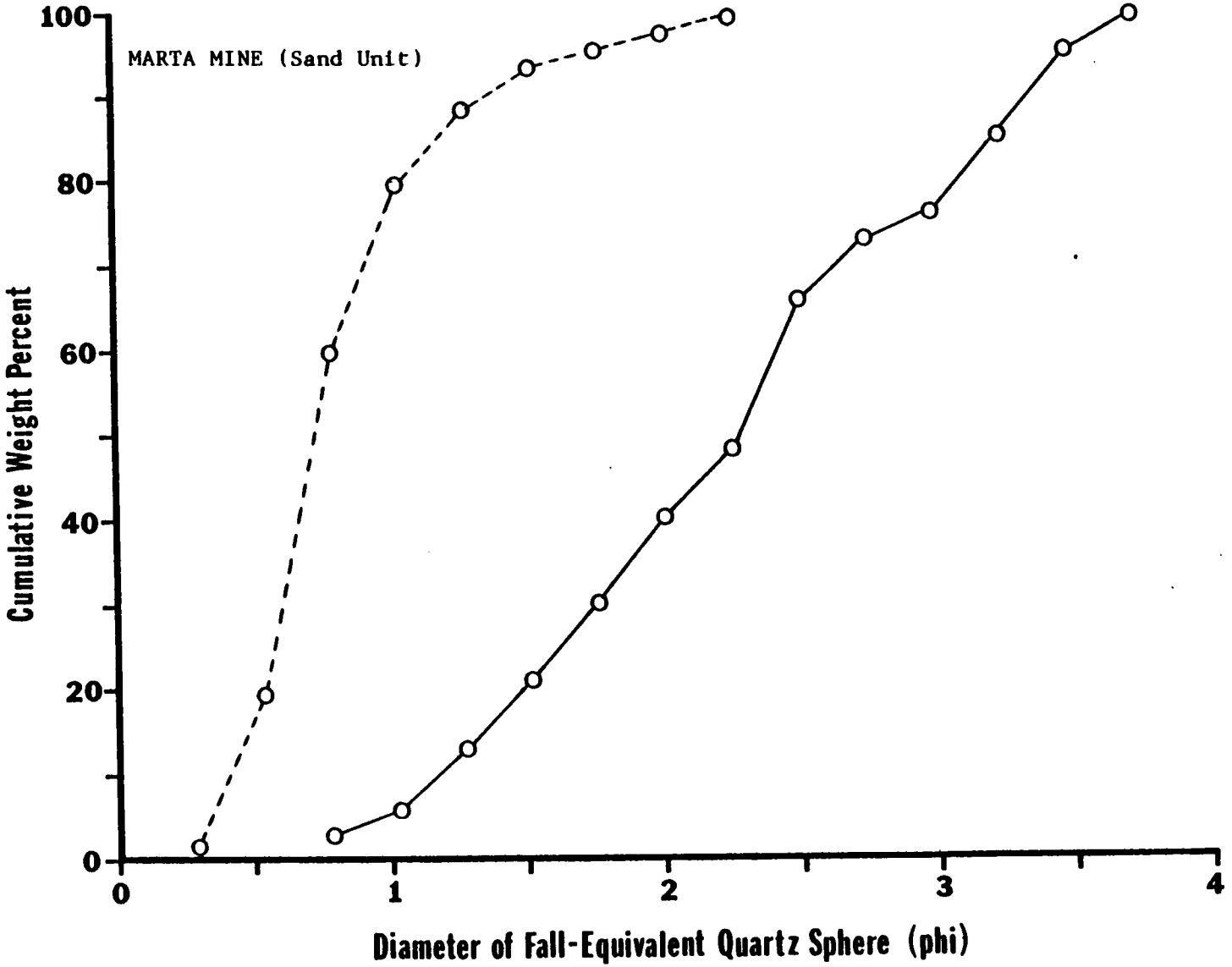
MARTA MINE (Sand Unit)
Cumulative Weight Percent
100
80
60
40
20
0
0
1
2
3
4
Diameter of Fall-Equivalent Quartz Sphere (phi)

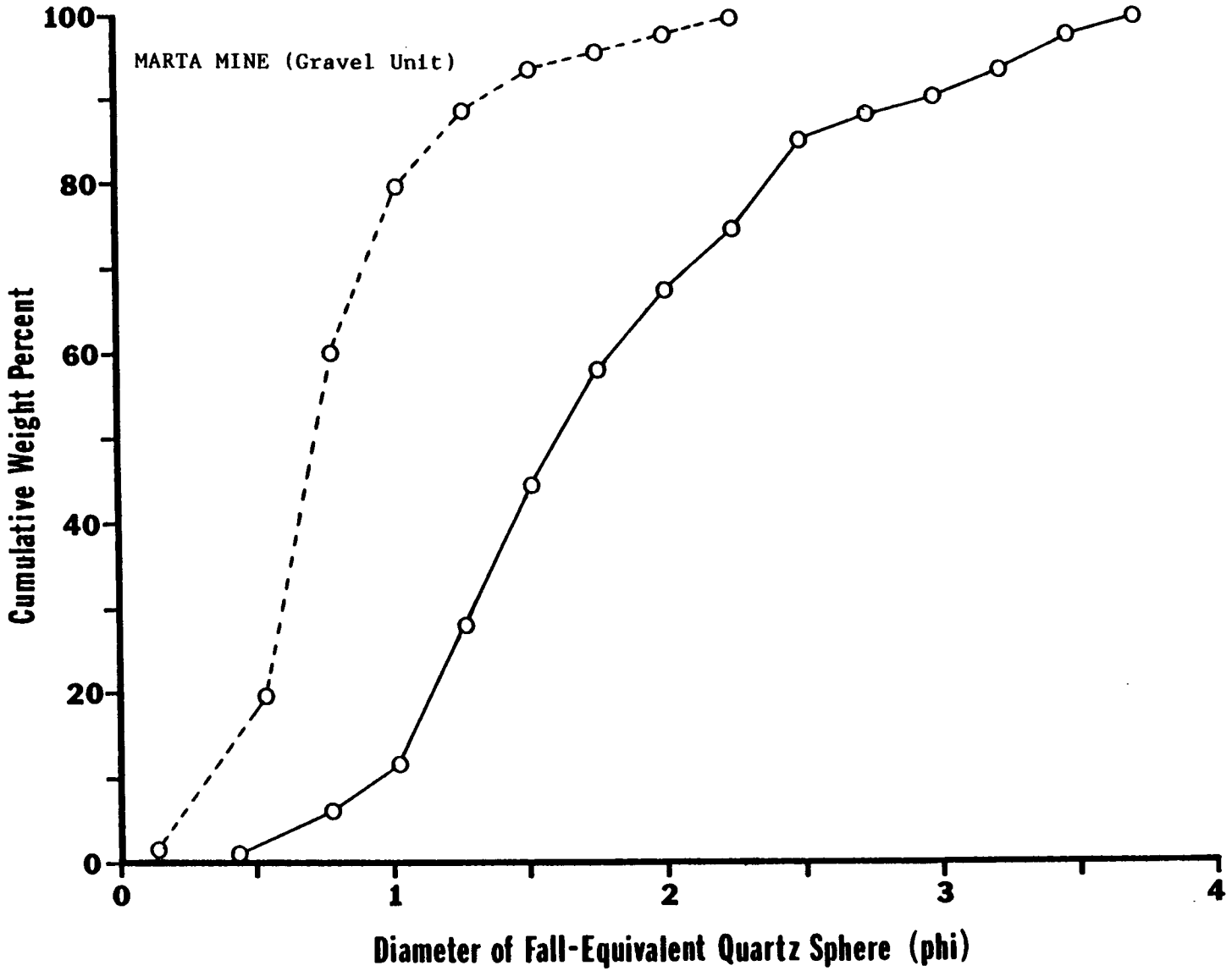
MARTA MINE (Gravel Unit)
Cumulative Weight Percent
100
80
60
40
20
0
0
1
2
3
4
Diameter of Fall-Equivalent Quartz Sphere (phi)

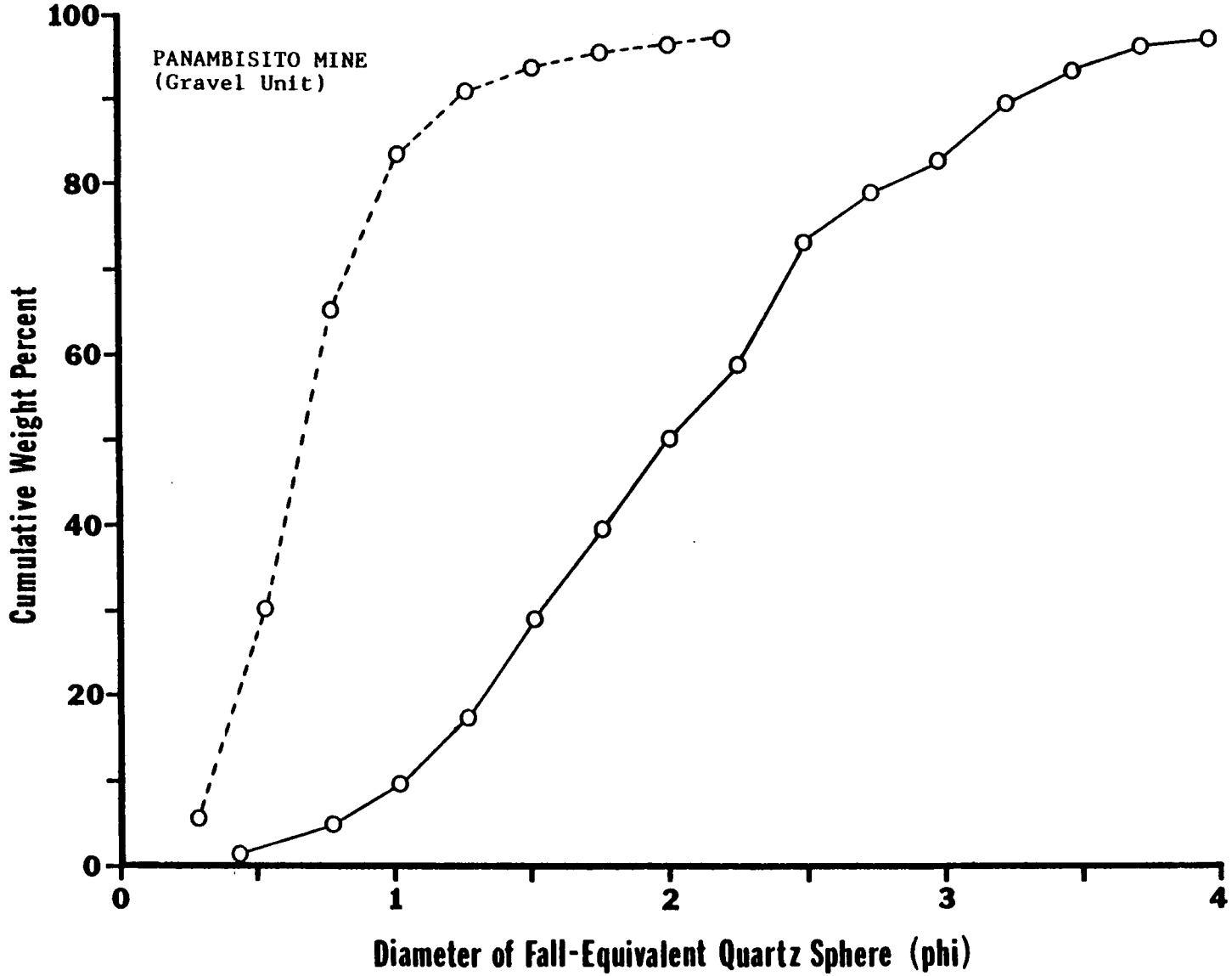
PANAMBISITO MINE
(Gravel Unit)
Cumulative Weight Percent
100
80
60
40
20
0
0
1
2
3
4
Diameter of Fall-Equivalent Quartz Sphere (phi)

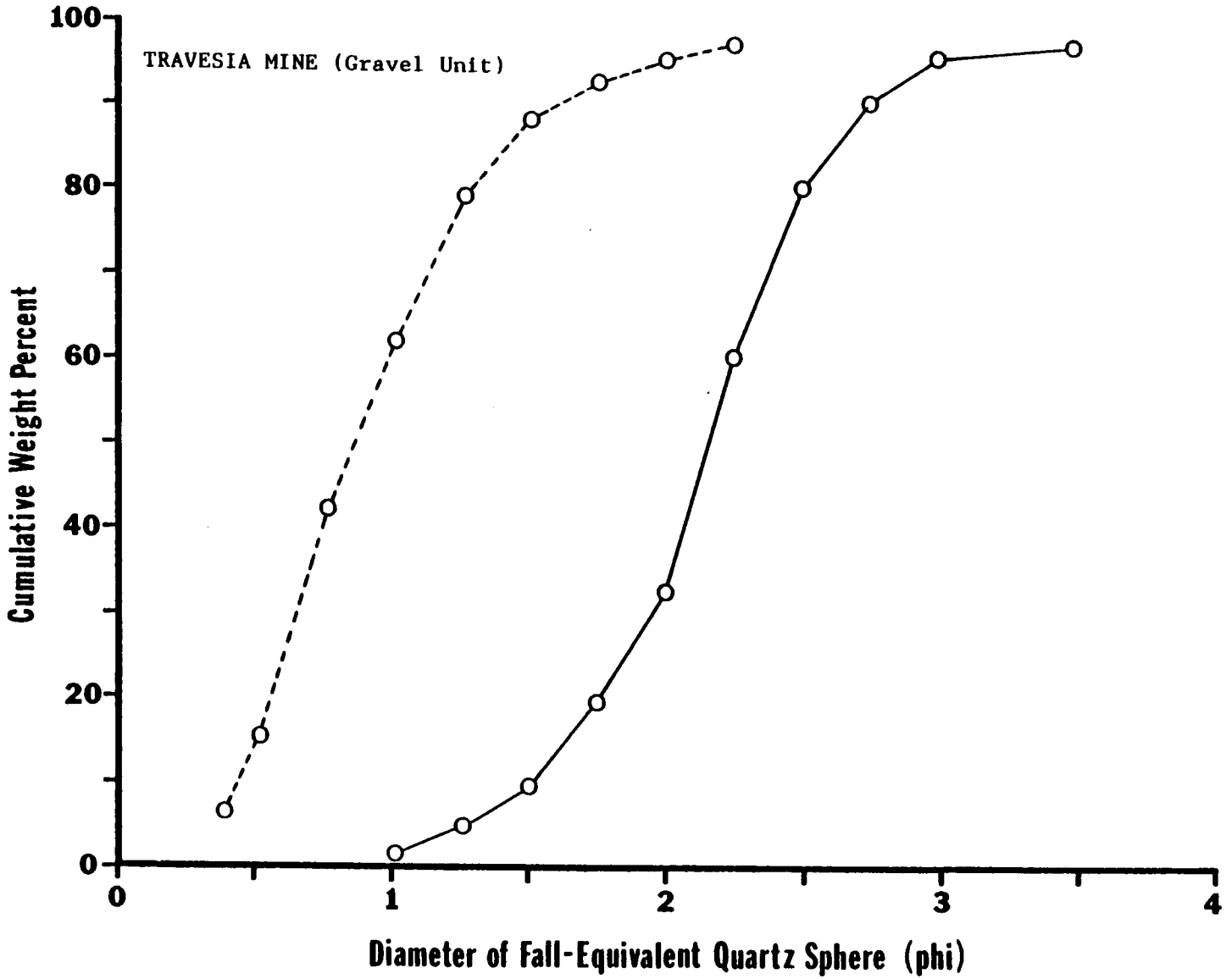
TRAVESIA MINE (Gravel Unit)
Cumulative Weight Percent
100
80
60
40
20
0
0
1
2
3
4
Diameter of Fall-Equivalent Quartz Sphere (phi)

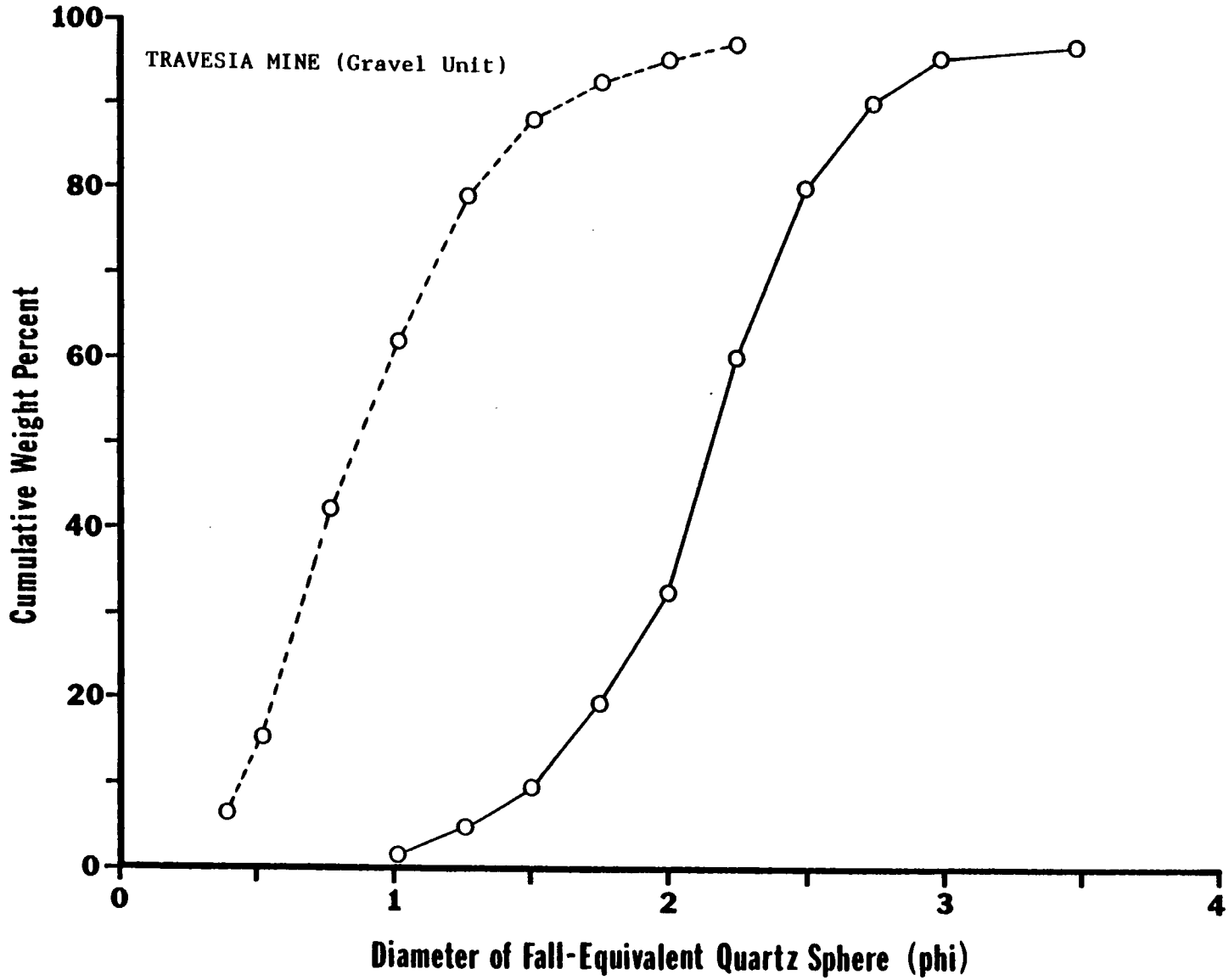
TRAVESIA MINE (Gravel Unit)
Cumulative Weight Percent
100
80
60
40
20
0
0
1
2
3
4
Diameter of Fall-Equivalent Quartz Sphere (phi)

DATE DUE
